Coordinated Rendezvous and Surveillance for Multiple Unmanned Aerial Vehicles (UAVs) subject to Actuator and Sensor Faults

Maria Palwasha Khan

A Thesis

in

The Department

of

Electrical & Computer Engineering

Presented in Partial Fulfillment of the Requirements

for the Degree of Master of Applied Science (Electrical & Computer Engineering) at

Concordia University

Montreal, Quebec, Canada

April 2008

Your file Votre référence
ISBN: 978-0-494-40885-8
Our file Notre référence
ISBN: 978-0-494-40885-8

Abstract

Coordinated Rendezvous and Surveillance for Multiple Unmanned Aerial Vehicles (UAVs) subject to Actuator and Sensor Faults

Maria Palwasha Khan

In this thesis, the problem of employing multiple UAVs for carrying out a *Coordinated Strike* and a *Multiple UAV Surveillance* mission has been addressed. The goal of the *Coordinated Strike* mission is for multiple UAVs to cooperate in order to simultaneously arrive at a high priority target to carry out a coordinated strike. The coordination strategy is based on coordination variables and coordination functions. A distributed system architecture is proposed that allows vehicles to communicate coordinating information across the team without reliance on a central ground controller. Simulations have been conducted to illustrate the performance of the coordination strategy under an actuator fault in single and multiple vehicles.

The Multiple UAV Surveillance problem has been investigated by developing a hypothetical *Border Surveillance Mission*, wherein a UAV team is tasked to monitor a region along a border between two countries. The goal of the UAVs is to cover the entire surveillance region, while minimizing the team cost, which is a function of each vehicle's fuel consumption and mission time. Three fault cases in a single vehicle in the team have been simulated, namely (1) actuator; (2) sensor; and (3) simultaneous actuator

and sensor faults. These faults necessitate a resource allocation problem to be solved, which is used to determine the configuration of the team engaged in the surveillance mission. The team chosen to perform the surveillance mission is the one that incurs the minimum cost for performing the mission.

With my deepest love and affection,

I dedicate this dissertation to my late grandfather:

Asghar Ali Kadri

Acknowledgments

I thank my supervisor, Dr. Khorasani for his insights, support and understanding through out my time of study.

I thank my parents and my brother for their unwavering love and support. They have been there for me through all the hurdles of my research, have never once doubted my abilities, and have always lifted my spirits. Their love has always been the wind beneath my wings. I shall be eternally grateful to them.

Finally, I would like to thanks all my friends and colleagues here at Concordia who have been a source of great strength for me.

TABLE OF CONTENTS

List of Tables

List of Figures

Nomenclature

Symbol	Description
N	Total number of threats
$d^4_{1/2,i,j}$	Distance from the ½ point on the ith edge to the jth threat
α	Constant scale factor
L_i	Length of edge i
$J_{threat,i}$	Threat cost associated with the ith edge
$J_{length,i}$	Length cost associated with the ith edge
J_i	Total cost associated with the ith edge
κ	Weighting factor
TOT_i	Time over target for the ith UAV
ξ_i	Waypoint path followed by the ith UAV to reach the target
V_i	Forward speed of the ith UAV
$S_{TOT,i}$	Set of feasible time over target ranges for the ith UAV
$\hat{J}_i(TOT)$	Coordination function for the ith UAV
(X_i^d, Y_i^d)	Desired inertial position of the i^{th} UAV

ψ_i^d	Desired heading of the i^{th} UAV
V_i^d	Desired velocity of the i^{th} UAV
h_i^d	Desired altitude of the i^{th} UAV
u_1, u_2	Input signals
T_S	Coordination variable
T_i	Time of arrival of the i^{th} vehicle
$L(W_i)$	Length of the waypoint path
v_i	Velocity of the i^{th} UAV
Δ_i	(1) Time interval between the arrival of the first and the i^{th} vehicles (2) Interval between the opening of the first time window and the opening of the i^{th} time window
τ_i	Duration of the i^{th} time window
CF_i	Coordination Function of the i^{th} vehicle
v	Velocity of the UAV
l_l	Path length in the low-threat region
l_h	Path length in the high threat region
C_f	Weighting factor
C_l	Weighting factor
C_h	Weighting factor
J_f	Fuel cost of the UAV

J_t	Threat cost of the UAV
$u_i(t)$	Actuator output
u_{ci}	Output of the controller and an input to the actuator
t_{Fi}	Time instant of the failure of the ith effector
k_i	Effectiveness coefficient of the control effector
ε_i	Minimum effectiveness of the control effector
CF_UAVi	Coordination Function of the ith UAV
UAVi ETA range	Set of time of arrival ranges of the ith UAV at the target
v_i	Velocity of the ith UAV
$\mathbf{h}$	Location of radar
H	Set of all radar locations
$\mathbf{w}_j$	Current waypoint
$\mathbf{w}_{j-1}$	Previous waypoint
ρ	Percentage of the power in the radar signal that is reflected by the UAV
$\mathbf{x}_i$	Situation state of the ith UAV
z_{io}	Current position of the ith UAV
z_{if}	Destination of the ith UAV

$\mathbf{u}_i$	Decision vector of the ith UAV
W_i	Waypoint path from the ith UAV's current position to its destination
θ_i	Estimated time of arrival of the ith UAV at its destination
$\Theta_i(\mathbf{x}_i)$	Set of estimated time of arrival ranges for the ith vehicle in situation state $\mathbf{x}_i$
λ	Scaling factor
τ	Scaling factor
J_{sm_i}	Total cost incurred by the ith UAV for carrying out surveillance of the area assigned to it
D_i	Distance or the length of the path covered by the ith UAV
LRA_i	Length of the rectangular area to be covered by the ith UAV
WRA	Width of the entire rectangular area
SR_UAV_i	Sensor range of the ith UAV
t_{s_i}	Surveillance mission time of the ith UAV
β	Scaling factor
γ	Scaling factor

Abbreviation	Description
UAV	Unmanned Aerial Vehicle
SEAD	Suppression of Enemy Air Defenses
ISR	Intelligence, Surveillance, and Reconnaissance
LOE	Loss of Effectiveness
ETA	Estimated Time of Arrival
TR	Target Recognition
A	Attack
ROR	Rate of Return
TOT*	Team-Optimal Time Over Target
WPP	Waypoint Path Planner
DTS	Dynamic Trajectory Smoother
CM	Coordination Manager
LIP	Lock-In-Place Failure
HOF	Hard-Over Failure
FTC	Fault tolerant control
FDI	Failure detection and identification

Chapter 1

Introduction

An Unmanned Aerial Vehicle (UAV) is a powered aerial vehicle that does not carry a human operator, uses aerodynamic forces to provide vehicle lift, can fly autonomously or be piloted remotely, can be expendable or recoverable, and can carry a lethal or non-lethal payload. Ballistic or semi-ballistic vehicles, cruise missiles, and artillery projectiles are not considered as UAVs [1].

UAVs have been identified as valuable assets for military as well as civilian (government and industrial) operations. The potential advantages of an UAV over a manned aircraft are significant and include but are not limited to: greater maneuverability, low risk to human operators (since an UAV can be remotely operated to perform dangerous missions), weight savings, and lower development costs. In the past decade, military investment in UAV research, systems and applied technologies has increased significantly. According to the Air Force Scientific Advisory Board, with advances in UAV technologies, these vehicles will be capable of fulfilling many of the current manned aircraft missions either autonomously or in conjunction with manned aircraft. Examples of the type of missions for which the UAVs are or will be employed by the United States Air Force are: Fixed and Moving Target Attack, Suppression of Enemy Air Defenses (SEAD), Intelligence, Surveillance, and Reconnaissance (ISR),

Radar Jamming, Theatre Missile Defense, and Air-to-Air Combat [2]. The civilian sector is also exploring the applications of UAVs for Land Management (e.g., wildfire monitoring, crop dusting), Homeland Security (e.g., border patrol, maritime surveillance), and Earth Science missions.

In the past decade, the focus of research has shifted from development of algorithms for a single UAV performing a mission to development of viable strategies that will allow a group of UAVs to cooperate to perform multiple tasks. Hence, to utilize the full capabilities of a team of UAVs performing a wide variety of mission dependent tasks, research efforts in both civilian and military domains have been focused on the development of efficient cooperative control algorithms.

With regard to UAVs, *Cooperative Control* means coordinating the activities of a team of vehicles so that they may work together to complete tasks in order to achieve a common goal. Effective group cooperation cannot be achieved without *coordination* of the actions of individual vehicles. However, each vehicle may not necessarily need to directly coordinate with every other vehicle in the team to achieve group cooperative behavior. Hence, *coordination* refers to the degree of interaction among team members. There are two types of coordination: *local coordination* and *global coordination.* In *local coordination*, an individual vehicle coordinates its actions only with either its nearest neighbors or team members in close physical proximity. Whereas, *global coordination* requires that each vehicle in the team coordinates its actions with every other vehicle in the team to achieve group cooperation.

The main objective of research into the *Cooperative UAV Control* problem is to develop and evaluate strategies (algorithms) for a team of UAVs working together to perform mission specific tasks in an extended area under varying operating conditions and constraints. For a given mission scenario, the *Cooperative UAV Control* problem formulation encompasses the following common sub-problems: Path Planning, Trajectory Generation, and Task Allocation. The complexity of these sub-problems depends on the chosen mission scenario, the assumptions made about the capabilities of the vehicles and the environment, and the constraints added by the mission designer. As these factors are varied, the *Cooperative UAV Control* problem formulation will also vary, with varying corresponding unique specialized solution strategies. Other problems that also need to be addressed are development of system architectures for the individual UAVs, the development of a team architecture (centralized, decentralized, or distributed), which determines how information is communicated across the team and how decisions are made, development of strategies for synchronizing the shared information across the team in the presence of factors such as partial network connectivity, and reduced communication range, and finally development of a viable coordination strategy.

1.1 Contributions

In this thesis, we have addressed the problem of employing multiple vehicles for carrying out two disjoint missions, i.e., *Coordinated Strike* and *Multiple UAV Surveillance*.

The goal of the *Coordinated Strike* mission is for multiple UAVs to simultaneously arrive at a high priority target to carry out a coordinated strike. We have used a coordination strategy based on coordination variables and coordination functions, originally developed by Chandler *et. al.* ([8], [9], [10], and [15]) and Beard *et. al.* ([4], [5], [6], [7], and [16]). Since the goal of the Coordinated Strike mission is for multiple vehicles to cooperate to achieve their joint mission objective, essential information must be communicated across the team. Instead of using a centralized system architecture, wherein each vehicle would only communicate with a central command and controller instead of its team members, we have utilized a distributed system architecture that allows vehicles to communicate coordinating information across the team without reliance on a central ground controller.

While Beard *et. al.* ([4], [5], [6], [7], and [16]) have only tested their coordination strategy under nominal conditions for the rendezvous problem, we have extended it to include an actuator fault in both single and multiple vehicles in order to determine the effect of actuator faults on the performance of the coordination strategy.

The type of actuator faults that are simulated in this thesis is the Loss of Effectiveness (LOE) [45]. In this type of fault, the output of the actuator is a fraction of the output of the controller, and is dependent on the value of the effectiveness coefficient (k_i) of the control effector. A perfectly functioning actuator has an associated value of $k_i = 1$ (where k_i can vary over the range: $[\varepsilon_i, 1]$, where ε_i is the

minimum effectiveness of the control effector). Hence, in the case of the LOE failure, the effectiveness coefficient is $k_i < 1$, which lowers the output of the actuator. The severity of the actuator fault depends on the value of the effectiveness coefficient, k_i. As the value of k_i decreases, the severity of the actuator fault increases.

Velocity has been used as the fault variable to simulate an actuator fault in single and multiple UAVs. The extent of the actuator fault has been simulated through gradual reduction of the maximum velocity of the UAV. While we have not modeled the actuator, we have assumed that the parameter k_i will have a direct impact on the velocity range of a vehicle. It is assumed that the percentage reduction in the value of k_i is directly proportional to the percentage reduction in maximum velocity of a UAV. Hence, the Loss of Effectiveness of a UAV's actuator will result in a lower maximum velocity of the UAV.

It is assumed that each UAV is operating under nominal conditions upon takeoff from their respective bases, and that the Loss of Effectiveness fault in the actuator of the affected vehicle occurs while the team is en route to the target. In response to the actuator fault, all UAVs re-generate and share coordinating information with one another in order to re-plan their routes to the target. However, if the degradation in a UAV's actuator is to such an extent that it can no longer rendezvous with the other vehicles at the target, a resource allocation problem is solved in order to determine which vehicles should engage the target. If a vehicle is dropped from the team for the joint attack mission, it is commanded to travel to the surveillance area.

For the *Multiple UAV Surveillance* problem, we have designed a hypothetical Border Surveillance mission. For this part of the mission, we have assumed a centralized system architecture wherein each UAV communicates with a central controller on a periodic basis. The goal of the UAVs is to carry out surveillance of the entire environment of operation while minimizing the team cost, which is a function of the amount of fuel consumed by each vehicle in the team and the time required to complete the mission. To emulate real world situations, where a fault in one or more of the vehicles in a team can occur at any time, we have simulated three cases of faults in different sub-systems of a single vehicle in a team in order to determine the effect of the faults on the performance of the team. The affected vehicle is assumed to be suffering from a fault in either its actuator or sensor or both its actuator and sensor.

As in the Coordinated Strike mission, the type of actuator fault simulated here is the Loss of Effectiveness (LOE). The type of sensor fault simulated here is called the Multiplicative-type sensor failure. In this failure type, a multiplicative factor is applied to the nominal value of the sensor. A scaling error in the sensor output is responsible for the multiplicative-type sensor failure.

The sensor range (sensor output) has been used as the fault variable to simulate the sensor fault in a single UAV. Despite the presence of either the Loss of Effectiveness actuator fault and/or the Multiplicative-type sensor failure, the goal of the surveillance mission remains the same, which is minimization of the team cost. However, a fault in either the sensor, or actuator or both requires the mission designer to

address a resource allocation problem, i.e, whether to carry out the mission using all three vehicles or only the healthy, perfectly functioning vehicles. The team chosen to perform the surveillance mission is the one that incurs the minimum cost for performing the mission.

1.2 Outline of Thesis

In Chapter 2, a literature review of the problem of Coordinated Rendezvous, Multiple UAV Search and Surveillance, and Fault Diagnosis and Identification in UAVs is given. In Chapter 3, the background into the Coordinated Rendezvous problem is given followed by the development of a mission scenario, and the development of the rendezvous strategy. Finally, simulation results showing rendezvous under nominal conditions and under an actuator fault in a single vehicle and multiple vehicles are presented. In Chapter 4, the solution strategy for the surveillance mission is detailed, and simulation results are presented to show the effect of sensor, actuator, and both sensor and actuator faults on the performance of the UAV team engaged in the surveillance mission. Finally, in Chapter 5, the conclusions drawn in this thesis are given, some directions for future research are indicated, and the contributions of this thesis are reiterated.

Chapter 2

Literature Review

2.1 Coordinated Rendezvous Problem

Coordinated Rendezvous is a type of *Cooperative Timing* problem that requires multiple UAVs to arrive simultaneously at their destination(s) to maximize the element of surprise. In [3], a generalized approach to solving cooperative control problems has been detailed. This approach can be applied to problems such as Spacecraft Formation Flying, Cooperative Timing, Cooperative Search, and Cooperative Forest Fire Surveillance. In [4]-[10], and [15], this approach has been applied to the coordinated rendezvous problem, and is divided into three steps. The first step requires the mission designer to define the cooperation objective (mission objective) of the team, and the cooperation constraints. Cooperation is said to be achieved when relationships between state variables, termed as cooperation constraints, are satisfied. The second step involves defining the *coordination variable* and *coordination functions*. The third and final step involves designing a cooperative control strategy for the team, which illustrates the process of how the team coordinates to achieve its mission objective.

Cooperation requires that an efficient method be developed to facilitate sharing of information between a team of vehicles. There are several ways in which information can be shared. For example, relative position sensors may enable vehicles to construct state information of other vehicles, information may be communicated between vehicles using a wireless network, or joint information may be pre-programmed into vehicles before the mission begins [7]. In the proposed approach to solving cooperative control problems, the strategy is to collect the information that must be shared across the team to enable cooperation into a single quantity called the *coordination variable*. The coordination variable represents the minimum amount of information needed by a team of vehicles to cooperate in order to achieve the team objective. Coordination functions parameterize the effect of changing the coordination variable on the objectives of individual vehicles. The information modeled by the coordination functions is used to determine an optimal value of the coordination variable for the team.

For the generalized coordinated rendezvous problem for a military application, the cooperative objective of a team of UAVs is to arrive at a pre-determined destination (a single target or multiple targets) simultaneously to maximize the element of surprise, while conserving fuel and minimizing its exposure to threats in the environment. The cooperation constraint is the requirement that all vehicles arrive at a single target or multiple targets simultaneously. The coordination variable is the estimated time of arrival (ETA) of the team at the target. The idea is that if all vehicles are aware of the team's arrival time at the target, they will be able to plan their trajectories in order to meet the cooperation objective. Each vehicle generates its coordination function, which

describes the range of total cost (i.e., combined threat exposure and fuel cost) incurred by a vehicle for achieving a given range of arrival times. Coordinated rendezvous is achieved by sharing of the coordination functions across the team and the subsequent selection of the coordination variable. A Coordination (Intercept, Rendezvous) Manager selects the coordination variable, i.e., team ETA such that the combined threat exposure and fuel expenditure of the team is minimized. To this end, it uses the coordination functions of team members to first select a common range of arrival times for the team, and then selects the arrival time with the minimum associated total cost (sum of individual vehicle (threat and fuel) costs) for the team.

In [4] and [5], a system architecture for a single UAV has been proposed, which shows how coordination functions are generated, how the team coordination variable is selected, and how the individual UAVs plan their trajectories to the target in order to satisfy the cooperation objective. The main functional blocks of this architecture are the Path Planner, the Target Manager, the Intercept Manager, and the Trajectory Generator.

The Path Planner of a UAV is responsible for generating threat avoiding straight line paths from the vehicle's current position to its destination (target). Depending on the vehicle's knowledge of the environment (i.e., its knowledge of the locations of threats, and targets in the environment), the Path Planner generates one or more candidate paths from the vehicle's initial position to the target. These paths minimize the vehicle's exposure to threats and allow it to conserve fuel. The role of the Target Manager is to assign a target to a UAV before the beginning of the mission.

Once teams have been formed and assigned to their respective targets, the task of the *Intercept Manager* is to ensure that individual vehicles comprising a team arrive at their assigned target simultaneously. The Intercept Manager of each vehicle uses the candidate paths generated by the Path Planner, and the team assignment created by the Target Manager to generate a set of time of arrival ranges, and the coordination function for the UAV. Next, to ensure that all the vehicles in a team reach their target simultaneously, all team members must share their time of arrival ranges and the information modeled by their coordination function. To this end, a cooperative, distributed decision and control system has been proposed in [7] in which each UAV sends its coordination function and time of arrival ranges to all its team members.

In [18], it is stated that there are three classes of distributed decision and control systems: Hierarchical ([10], [11], and [12]), Behavioural, and Cooperative [7]. The Cooperative class is characterized by a minimum level of global information to ensure team cohesion and coherence. In the cooperative control architecture proposed in [7], each vehicle in the team implements an identical copy of the Intercept (Coordination, Rendezvous) Manager algorithm, which is essentially a centralized algorithm implemented by each vehicle. It is assumed that the information shared across the team is synchronized by the Communication Manager of each vehicle. Hence, the Intercept Manager of each vehicle receives identical input data, i.e., coordination functions from all the vehicles. The Intercept Manager then selects the same team coordination variable, i.e., team ETA.

For the rendezvous mission, team ETA is chosen such that the total team cost, i.e., the combined threat cost and fuel expenditure of the vehicles forming the team is minimized. Once the team ETA is determined, the Intercept Manager of each vehicle generates a velocity and a set of waypoints for the vehicle to follow to reach its target. The chosen velocity and waypoint path allow the vehicle to reach the target at the given team ETA. These set of waypoints and velocity are then passed to the *Trajectory Generator*. The objective of the Trajectory Generator is to smooth the straight-line waypoint path that the UAV must follow to reach its target into a time parameterized trajectory.

In [6] and [7], the cooperative control strategy developed in [4] and [5] is applied to three cooperative timing missions: simultaneous intercept, tight sequencing, and loose sequencing. In [8] and [9], the Intercept Manager has been modeled as a finite state machine. Different phases of the mission are planned in each state of the finite state machine.

In [10], [11], and [12], a hierarchical, distributed architecture has been developed to address the general problem of cooperative control, and is applied to a cooperative rendezvous mission [10]. The hierarchical architecture is redundant, with the same agent hierarchy on each vehicle, and consists of three decisions layers, and one control layer. At decision level 3 is the team agent, which is responsible for accomplishing the mission objective (cooperation objective). It divides the mission objective into sub-objectives for the sub-teams, and allocates resources and tasks to the sub-teams accordingly. At

decision level 2 is the sub-team agent. This agent performs resource allocation (i.e., assigns vehicles in the sub-team to multiple targets), and coordinates the actions of the vehicles in the sub-team to perform tasks that require more than one vehicle to accomplish. For the cooperative rendezvous mission, the sub-team agent performs rendezvous coordination. At decision level 1 is the vehicle agent, which maintains models of the area of operation, threats and targets, and is responsible for the tasks of path planning, and trajectory generation for an individual vehicle. At the lowest level (control level) is the regulation agent, which provides commands to the UAV to accomplish tasks such as trajectory generation, changing speed, activating sensors, and releasing weapons.

Depending on the mission scenario and the desired level of detail, the coordinated rendezvous problem can encompass the following sub-problems: Path Planning, Trajectory Generation, and Task Allocation.

A Path Planning problem always needs to be solved to generate a straight-line waypoint path from a UAV's current position to its desired position such that the mission objective and cooperation constraints (mission dependent) are satisfied. If the kinematic constraints of a UAV, such as constraints on maximum velocity, and turning radius and their effect on the maneuvers a UAV can make, are taken into account, it becomes necessary to solve a Trajectory Generation problem. In [13], it is stated that the objective of a Trajectory Generation problem is to develop a trajectory that is possible to implement in real-time, allows a UAV to traverse between a sequence of waypoints in a

time-optimal manner, and that satisfies the kinematic and dynamic constraints of a UAV. For the rendezvous problem, in order to satisfy the simultaneous arrival constraint, the generated trajectory should be equal in length to the waypoint path produced by the Path Planning algorithm.

In [14], various path planning and trajectory generation schemes have been compared and contrasted using the following metrics: threat avoidance, ability to satisfy dynamic constraints of a UAV, computational efficiency, and the ability to generate trajectories rather than paths. The path planning and trajectory generation strategies that have been investigated are Rectilinear Grid, Voronoi Grid, Voronoi Path Filleting, Mass-Spring-Damper System [17], Chain-Link System, Voronoi Grid Approximation, Polynomial Basis Functions, Cubic Spline Basis Functions, Voronoi Decomposition Approach, and Non-Dimensional approaches. In [4]-[10], [15], and [16], the Voronoi Grid (i.e., a Voronoi diagram) approach is used to construct a single waypoint path or multiple waypoint paths from a vehicle's current position to its target. The generated waypoint paths satisfy the mission objective and cooperation constraints. To find the optimal paths, graph search algorithms, such as A*, Dijkstra, or k-best path algorithms are used to search the Voronoi diagram. To ensure that the generated paths are dynamically feasible and are flyable by the UAVs, the following trajectory generation schemes have been used: Chain-Link System [9], [16], Voronoi Path Filleting [10], [15], and a real-time non-linear filter whose mathematical structure is similar to the kinematics of the UAV [4]-[7].

The Task Allocation problem involves developing an assignment algorithm that assigns tasks to a team of vehicles. In [4] and [5], a task assignment algorithm based on the satisficing decision theory [44] has been detailed. However, in [6]-[9], it has been assumed that the UAVs have been assigned to targets (tasks) before the beginning of the mission, thereby not requiring a Task Allocation problem to be solved. However, to simulate real missions, a Target Manager should be included in the rendezvous problem, and a respective Task Allocation scheme should be developed.

2.2 Multiple UAV Search and Surveillance Problem

The main objective of research into the *Multiple UAV Search* problem is to develop and evaluate strategies for a team of UAVs searching an environment of known dimensions for (stationary and/or mobile) targets under varying operating conditions and constraints. Searching an area of interest using a group of vehicles is a problem that finds use in both military and civilian applications. Some of the possible missions that could benefit from multiple UAVs conducting search are: search-and-rescue operations, search-and-destroy missions for previously detected enemy targets, seek-destroy missions for land mines, intelligence gathering missions, and surveillance missions such as border patrol.

According to [19], the problem of searching an unknown environment has been actively studied in classical search theory, where problems such as optimal distribution

of search effort, maximization of the probability of detection of stationary targets, and establishment of optimal values of various search parameters have been concentrated on. While additions have been made to the search theory literature by inclusion of mobile, multiple, and intelligent targets in the problem formulation, solution strategies have only been developed for a single searcher, and hence are inapplicable to multiple searchers. Moreover, the authors in [19] have pointed out that other realistic considerations such as communication constraints, a vehicle's ability to make autonomous decisions, information constraints (i.e., availability of only partial information to a vehicle), and distributed decision making issues have not been taken into account in search theory literature.

The *Multiple UAV Search* problem can be formulated in a number of different ways, thus requiring the development of corresponding unique solution strategies. The variations in the problem formulation are due to the varying objectives of the UAV team, the imposed constraints under which the vehicles are operating, the assumptions made about the UAVs' capabilities, and the environment of operation. The search environment may contain obstacles (e.g., no fly zones such as mountains), multiple, stationary and/or mobile, intelligent, known and/or unknown targets, and threats. Hence, the composition of a search environment can dictate whether a static or a dynamic solution strategy is suitable for solving the search problem. As for constraints, some of the prominent ones in the UAV literature are constraints on a vehicle's maneuverability, velocity range, endurance time (dependent on the maximum amount of fuel a vehicle can consume during a mission), and communication ability (limited range of

communication). Examples of assumptions made are (but not limited to) the following: (1) Vehicles may or may not be capable of wireless communication, (2) The information base of the vehicles, representing the state of the environment, might be centralized or decentralized, (3) The sensors of the vehicles might have the same or different accuracy and ranges, (4) The vehicles may or may not be autonomous (capable of independent decision making, and computational capabilities), and (5) The vehicles may or may not be identical in terms of their abilities to perform tasks.

A small sample of papers has been chosen and described briefly below in order to illustrate the various aspects of the *Multiple UAV Search* problem studied in literature, and the corresponding solution strategies.

In [19], the authors have addressed the problem of multiple UAVs carrying out a search and surveillance mission based on the uncertainty map of a given unknown environment. The uncertainty map represents the *a priori* knowledge of the location of targets, and is comprised of real numbers between 0 and 1. The search environment is divided into identical hexagonal cells, where each cell has an associated uncertainty value, which represents the extent of the lack of information about a cell. The UAVs are directed to fly multiple sorties (or missions). For each mission, the objective of the UAVs is to maximize the reduction in uncertainty of the environment under a limited fuel constraint, which also constrains the length of the search path each vehicle takes since the vehicles have to return to their respective base stations for re-fueling at the end of each mission.

The search algorithm, based on the k-shortest path algorithm, directs individual UAVs to search (independently of their team members) through the area of maximum uncertainty in the environment while satisfying constraints on their endurance time and on the search path. The authors in [19] have compared the performance of their algorithm with that of random search and greedy search algorithms, and have shown that their algorithm reduces the uncertainty in the environment at a faster rate. However, there are several drawbacks of the proposed search strategy. Firstly, the uncertainty map remains static during a given search mission. It is updated only after the UAVs have returned to their respective base stations, where data acquired by all UAVs is combined through communication between base stations to create a global uncertainty map for all the vehicles.

Secondly, only the perfect information case is assumed for the update of the uncertainty map, i.e., one in which all base stations share the data collected by their respective UAVs to create a global uncertainty map. In [20], the authors have addressed this problem by testing the performance of the k-shortest path based search algorithm under four different information structures, which are: a fully connected communication network, a partially connected communication network, a fully connected communication network with delay in information, and a partially connected communication network with delay in information. The third drawback of the search algorithm is that the search route of each vehicle is generated off-line before the beginning of the next search mission based on the local copy of the uncertainty map

available to the vehicle. Finally, direct communication between searchers has not been addressed since communication only takes place between base stations.

In [21], the authors have addressed the first, third and fourth drawbacks of [19] by introducing a game theoretical framework in which each UAV (agent) updates its uncertainty map at every time step after using the position and route information (up to that time) of the other UAVs. Hence, at any given time, all UAVs have the same uncertainty map, and are aware of the past route and present location of their team members. At each time step, the objective of the UAVs forming the team is to select their future paths such that the reduction in uncertainty of the environment is maximized. To this end, the authors have proposed three search strategies based on notions in game theory to direct the UAVs to choose paths to maximize the reduction in uncertainty in the environment. These are Non cooperative search strategy using Nash Equilibrium, Security Strategy, and Cooperative Strategy.

In [22], an agent based negotiation scheme has been presented to address the problem of communication between vehicles for the search problem presented in [19]. The vehicles have a limited sensor range and can communicate with their neighboring vehicles only. The objective of each UAV in the team is to coordinate with its neighboring UAVs to select search routes such that the collective uncertainty reduction of the team is maximized. In this scheme, at the beginning of each time step, information is shared between every agent, which is followed by a negotiation process,

based on which, every agent selects the next cell in its search route. This process continues until the given area is completely searched.

As in [19], reduction in uncertainty in the environment has been used as a performance measure to show that the proposed search strategy outperforms the random and greedy search strategies for the cases of complete and partial information exchange among vehicles. However, the effects of communication delays and loss of communication on the performance of the search strategy have not been studied. Moreover, the negotiation scheme has a large communication overhead. In [23], the authors have presented self assessment schemes for the search problem in [19]. As in [22], each vehicle communicates and coordinates with its neighboring vehicles to select search routes such that the team's collective uncertainty reduction is maximized. However, the self assessment scheme requires a low communication and computational overhead, is scalable to a large number of vehicles, facilitates fast decision making, and can be used with partial or complete information sharing schemes during the search mission.

In [24], the authors have proposed a cooperative search approach for a team of vehicles, where the objective of each vehicle is to follow a trajectory that would result in minimization of the uncertainty about the environment, subject to maneuverability constraints. The proposed cooperative search approach solves two interdependent tasks: online update of a vehicle's search map, and utilization of the search map to online generate a vehicle's search trajectory. Each vehicle continuously updates its search map

(a global search map) during the mission by processing information gathered about the search environment through its sensors and through communication with other vehicles. A q-step ahead planning approach is used by each UAV to generate its path online, independently of the other vehicles. Path selection is carried out using a multi-objective cost function, which is comprised of the following three sub-goals: 1) Follow the path of maximum uncertainty in the search map, 2) Follow the path that leads to the region of maximum uncertainty (on average) in the environment, and 3) Follow the path that results in minimum overlap between the regions being searched by other vehicles.

In [25], multiple UAVs must autonomously search a given area such that, given some *a priori* information about target distribution, the vehicles can identify the maximum number of stationary targets during their life time, which is determined by the amount of fuel carried by the vehicles. To address this problem, the authors have formulated a discrete time stochastic decision model, which has been implemented with a Dynamic Programming algorithm, and in which gain is defined as the reduction in probability of there being an undiscovered target in a searched area. The objective of the vehicles is to maximize the total gain (equal to the sum of the individual vehicle gains) over their life time. In order to plan trajectories, vehicles use their cognitive maps, which represent the state of the environment. Each vehicle updates its own cognitive map (divided into unit sized cells) at every time step based on information gained from its sensors and the location and heading information of its team members. At every time step, each vehicle chooses a path that is q steps ahead of its current position (i.e., q step ahead planning), and cooperates with its team members by considering them as

stochastic elements. The problem in [25] has been extended in [26] to include the following information in the problem formulation: 1) uneven target distributions in the environment; 2) inclusion of an event that a detected target might not be a real target; and 3) inclusion of threats in the environment.

In [27]-[31], the authors have considered a team of heterogeneous UAVs engaged in a search–and-destroy mission over a given region, divided into cells, containing multiple stationary targets but no threats. The locations of some of the targets are suspected *a priori*, while those of others must be discovered through search. The UAVs are drawn from two classes: Target Recognition (TR) UAVs, and Attack (A) UAVs. Each UAV is equipped with sensors and is capable of communicating with the other UAVs. The objective of the UAVs is to cooperatively search the environment, confirm suspected targets, discover and confirm new targets, attack these targets, and confirm their destruction through battle damage assessment. All these tasks must be performed by the UAV team in such a way that the entire environment is searched as rapidly as possible, and all targets are neutralized. In [27], [29], and [30], it has been assumed that before the beginning of the mission and during its progress, all UAVs have instantaneous and noise-free access to a centralized information base. In [27], a search algorithm has been developed for directing the UAVs to search for unknown targets, and an assignment algorithm for assigning UAVs to the known or newly discovered target locations. Simulations have been conducted to show that: (1) Team composition (ratio of TR UAVs to A UAVs) affects the target neutralization time but has relatively no effect on the total mission time; and (2) As the number of unknown targets in the search

environment increases, a *search driven algorithm* (one in which a UAV follows a path of least certainty, i.e., a path along which chances of finding targets is maximum) neutralizes all the targets as well as searches the entire environment faster than the non-search driven algorithm (one in which a UAV chooses its path randomly).

In [28], the authors have extended their results in [27] by decentralizing the information base of the vehicles. In [29] and [30], prediction has been included in the assignment process. The motivation for adding prediction to the assignment process is that it allows UAVs to bid for tasks that may become available in the future, and provides assignments for UAVs that do not have the expertise to perform any currently available tasks. In [31], the following items have been added to the problem in [27]: limited communication range and periodic communication between vehicles, decentralization of the information base of the vehicles, and decentralization of the decision making process.

In [32], two algorithms, namely Best Leader Cooperative Search, and Optimal Best Path Cooperative Search have been proposed for a cooperative search problem involving a team of UAVs engaged in searching an environment with unknown opportunities and hazards. The objective of the team is to maximize its visits to the regions of opportunity, while minimizing visits to the regions of hazard subject to two constraints: (1) the UAVs must always remain within a communication range of one another, and (2) there should be no collisions between UAVs.

In [33], a search-theoretic approach based on the concept of rate of return (ROR) maps has been used to develop cooperative search plans for a team of UAVs searching a given environment, divided into cells, for multiple, stationary, and non-hostile targets. The objective in search theoretic problems is to find the optimal allocation of effort in an environment within a given constraint on effort. The ROR map shows the benefit of searching a cell with a small increment of effort. The ROR in a cell decreases as a cell is searched and may suddenly decrease if a target is found. Two cooperative search strategies and a non-cooperative search strategy have been compared to show the benefits of cooperative search. In the non-cooperative search strategy, i.e., random search, UAVs move in random directions within the cells (rectangular search regions) without using *a priori* information about target locations. One of the cooperative search strategies is the greedy search in which UAVs search the cells with the highest ROR, while the other assigns a UAV to search the cell with the highest ROR that has not been assigned to another searcher.

In [34], a group of UAVs is used to search a predefined ground area, containing multiple stationary and relatively slow mobile targets and decoys. The UAVs must systematically search the given area until a target is found and confirmed. The objective of the team is to minimize the total path length covered by the individual vehicles while exhaustively searching the given area, and performing a second sighting of potential targets. The proposed approach depends on prior definition of search lanes, and takes into account realistic considerations such as wind disturbances, vehicle faults, and existence of decoys, and the resulting delays in the flight plans. However, uneven

probability of target distribution, dynamics in the information about target location, and the role of communication between vehicles have not been addressed.

In search theory literature, most problem formulations consider a cellular environment in which uncertainty about target existence is modeled in a probabilistic manner by assigning an uncertainty value (or probability of target existence) to each cell. The uncertainty value (ranging between 0 and 1) associated with a cell reduces as a function of time spent by the UAV searching the cell. Each vehicle carries a probability map, which contains the probability of target existence (uncertainty value) associated with each cell. It is assumed that the uncertainty value associated with each cell is precisely known at the beginning of the search mission. The UAVs are then tasked to search the cells with the highest probability of target existence. However, the authors in [35] argue that the probabilities of target existence associated with each cell are often determined as a result of prior intelligence gathering missions, and are most likely not exactly known due to poor intelligence or noisy sensors. Hence, they have proposed a new framework for search operations that takes into account the uncertainty in information about target existence. The proposed approach uses the Beta distribution to model the uncertainty in the prior probability of target existence in each cell, and generates search actions that are robust to this uncertainty. Use of the Beta distribution allows one to analytically predict the number of observations needed by a UAV in a particular cell to determine above a specific threshold of confidence whether a target does or does not exist in the given cell. In [36], the authors have extended their

framework in [35], which accounted for uncertainty in probability of existence for stationary targets to include dynamic targets.

In [37], the authors have considered two UAVs engaged in a search and destroy mission over a given search space, which contains randomly distributed targets, and a number of non-targets, which are either decoys used to deceive the UAV sensors, or are civilian structures whose radar signature may be confused with that of a real target. Two engagement strategies, namely cooperative and non-cooperative search and attack have been compared to quantify the benefits of cooperation. In the cooperative strategy, the two UAVs divide the search area, and independently search for targets until a potential target is discovered. Once a target is discovered, and identified as a real target (and not a decoy), the discovering UAV informs the other UAV of its decision to attack, and subsequently attacks the target. The role of the second UAV is to travel to the location of the discovered target and perform battle damage assessment. If the target was not destroyed by the first UAV, the second UAV will attack. However, if the target has been destroyed, the second UAV will travel back to its search region to continue with its search. The simulations results show that the advantages of cooperation are dependent upon the target density, the kill probability of an individual attack, and the probability of correct identification of a target.

To summarize, references [19]-[26], and [32]-[37] address the *Multiple UAV Search* problem, wherein cooperative and non-cooperative search strategies are developed. References [19]-[24] assume that a team of UAVs is involved in both a

search and surveillance mission. Whereas, references [27]-[31], and [37] address the *Cooperative Search and Destroy* problem by developing algorithms for both the *Multiple UAV Search* and task allocation problems.

The *Multiple UAV Surveillance* problem is addressed by references [3], and [38]-[41]. According to the authors in [41], surveillance is different than search, wherein the goal is to locate targets present in the search environment. However, for a surveillance mission, the location of the target (or targets) is already known to the UAVs, and the goal of each UAV in the team is to use its resources (camera, sensor) to closely observe the given target (a geographical region for border patrol, a region of specified radius in open-ocean for maritime surveillance, the perimeter of a wildfire, etc.). According to the authors in [3], numerous applications require aerial surveillance. Civilian applications include monitoring forest fires, oil fields, pipelines, oil spills, and tracking wildlife, whereas military and homeland security applications include border patrol, maritime surveillance, monitoring the perimeter of nuclear power plants, and mobile combatant surveillance.

The authors in [3] have presented an overview of a cooperative control strategy for a team of UAVs performing two different aerial surveillance missions. In the first mission, a team of UAVs equipped with imaging sensors is tasked to persistently image a known target. The second mission is cooperative identification, where each UAV in the team is required to fly along different approach angles over a target simultaneously. The cooperative control strategy involves four phases, which are the definition of a

cooperation objective and cooperation constraints, the definition of coordination variable and coordination functions, and the development of a centralized cooperation strategy, which is transformed into a decentralized strategy using consensus schemes.

In [38], [39], and [40], perimeter surveillance algorithms have been developed for a team of multiple, low-altitude, short endurance (LASE) UAVs, which are tasked to cooperatively monitor and track the propagation of a forest fire. By definition, perimeter surveillance is the process of gathering data at all points of the perimeter and transmitting it to a base station for analysis. The objective of the team is to cooperatively gather information about the state of the perimeter (i.e., to capture images along the perimeter of the fire and then share them with one another), and to upload the location of the changing fire perimeter with associated imagery to a base station as frequently and with as little delay as possible. Hence, the two performance metrics that are used to measure the performance of the proposed centralized and decentralized monitoring algorithms are: (1) the information update frequency at the base station, and (2) the maximum time delay required to transmit information to the base station.

Each vehicle is equipped with an infrared camera and is subjected to a limited communication and flight range (due to limited fuel), and a turning constraint. A path planning algorithm and a centralized cooperation scheme has been developed in [38], which is extended in [39] to include a decentralized cooperative monitoring scheme, and a real-time tracking algorithm that allows a UAV to track the perimeter of a fire using an onboard infrared sensor. The decentralized perimeter surveillance algorithm is solved

using the notion of coordination variables, wherein agents must share the minimum amount of information in order to cooperate. Information shared among agents is the perimeter length, and the number of agents forming the team. The advantages of the decentralized approach, initially proposed in [40], include the ability to monitor a changing fire perimeter, the ability to systematically add and remove UAVs from the team, and the ability to supply time-critical information to forest fire fighters.

2.3 Fault Detection and Isolation of Sensor and Actuator Failures in UAVs

A fault is defined as an unexpected change that leads to the corruption of the overall performance of the system [48]. In any system, the occurrence of a fault will negatively affect the performance of the system and cause it to deviate from the norm. However, for critical and complex autonomous systems such as UAVs, the severity of faults in its subsystems, such as sensors, actuators, communication systems, and the guidance system can have drastic consequences. Hence, it is imperative that if a fault occurs in any of the subsystems of a UAV, it should be detected, and isolated in a timely manner, and algorithms should be designed that allow the vehicle to (partially) recover from these faults.

In the *Coordinated Rendezvous* and *Multiple UAV Search and Surveillance* literature the effect of faults in the critical subsystems on the performance of a UAV has been largely ignored. In these areas, the main focus has been on the development of

efficient algorithms that allow a single vehicle or team of vehicles to effectively carry out the requirements of the given mission. However, this does not mean that fault detection and isolation techniques have not been investigated for UAVs. A brief description of a small sample of the papers addressing fault detection and isolation of sensor and actuator failures in UAVs is given below.

In [45], an Integrated Retrofit Reconfigurable Flight Controller has been developed and implemented to compensate for control effector damage. The adaptive control system is capable of detecting and identifying flight-critical actuator failures and control effector damage, and is able to reject the state-dependent disturbances that arise due to the asymmetry of the damaged vehicle. The types of actuator faults that have been presented are: (1) Lock-In-Place (LIP) Failure; (2) Hard-Over Failure (HOF); (3) Float Type of Failure; and (4) Loss of Effectiveness (LOE).

In [46], a sensor fault detection and diagnosis system has been developed for, and tested on an autonomous helicopter. The authors have utilized a model based Fault Detection and Identification (FDI) approach and have used Luenberger observers for observer-based residual generation. In the model-based FDI approach, all the information on the system can be used to monitor the behavior of the plant, including the knowledge about its dynamics [46]. The five different types of sensor failures that have been modeled are: (1) Total sensor failure; (2) Stuck with constant bias sensor failure; (3) Drift or additive-type sensor failure; (4) Multiplicative-type sensor failure; and (5) Outlier data sensor failure.

Total sensor failure is a catastrophic failure, in which at a given point in time, the sensor stops functioning. The output of the sensor is then a constant zero. This failure can be caused by electrical or communication problems. In (stuck with constant bias sensor failure), the sensor gets stuck with a constant bias, and the output (thereafter) remains constant [46]. Drift or additive-type sensor failure is a very common failure in analog sensors [46]. It is caused by internal temperature changes or calibration problems. The sensor output has an added constant term (the drift) [46]. A scaling error in the sensor output is responsible for the multiplicative-type sensor failure. In this failure type, a multiplicative factor is applied to the sensor nominal value [46]. Outlier data sensor failure occurs in GPS sensors. It is a temporal failure. The GPS sensor outputs a single point with a large error. However, the measurements following this error are correct. Possible causes of the error are failures in the GPS internal signal processing algorithms, and temporary satellite signal blocking.

The authors in [47] have developed an approach based on the Interacting Multiple Model (IMM) Kalman Filter for sensor and actuator failure detection and identification (FDI) and fault tolerant control (FTC). The FDI-FTC approach has been tested on a linear simulation of Bell Helicopter's Eagle-Eye UAV. Simulation results show that the proposed approach is able to: (1) rapidly and reliably detect and identify all single and multiple (simultaneous) sensor failures; (2) detect and identify all single actuator failures; and (3) to detect, identify and control the UAV under combined, simultaneous actuator and sensor failures [47].

2.4 Conclusion

In this Chapter, we have presented the Coordinated Rendezvous and Multiple UAV Search and Surveillance problems in detail. Coordinated Rendezvous is a type of *Cooperative Timing* problem that requires multiple UAVs to arrive simultaneously at their destination(s) to maximize the element of surprise. The main objective of research into the *Multiple UAV Search* problem is to develop and evaluate strategies for a team of UAVs searching an environment of known dimensions for (stationary and/or mobile) targets under varying operating conditions and constraints. The *Multiple UAV Surveillance* problem is different than the *Multiple UAV Search* problem, wherein the goal is to locate targets present in the search environment. However, for a surveillance mission, the location of the target(s) is already known to the UAVs, and the goal of each UAV in the team is to use its resources (camera, sensor) to closely observe the given target (a geographical region for border patrol, a region of specified radius in open-ocean for maritime surveillance, the perimeter of a wildfire, etc.).

The focus of this thesis is on determining: (1) the effect of the actuator fault on the coordination algorithm in the Coordinated Rendezvous/Strike mission; and (2) the effect of actuator and sensor faults on the performance of UAV team performing the Multiple UAV Surveillance mission. While fault detection and isolation of sensor and actuator faults or failures is not the subject of this thesis, for sake of completeness, we have included some literature on this subject matter as well.

Chapter 3

Coordinated Rendezvous Mission

3.1 Background Information

Coordinated Rendezvous is a type of cooperative timing problem, in which multiple vehicles must jointly reach a single destination or multiple destinations while minimizing their combined exposure to threats in the environment of operation and conserving fuel.

In [4] and [5], the authors have addressed the coordinated rendezvous problem involving a team of UAVs, which must simultaneously arrive on the boundary of the radar detection region of multiple targets, while avoiding multiple threats. The approach has been illustrated through a case study involving 5 UAVs, 6 targets, and 36 threats. The locations of the targets are known before the start of the mission. The threats in the environment are of two types: known and pop-up. The locations of known threats are known by the UAVs at the start of the mission whereas the locations of pop-up threats become apparent only when they come within a vehicle's sensor range. It is assumed that individual UAVs fly at different, pre-assigned altitudes, thereby ensuring collision avoidance. Moreover, multiple UAVs can be assigned to a single target, while some targets can be unassigned. The mission objective (for the UAVs) is to visit all the targets, while minimizing the risk to each individual UAV [5]. To reduce risk to the UAVs, the

distance between the UAVs and the threats should be maximized, and the targets should be simultaneously engaged by multiple UAVs in order to increase the element of surprise.

To address the coordinated rendezvous problem, the authors in [4] and [5] have proposed the system architecture shown in Figure 3.1.

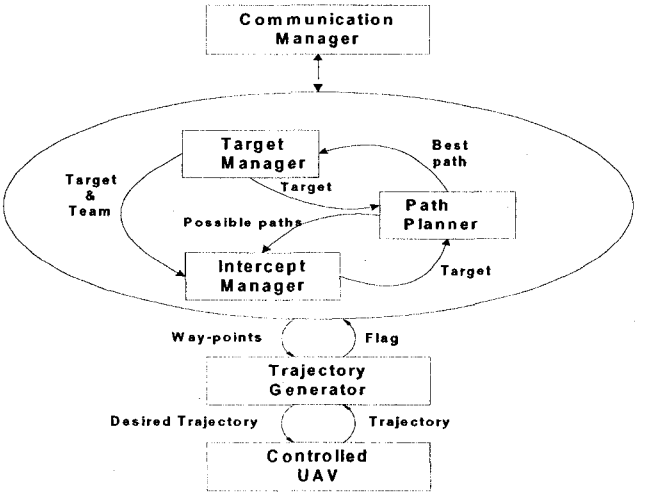

Figure 3.1: System architecture for a single UAV [4], [5].

The four main functional blocks of the system architecture are the *Path Planner*, *Target Manager*, *Intercept Manager* and the *Trajectory generator*, which solve the problems of UAV Path Planning, Multi-Vehicle Task Allocation, Coordinated UAV Intercept, and Trajectory Generation. Each vehicle implements each of these functional blocks separately. The decisions reached by these functional blocks have to be synchronized among the different UAVs [5]. Synchronization of information is carried out by the *Communication Manager*.

The *Path Planner* is responsible for generating a set of feasible candidate paths between the UAV and each target. The paths are generated from each vehicle's current (initial) position to the location of each target. The development of paths involves two stages. In the first stage, a threat based Voronoi diagram is created to generate possible paths from each UAV's initial position to the location of each target. Each edge of the Voronoi diagram is assigned two costs: the threat cost and the length cost (or the fuel cost).

While traveling along the i^{th} edge, the threat cost incurred by a UAV is based on its exposure to radar sites located at all the threats present in the environment. It has been assumed that the radar signature of a UAV is uniform in all directions and is inversely proportional to the distance from the UAV to the threat to the fourth power, that is $1/d^4$. The threat cost associated with the i^{th} edge is calculated at three points along the edge, and is given by:

$$J_{threat,i} = \frac{\alpha L_i}{3} \sum_{j=1}^{N} \left(\frac{1}{d_{1/6,i,j}^4} + \frac{1}{d_{1/2,i,j}^4} + \frac{1}{d_{5/6,i,j}^4} \right) \tag{3.1}$$

where

- N: the total number of threats
- $d_{1/2,i,j}^4$: the distance from the ½ point on the i^{th} edge to the j^{th} threat
- α: the constant scale factor
- L_i : the length of edge i

The length cost associated with the i^{th} edge is given by:

$$J_{lenght,i} = L_i \tag{3.2}$$

The total cost incurred by a UAV for traveling along the i^{th} edge of the Voronoi diagram is a weighted sum of the threat cost and the length cost associated with the given edge, and is given by the equation:

$$J_i = \kappa J_{length,i} + (1-\kappa) J_{threat,i} \tag{3.3}$$

where

$0< \kappa <1$: weighting factor that allows weight to be placed on either exposure to threats or path length

Once the total cost associated with each edge is determined, the second stage involves searching the Voronoi diagram to find the set of **k** lowest cost candidate paths between the initial location of each UAV and the location of each target. A variation of Eppstein's k-best paths algorithm has been used to search the Voronoi diagram. A shortest path algorithm is used to produce a shortest path such that a performance objective (cost) is minimized. A k-shortest paths algorithm produces a list of k paths, with monotonically increasing costs, starting from the shortest path.

Each vehicle's *Target Manager* selects a set of potential targets for the vehicle, which is then communicated (through the communication manager) to all the other

vehicles to select a team assignment. The *Target Manager* assigns a UAV to a target such that the following constraints are satisfied: 1) Each target should have (if possible) multiple UAVs assigned to it; 2) The overall team cost (sum of the individual UAV costs) should be minimized; and 3) The number of targets destroyed should be maximized. While assigning targets to UAVs, the *Target Manager* takes into account four competing objectives, which are: The group path length to the target should be minimized (*ShortPath*); The group threat exposure should be minimized (*AvoidThreats*); To maximize survivability, the number of vehicles engaging each target should be maximized (*MaxForce*); and The number of targets visited should be maximized (*MaxSpread*). The *ShortPath* and *AvoidThreats* objectives are used by the target manger to determine target assignments for individual vehicles whereas the *MaxForce* and *MaxSpread* objectives are used to determine target assignments for teams of vehicles. The target assignment problem has been solved using the satisficing and social welfare paradigms [44].

Once the teams have been formed and assigned to their respective targets, the task of the *Intercept Manager* is to ensure that individual vehicles comprising a team arrive on the radar detection boundary of their assigned target simultaneously. Coordinated intercept is achieved by selection of the coordination variable, which is the minimal amount of information needed by the vehicles to achieve the task of simultaneous intercept. The team-optimal *time over target* (TOT*) has been chosen as the coordination variable. As shown in Figure 3.2, the Cooperative Path Manager selects the TOT* value for the team. Each vehicle implements an identical copy of the

Cooperative Path Manager algorithm. The process of selecting the TOT* value is shown in Figure 3.2 and is described briefly as follows.

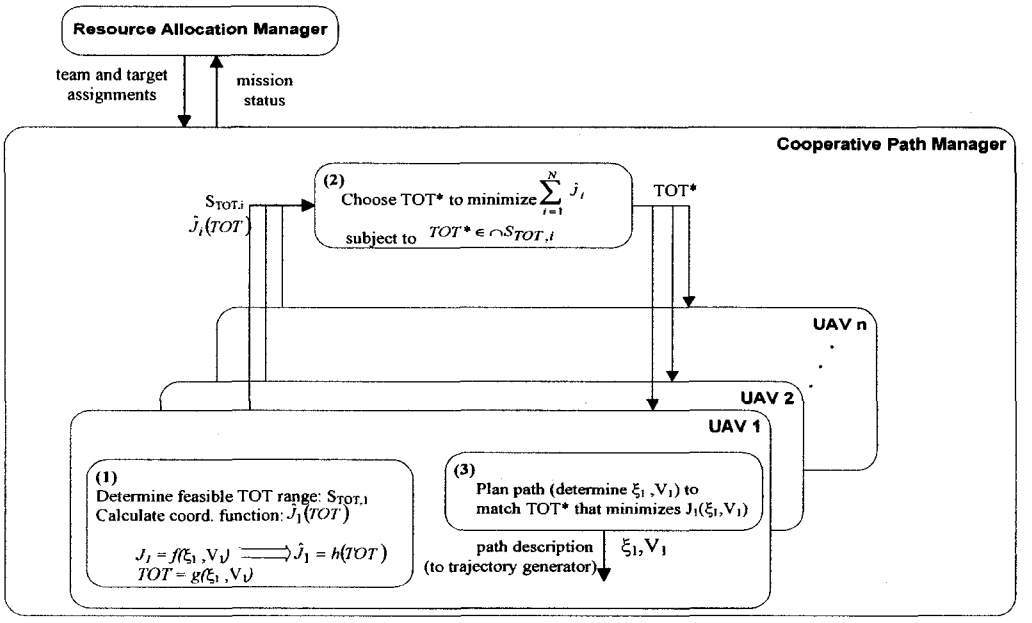

Figure 3.2: Cooperative path planning algorithm [4], [5].

At first, the *Intercept Manager* of each vehicle calculates a set of feasible time over target ($S_{TOT,i}$) ranges, and the coordination function, $\hat{J}_i(TOT)$. The $S_{TOT,i}$ for each UAV are based on the feasible candidate paths for that UAV found from a search of the Voronoi diagram, and the feasible range of its velocity. Each vehicle's coordination function, $\hat{J}_i(TOT_i)$ is determined from the following relations:

$\mathbf{TOT_i = f(\xi_i , V_i)}$ is the time over target for the i^{th} UAV

where

ξ_i: the waypoint path followed by the i^{th} UAV to reach the target,

V_i: the forward speed of the i^{th} UAV.

$\mathbf{J_i = g(\xi_i , V_i)}$ is the total cost (threat and fuel) incurred by the i^{th} UAV to travel along the waypoint path ξ_i at a speed V_i.

For a given vehicle, $\hat{J}_i(TOT_i)$ parameterizes the total cost incurred by the vehicle ($\mathbf{J_i = g(\xi_i , V_i)}$) versus the vehicle's time over target ($\mathbf{TOT_i = f(\xi_i , V_i)}$), and is given by:

$$\hat{J}_i(TOT_i) = J_i(\xi_i , V_i) \tag{3.4}$$

For a specific waypoint path, ξ_i and forward speed, V_i, the time over the target for the i^{th} vehicle, TOT_i takes on a unique value (and is equal to the length of the waypoint path divided by the forward speed of the vehicle). For achieving a given TOT_i, a vehicle incurs a combined fuel (or length) and threat cost, given by $J_i = g(\xi_i , V_i)$, which has been defined in Equation (3.3). Hence, the coordination function of the i^{th} vehicle models the cost to the vehicle for achieving a particular time over target (TOT_i).

Each vehicle then sends its coordination function and time over target ranges to the other vehicles forming the team through its *Communication Manager*. Based upon its own coordination functions and time over target ranges and those received from its team members, each vehicle's Cooperative Path Manager selects the TOT* value (the team-optimal time over target) such that the following conditions are satisfied: 1) the

chosen TOT* value is common to all UAVs, and 2) the collective threat exposure of the team (i.e., the sum of the coordination functions of the individual vehicles forming the team) is minimized. The chosen TOT* is given by:

$$\text{TOT}^* = \arg\min \sum_{i=1}^{N} \hat{J}_i \tag{3.5}$$

subject to

$$\text{TOT}^* \in \cap S_{\text{TOT},i}$$

It is assumed that the information shared across the team is synchronized and hence, the TOT* value calculated by all vehicles forming a team is identical. Once the TOT* value is calculated, the *Intercept Manager* of each vehicle generates a velocity and a set of waypoints for the vehicle to follow to reach its target. These set of waypoints and velocity are then passed to the *Trajectory Generator*.

Each vehicle's *Trajectory Generator* is then responsible for planning a threat-avoiding trajectory to the target while satisfying the TOT* value, and the constraints on the vehicle's velocity and maximum turning radius. The Trajectory Generator is calculated using the following differential equations (kinematics):

$$\begin{aligned} \dot{X}_i^d &= V_i^d \cos\psi_i^d \\ \dot{Y}_i^d &= V_i^d \sin\psi_i^d \\ \dot{\psi}_i^d &= u_1 \\ \dot{V}_i^d &= u_2 \\ \dot{h}_i^d &= 0 \end{aligned} \tag{3.6}$$

where:

(X_i^d, Y_i^d) : desired inertial position of the i^{th} UAV

ψ_i^d : desired heading of the i^{th} UAV

V_i^d : desired velocity of the i^{th} UAV

h_i^d : desired altitude of the i^{th} UAV

u_1, u_2 : input signals that are constrained by the heading rate constraint and the acceleration constraint

For the coordinated rendezvous strategy proposed in [4] and [5], teams are created and assigned to targets before the beginning of the mission. Moreover, the initial TOT* value is also selected before the beginning of the mission by the Cooperative Path Manager (residing on each UAV) based on the location of the targets (all are known), and the known threats. All vehicles in a team then follow paths that allow them to arrive simultaneously at their respective target at the time TOT*. When a UAV encounters a pop-up threat, its Target Manger, Intercept Manager, and Path Planner have to be reinstantiated with the new threats list (containing the previously known threats and the new pop-up threat(s)). Hence, a new TOT* is generated for the team and each vehicle re-plans its path to the target such that the new TOT* value is satisfied and the team cost is minimized.

In [6] and [7], the authors have shown that their cooperative control strategy developed in [4] and [5], based on the principle of coordination variable and

coordination functions can be applied to cooperative control problems other than coordinated rendezvous. To this end, they have applied their cooperative control strategy to three cooperative timing problems: *Simultaneous Arrival (Coordinated Rendezvous)*, *Tight Sequencing*, and *Loose Sequencing*. To illustrate their approach to these problems, the authors have considered a team of 3 UAVs, which must travel through a 5 sq-km battle area, populated with one target and 33 threats (radars). For each cooperative timing problem, the objective is to coordinate the arrival of the team of UAVs at the target such that the team's exposure to threats is minimized and a given timing constraint (different for each cooperative timing mission) is satisfied. Individual vehicles must also satisfy velocity and heading rate constraints.

The *Simultaneous Arrival* problem constrains N vehicles to arrive at their destinations (single or multiple) simultaneously. The coordination variable is the time of arrival of the team at the target(s), and the coordination function of each vehicle describes the range of total cost incurred by the vehicle for achieving a given range of arrival times. The simultaneous arrival constraint is given by:

$$T_1 = T_2 = ... = T_N = T_S$$

where

T_S : the coordination variable

$T_i = L(W_i)/v_i$: the time of arrival of the i^{th} vehicle

where:

$L(W_i)$: the length of the waypoint path, W_i

v_i : velocity of the ith UAV

The *Tight Sequencing* problem requires that all vehicles on the team should arrive at their target(s) in a specified sequence, and enforces specified intervals between the arrival times of the vehicles composing the team. Hence, the tight-sequencing constraint for a team of N vehicles is given by:

$$T_1 = T_S$$

$$T_i = T_S + \Delta_i, \qquad i = 2,...,N$$

where

Δ_i : the time interval between the arrival of the first and the ith vehicles

T_S : the coordination variable, and is the time of arrival of the first vehicle at its target

The *Loose Sequencing* problem requires all vehicles on the team to arrive at their target(s) in a specified sequence, with the time intervals between arrival times of individual vehicles given as acceptable ranges. The loose sequencing constraint for a team of N vehicles is given by:

$$T_S \le T_1 \le T_S + \tau_1$$

$$T_S + \Delta_i \le T_i \le T_S + \Delta_i + \tau_i, \qquad i = 2,...,N$$

where

Δ_i : the interval between the opening of the first time window and the opening of the ith time window

τ_i : the duration of the i^{th} time window

T_S : the coordination variable, and is the time of arrival of the first vehicle at its target

The team of three vehicles flies three different missions: simultaneous arrival, tight sequencing, and loose sequencing. The environment of operation remains the same for all three missions. For each timing mission, the coordination function for each vehicle describes the range of total cost incurred by the vehicle for achieving a given range arrival times. The coordination variable for the simultaneous arrival mission is the arrival time of the entire team at the target, whereas for the tight sequencing and loose sequencing missions, the time of arrival of the first vehicle at the target is chosen as the coordination variable.

To address the cooperative timing problems, the authors in [7] have proposed a distributed cooperative control architecture, as shown in Figure 3.3.

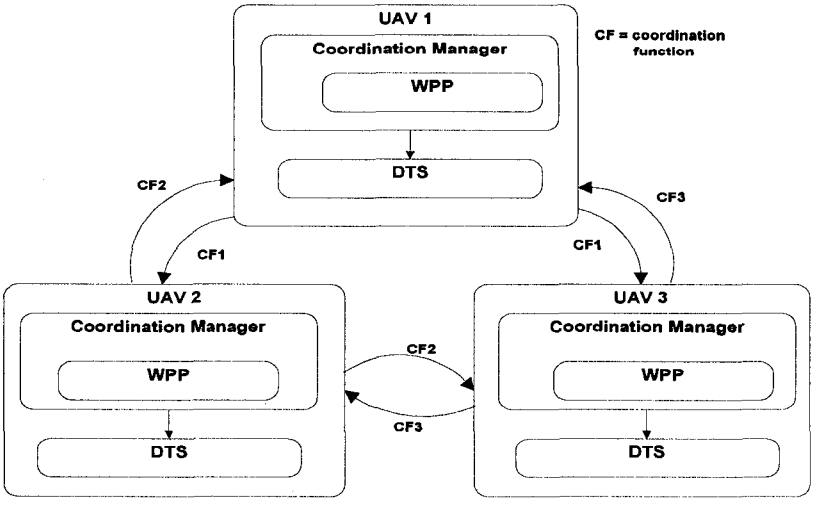

Figure 3.3: Cooperative control architecture for team of UAVs [7], where WPP denotes the Waypoint Path Planner, DTS denotes the Dynamic Trajectory Smoother, and CF_i denotes the Coordination Function of the i^{th} vehicle.

According to this architecture, the coordination variable is selected based on a consensus among the individual vehicles. The architecture of the individual vehicles is illustrated by Figure 3.4, and includes a Coordination Manager (CM), a Waypoint Path Planner (WPP), and a Dynamic Trajectory Smoother (DTS). Each vehicle implements each of these functional blocks separately.

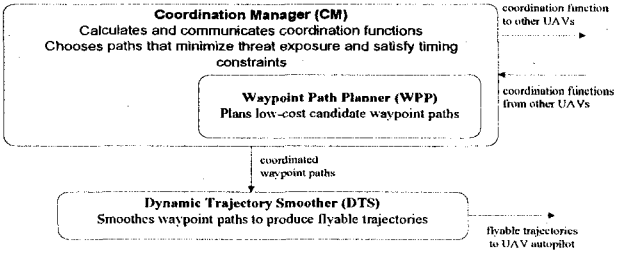

Figure 3.4: Trajectory-planning architecture [6], [7].

As in [4] and [5], the Coordination Manager implemented on each UAV is identical. As shown in Figure 3.4, the Coordination Manager of a vehicle computes the coordination function, sends it to the other vehicles in the team, receives the coordination functions from the other vehicles in the team and then subsequently chooses the team-optimal coordination variable. Since all the vehicles are aware of each other's coordination functions, it is assumed that the Coordination Manager of each vehicle computes the same team-optimal coordination variable.

Figure 3.5 shows the time of arrival of the individual vehicles at the target for the three different cooperative timing missions. For each of the missions, the x-axis denotes the arrival time and the y-axis denotes the total cost incurred by the individual vehicle for achieving a given arrival time. Each line segment represents the total cost incurred by a given vehicle for achieving a given arrival time while traveling along a specific waypoint path, W_i at a velocity, v_i . Hence, the line segments for an individual UAV represent the vehicle's coordination function. From Figure 3.5, we can see that each line segment is monotonically increasing. This is because the authors in [7] have set up the environment in a manner (i.e., chosen the position of the threats, the target, the UAVs, and the value of the weighting factor κ) that ensures the individual vehicle cost for a given waypoint path is minimum at the earliest possible arrival time (which is also associated with the maximum possible velocity at which the vehicle can fly along the given waypoint path).

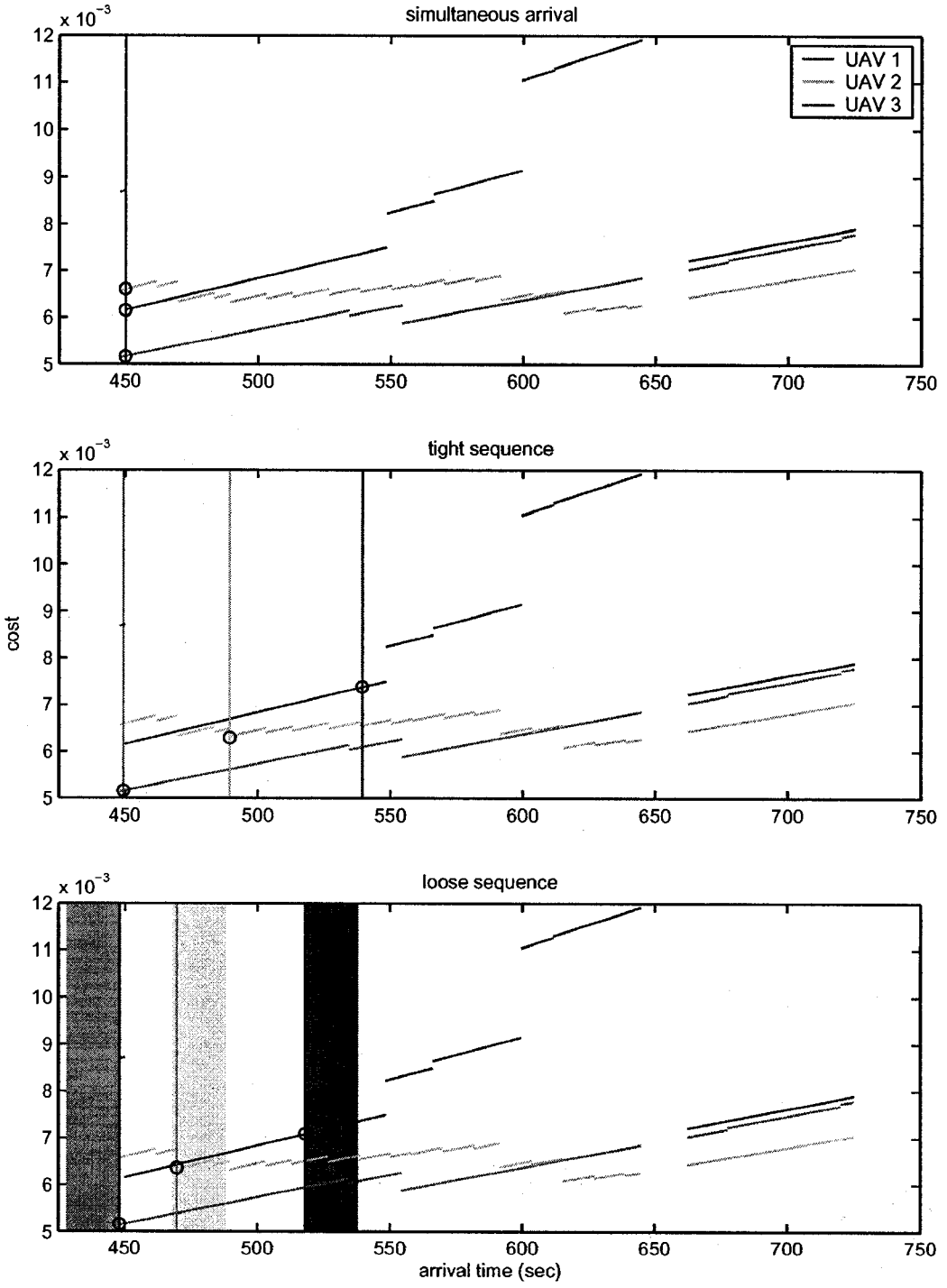

Figure 3.5: Coordination Functions for the three cooperative timing missions [7].

For all three missions, the process of obtaining the arrival time of the individual members of the team is different. For the simultaneous arrival mission, the best coordination variable for the team (i.e., arrival time for all members in the team) is chosen such that the collective threat exposure of the team is minimized. In Figure 3.5, the arrival time for all the team members engaged in the simultaneous arrival mission is 450 seconds. This arrival time is chosen such that the sum of the total costs of the individual vehicles (note that the value of each vehicle's cost is represented by a circle) is minimized. It should be noted that the minimum value of an individual vehicle's total cost does not necessarily correlate with the team's arrival time. Hence, the chosen arrival time is best from a team's perspective, and not necessarily ideal from an individual vehicle's perspective.

For the tight sequencing mission, the coordination variable, i.e., the time of arrival of the first vehicle (UAV1) at the target is chosen such that the total cost incurred by the vehicle to reach the target is minimized. In the middle plot of Figure 3.5, the desired arrival time of UAV1 at the target is 450 seconds. This arrival time corresponds to the minimum possible value of the total cost incurred by UAV1. Earlier, we stated that the tight-sequencing problem enforces specified intervals between the arrival times of the team members. For the tight-sequencing mission in Figure 3.5, there is a 40-sec interval between the arrival times of UAV1 and UAV2, and a 50-sec interval between the arrival times of UAV2 and UAV3. Hence, in the tight-sequencing plot, the second vertical line represents the arrival time of UAV2 at the target (490 seconds) and the third vertical line represents the arrival time of UAV3 at the target (540 seconds).

For the loose sequencing mission, each vehicle has a desired arrival-time window within which it should arrive at the target. In the loose-sequencing plot in Figure 3.5, the shaded regions represent the desired arrival-time (at the target) windows of the individual vehicles. The arrival-time windows of UAV1 and UAV2 are 20 seconds wide, whereas the arrival-time window of UAV3 is 30 seconds wide. Given these arrival-time windows, the coordination variable, i.e., the time of arrival of the first vehicle (UAV1) at the target is chosen to be the upper limit of its time window. Hence, the arrival time of UAV1 is selected to be approximately 450 seconds. If there are several paths that the first vehicle can follow to achieve the team-optimal arrival time, it selects the path at which it incurs the minimum cost. The arrival time of every other vehicle in the team is chosen from within its desired arrival-time window, and is associated with the minimum cost (combined fuel cost and threat cost) incurred by the vehicle.

Once the team coordination variable has been generated, each vehicle's Coordination Manager uses the Waypoint Path Planner to generate a velocity and a set of waypoints for the vehicle to follow. This set of waypoints is then passed to the Dynamic Trajectory Smoother, which produces a flyable trajectory, subject to the dynamic constraints of the vehicle.

The authors in [8] and [9] have focused on the implementation of the rendezvous manager. In [8], the rendezvous manager is implemented as a state chart. As shown in Figure 3.6, the rendezvous manager plans the UAV team mission in four phases.

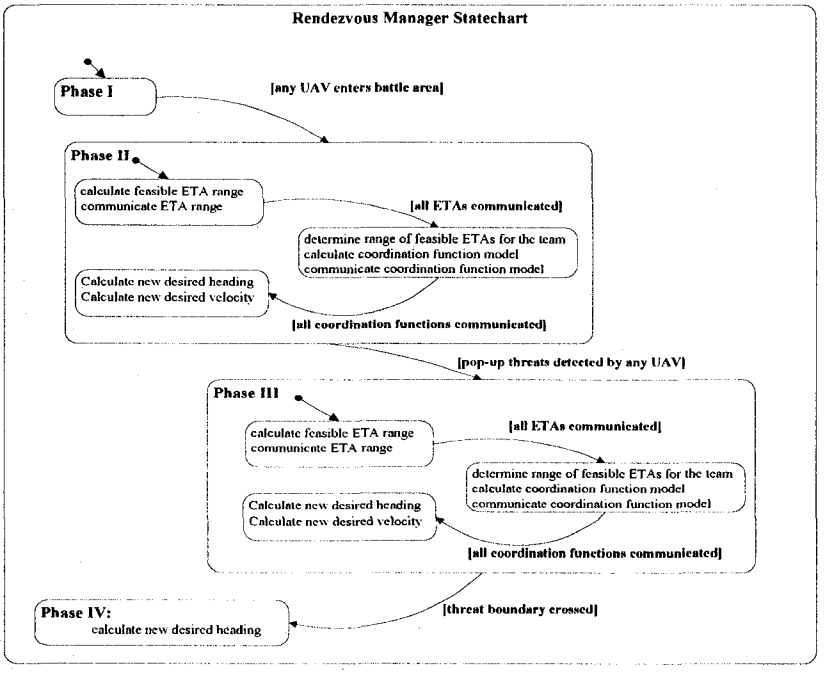

Figure 3.6: Rendezvous manager statechart [8].

The goal of the mission is for a team of three UAVs to simultaneously arrive at a single known target while maximizing the survivability of the team, which is a sum of the individual vehicle costs. Each vehicle's cost is a sum of its fuel cost, J_f, and its threat cost, J_t, which are given by the following equations:

$$J_f = C_f v(l_l + l_h) \tag{3.7}$$

$$J_t = C_l\left(\frac{l_l}{v}\right) + C_h\left(\frac{l_h}{v}\right) \tag{3.8}$$

where

v : velocity of the UAV

l_l : path length in the low-threat region

l_h: path length in the high threat region

C_f, C_l, and C_h: weighting factors

In the first phase of the mission, the UAVs are en route to the battle area, which is divided into high threat and low threat regions by a threat boundary along which threats can pop-up. Once the UAVs enter the battle area, phase II begins. In this phase, assuming no pop-up threats along the boundary, the rendezvous manger of each vehicle follows the cooperative control strategy explained in [4] and [5] to select a team-optimal ETA (coordination variable) such that the team's combined threat exposure is minimized and fuel is conserved. Next, the Rendezvous Manager of each UAV plans a trajectory to the target that avoids the known threats, and ensures that the team-optimal ETA is matched and the vehicle's constraints on velocity, heading rate and fuel are satisfied. The UAVs travel along these trajectories until a pop-up threat is detected, which leads to the third phase of the mission. In the third phase, individual vehicles have to recalculate their coordination functions, and ETA ranges, which are then used by each vehicle's Rendezvous Manager to determine a new team-optimal ETA. Subsequently, each vehicle plans a new trajectory (to the target) that avoids the pop-up threat(s), satisfies the team-optimal ETA, and does not violate its dynamic constraints. Thus, whenever a new pop-up threat is encountered, a new coordination variable has to be determined and all the vehicles have to re-plan their trajectories. Once the threat boundary is crossed, phase IV begins. In this final phase, the UAVs re-calculate their desired heading to the target while ensuring simultaneous intercept.

In [9], the rendezvous manager is modeled as a state machine, and runs concurrently on each UAV participating in the rendezvous mission. The mission objective is for three UAVs to arrive at their individually assigned targets simultaneously while satisfying two competing constraints. The first constraint requires the vehicles to have sufficient fuel to be able to return to base while the second requires the vehicles to minimize their exposure to both known and pop-up threats en route to their targets.

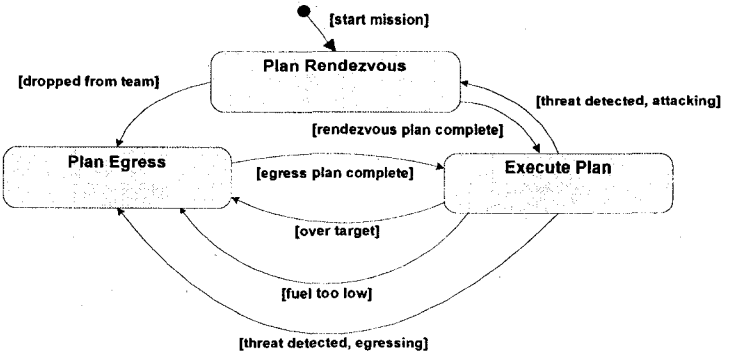

Figure 3.7: Rendezvous manager state machine [9].

As shown in Figure 3.7, there are three states in the Rendezvous Manager state machine. At the beginning of the mission, the Rendezvous Manager of each vehicle is in the Plan Rendezvous state. In this state, using the locations of the targets and the known threats, the Path Planner of each vehicle (comprising the team) determines multiple candidate paths for the UAV through the threats to its target. The Rendezvous Manager of each vehicle then determines the coordination function and range of arrival times for the vehicle, and sends this information through the Communication Manager (shown in Figure 3.1) to all the vehicles in the team. Then, using the coordination functions and

range of arrival times of all team members, each Rendezvous Manager calculates feasible team ETA ranges. Next, the Rendezvous Manager of each vehicle selects the same optimal team ETA, which ensures the minimization of the collective threat exposure of the team while ensuring that the UAVs would have sufficient fuel to return to base. Finally, the Rendezvous Manager selects the best paths for the individual UAVs to achieve the team ETA.

Within the Plan Rendezvous state, interactions between a Resource Allocation Manager (shown in Figure 3.2) and the Rendezvous Manager of each vehicle are also modeled. The Resource Allocation Manager is called whenever there is a change in the threat scenario, i.e., when a UAV encounters a pop-up threat. At this point, including the position of the pop-up threat in the threats list, the Rendezvous Manager of each vehicle computes the minimum team cost for all possible team compositions (one UAV, two UAVs, three UAVs, and so on), and communicates this information to the Resource Allocation Manager, which determines the optimal composition of the UAV team suitable for performing the given mission based on the threat risk threshold for the specified mission.

Once the team ETA is determined, and individual vehicle paths to their respective targets are determined, the Rendezvous Manager state machine transitions from the Plan Rendezvous state to the Execute Plan state. In the Execute Plan state, the Rendezvous Manager generates heading and velocity commands for the UAV to follow along the waypoint path determined in the Plan Rendezvous state. If a UAV reaches its

target as planned, a transition to the Plan Egress state takes place. In the Execute Plan state, a radar function is implemented, which scans the battle area for pop-up threats. If a pop-up threat is detected, the Rendezvous Manager will either transition to the Plan Egress state or the Plan Rendezvous state. A transition to the Plan Egress state takes place if the risk threshold of the UAV is low, and the Resource Allocation Manager determines that it should be dropped from the team. On the other hand, if the risk threshold of the UAV is high, and it is not dropped from the team, a transition to the Plan Rendezvous state takes place, where calculations for rendezvous are carried out. In the Execute Plan state, the fuel level of a UAV is monitored, and its range to the assigned target is calculated. If the UAV is low on fuel, it drops out of the mission, and a transition to the Plan Egress state takes place, where the vehicle plans its path to its home base.

In the Plan Egress state, a path to an egress point is calculated. The egress point can be the home base if a UAV is running low on fuel, or if it is dropped from the team by the Resource Allocation Manager, or another pre-planned location where a UAV would join its other team members upon the successful completion of its mission.

3.2 Problem Formulation

The mission scenario developed in this thesis encompasses both the rendezvous and surveillance problems. A team of three UAVs starting from geographically separate locations (airbases) is tasked to arrive simultaneously at a pre-determined high-valued target location in order to carry out a successful attack. While traveling to the target, the team must pass through an enemy stronghold containing multiple radar sites whose positions are known due to a previous ISR (Intelligence, Surveillance, and Reconnaissance) mission. It is assumed that the radars are of equal power and are not able to communicate with one another. During this phase of the mission, the UAVs must pass through the region while minimizing their exposure to the radar sites and conserving fuel. It is assumed that none of the UAVs is lost during the joint strike mission. Upon successful completion of the mission, the UAVs are tasked to arrive on a militarized border between two countries. Upon arrival at the border, the team's mission is to conduct a surveillance mission in a specified 'rectangular' region.

Each UAV is assumed to be equipped with a sensor with which it collects data and information about the environment it is currently traveling through. Moreover, each UAV is assumed to have wireless communication capabilities. The vehicles are also assumed to be able to avoid collisions with one another by flying at different, pre-assigned altitudes. The dynamics of the vehicles have been ignored since we have chosen to generate straight-line waypoint paths from UAV positions to the target instead of generating trajectories. The generation of trajectories would have required us to

satisfy dynamic constraints, i.e., constraints on an individual vehicle's velocity as well as its turning rate. Moreover, our goal is not to model the system, but rather to test the robustness of the coordination (or cooperative control) algorithm.

We have used the Rendezvous Strategy developed by Chandler et al ([8], [9], [10], and [15]) and Beard et al ([4], [5], [6], [7], and [16]), and extended it to include an actuator fault in both single and multiple vehicles in order to determine its effect on the performance of a team of vehicles. According to [45], there are four types of actuator and control effector failures. These are: (1) Lock-In-Place (LIP) Failure; (2) Hard-Over Failure (HOF); (3) Float Type of Failure; and (4) Loss of Effectiveness (LOE). In the case of Lock-In-Place failure, the effector freezes at a certain condition and does not respond to subsequent commands [45]. In a Hard-Over Failure, the effector moves to the upper or lower position limit regardless of the command. The speed of response is limited by the effector rate limit [45]. The Float failure occurs when the effector floats with zero moment and does not contribute to the control authority [45]. Loss of Effectiveness is characterized by lowering the effector gain with respect to its nominal value. The different types of actuator and control effector failures can be parameterized as follows [45]:

No-Failure Case: $u_i(t) = u_c(t), \quad k_i(t) = 1, \quad \forall t \geq t_o$

Loss of Effectiveness: $u_i(t) = k_i(t)u_c(t), \quad 0 < \varepsilon_i \leq k_i(t) < 1, \quad \forall t \geq t_{Fi}$

Float type of failure: $u_i(t) = 0, \quad k_i(t) = 1, \quad \forall t \geq t_{Fi}$

Lock-In-Place Failure: $u_i(t) = u_{ci}(t_{Fi}), \quad k_i(t) = 1, \quad \forall t \geq t_{Fi}$

Hard-Over Failure: $u_i(t) = u_{im} \quad or \quad u_{iM}, \quad k_i(t) = 1, \quad \forall t \geq t_{Fi}$

where

$u_i(t)$: actuator output

u_{ci} : output of the controller and an input to the actuator

t_{Fi} : the time instant of the failure of the i^{th} effector

$k_i \in [\varepsilon_i, 1]$: the effectiveness coefficient of the control effector, where ε_i is the minimum effectiveness of the control effector

The type of actuator fault simulated in this thesis is the Loss of Effectiveness (LOE). As seen from the above definitions, in the No-Failure Case, the output of the actuator is equal to the output of the controller, and the effectiveness coefficient (k_i) is equal to its nominal value, 1. In case of the LOE failure, the effectiveness coefficient is less than 1, which in turn lowers the output of the actuator. Hence, the severity of the actuator fault depends on the value of the effectiveness coefficient. As the value of k_i decreases, the severity of the actuator fault increases.

In the simulation results (given in Section 3.4), velocity has been used as the fault variable to simulate an actuator fault in single and multiple UAVs. The extent of the actuator fault has been simulated through gradual reduction of the maximum velocity of the UAV. While we have not modeled the actuator, we have assumed that the value of k_i will have a direct impact on the velocity range of a vehicle ($[v_{min}, v_{max}]$).

Hence, the Loss of Effectiveness of a UAV's actuator will result in a lower maximum velocity value.

It is assumed that each UAV is operating under nominal conditions upon takeoff from their respective bases, and that the Loss of Effectiveness fault in the actuator of the affected vehicle occurs while the team is en route to the target. In response to the actuator fault, a new time of arrival at the target must be generated for the team, and the affected vehicle as well as the healthy vehicles must re-plan their routes to the target. However, if the degradation in a UAV's actuator is to such an extent that it can no longer rendezvous with the other vehicles at their pre-determined destination, a resource allocation problem must be solved in order to determine which vehicles should engage the target. If a vehicle is dropped from the team for the joint attack mission, it is commanded to travel to the surveillance area.

3.3 Solution Strategy

The proposed cooperative control strategy is applicable to general cooperative control problems. It is based on the notion of coordination variable and coordination functions. The goal of the cooperation strategy is to allow the team to meet its cooperation objective while satisfying given constraints.

The cooperation objective defines the goal of the UAV team. In the mission scenario developed here, the cooperation objective requires a team of three UAVs to arrive at a pre-determined target location while minimizing their collective exposure to radars, and conserving fuel. The cooperation constraint requires the team to simultaneously arrive at the target.

In order for the team of UAVs to satisfy the cooperation objective and cooperation constraint, coordinating information must be shared across the team. In our approach, we have employed a distributed, cooperative control architecture, which requires a minimum level of global information to be shared across the team to ensure team coherence and cohesion. This is termed the coordination variable, which for the rendezvous (coordinated strike) problem, has been chosen as the estimated time of arrival, T_S, of the UAV team at the target.

As shown in Figure 3.8, each vehicle implements an identical copy of a centralized *Coordination Manager* algorithm, which selects the estimated time of arrival of the team based on its own coordination function and the coordination functions it receives from the individual vehicles. The process involved in selecting the team ETA (estimated time of arrival of the team) is described using the distributed, cooperative control architecture shown in Figure 3.8.

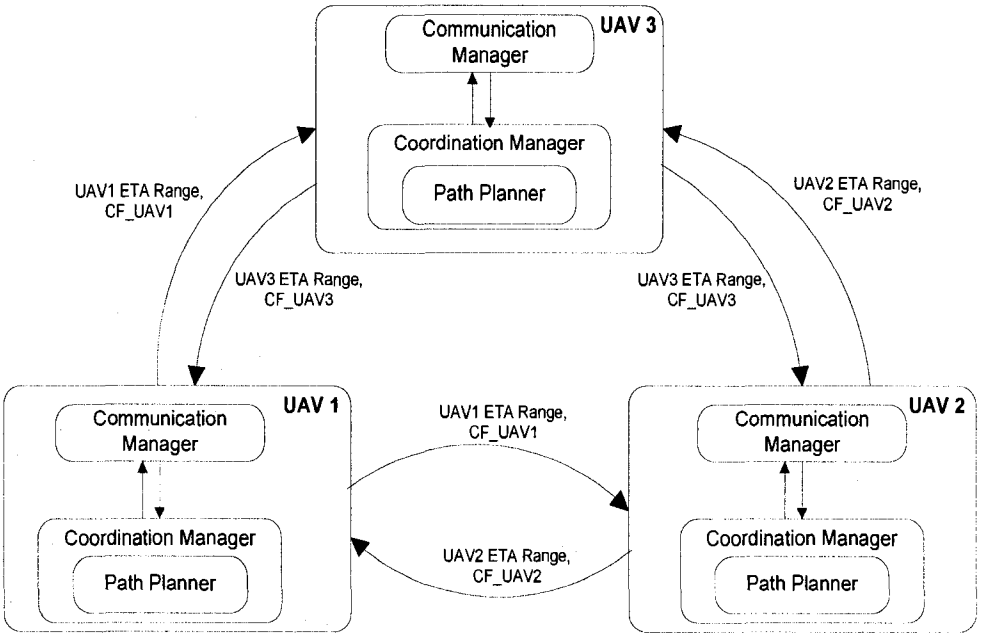

Figure 3.8: Distributed cooperative control architecture for a team of 3 UAVs, where CF_UAVi denotes the Coordination Function of the i^{th} UAV and UAVi ETA range denotes the set of time of arrival ranges of the i^{th} UAV at the target.

As shown in Figure 3.8, each UAV is composed of three functional blocks. These are the *Communication Manager*, the *Path Planner*, and the *Coordination Manager*.

The *Path Planner* is responsible for generating shortest paths (paths that have the lowest associated total cost) between the UAV and each target. Given the position of the UAV in the environment, the radar (threat) distribution, and the location of the target, there might be either a single shortest path or multiple shortest paths over the velocity

range of a UAV. The Path Planner also determines the total cost (a function of the threat cost and the fuel cost) incurred by the vehicle for traveling along each path.

The *Coordination Manager* of each vehicle receives (from the Path Planner) either a single shortest path or the list of possible shortest paths that the vehicle can follow to arrive at the target. The Coordination Manager calculates the possible time of arrival ranges (at the target) of a UAV, and the coordination function, which describes how the vehicle's total cost varies as a function of its arrival time range at the target.

The *Communication Manager* of each vehicle facilitates the sharing of information between the UAVs. The Coordination Manager of each UAV sends the possible time of arrival ranges of the UAV at the target, and the information modeled in the coordination function to the other vehicles in the team through the Communication Manager. Based upon the coordination functions and associated time of arrival ranges for all members of the team, the centralized Coordination Manager algorithm implemented on each vehicle chooses the team ETA. It is assumed that the Communication Manager synchronizes the information transmitted across the team. Hence, an identical value of the team ETA is chosen by all UAVs. The team ETA is chosen such that the overall cost (combined threat exposure and fuel cost) incurred by the team for achieving simultaneous intercept is minimized. Based upon the team ETA, the Coordination Manager of each vehicle generates a velocity and selects the waypoint path from the list of possible paths (if multiple paths are available) for the vehicle to follow to reach its target. The waypoint path that is selected is the one that allows the

vehicle to achieve the team ETA. The design of each functional block is explained in detail as follows.

The *Path Planner* is called at the beginning of the mission, or after an event has taken place (such as a change in the vehicle's condition), or when the vehicle reaches its destination. It generates a feasible velocity for the vehicle and also produces candidate waypoint path(s) between the UAV's current position and its destination(s). The development of each vehicle's path(s) involves three stages. In the first stage, a threat based Voronoi diagram [42] is created using the initial positions of all UAVs, the position(s) of the target(s), and the known threat locations (It is assumed that the positions of all threats are known before the beginning of the mission). In the second stage, each edge of the Voronoi diagram is assigned two costs: the threat cost and the fuel cost. These two costs are then summed to produce a total cost associated with each edge of the Voronoi diagram.

Each vehicle incurs a threat cost for traveling along a given path to its destination. Since the threats in the environment are multiple radar sites, the threat cost is based on the radar equation. Radar is a system that uses electromagnetic waves to identify the range, altitude, direction, or speed of both moving and fixed objects. A transmitter emits radio waves, which are reflected by the target and detected by a receiver, hence enabling the radar to detect objects. As in [4] and [5], it has been assumed that the radar signature of a UAV is uniform in all directions and is inversely proportional to the distance from the UAV to the threat to the fourth power, that is $1/d^4$.

The threat cost is a function of two factors: 1) distance between the vehicle and the threat, and 2) the duration of time for which the vehicle is exposed to the threat (i.e., the velocity of the vehicle). The threat cost of the i^{th} UAV associated with each edge of the Voronoi diagram is based on the velocity at which the vehicle travels along the edge and its distance to every threat in the environment, and is given by:

$$\hat{\mathbf{J}}_{threat}(v_i, \mathbf{h}, \mathbf{w}_j, \mathbf{w}_{j-1}) = \frac{\rho}{v_i} \int_{s=0}^{1} \frac{1}{\left\| \mathbf{h} - (\mathbf{w}_{j-1} + s(\mathbf{w}_j - \mathbf{w}_{j-1})) \right\|^4} ds \qquad (3.9)$$

where:

v_i: velocity of the i^{th} UAV.

$\mathbf{h}$: the location of a radar ($\mathbf{h} \in H$, where H is the set of all radar (threat) locations, which are known to all UAVs in the team before the beginning of the mission).

$\mathbf{w}_j$: current waypoint.

$\mathbf{w}_{j-1}$: previous waypoint.

$s \in [0,1]$: parameterizes the straight-line path from $\mathbf{w}_{j-1}$ to $\mathbf{w}_j$.

$\rho \in [0,1]$: is the percentage of the power in the radar signal that is reflected by the UAV, and indicates the vehicle's vulnerability to being detected by radar.

$\rho = 0$ implies the UAV is in the stealth mode, and is not vulnerable to threats.

$\rho = 1$ indicates that the UAV will always be detected by radar.

The closed-form solution to the integral in (3.9) is given by:

$$\hat{\mathbf{J}}_{threat}(v_i, \mathbf{h}, \mathbf{w}_j, \mathbf{w}_{j-1}) = \frac{\rho}{2v_i b^2 \left\|\mathbf{w}_j - \mathbf{w}_{j-1}\right\|^3}\left[\frac{1-a}{(1-a)^2+b^2} + \frac{1}{b}\tan^{-1}\left(\frac{1-a}{b}\right) + \frac{a}{a^2+b^2} + \frac{1}{b}\tan^{-1}\left(\frac{a}{b}\right)\right]$$

where:

$$a = \frac{(\mathbf{h}-\mathbf{w}_{j-1})^T(\mathbf{w}_j - \mathbf{w}_{j-1})}{\left\|\mathbf{w}_j - \mathbf{w}_{j-1}\right\|^2}$$

$$b = \frac{\left\| \left[\left\|\mathbf{w}_j - \mathbf{w}_{j-1}\right\|^2 I - (\mathbf{w}_j - \mathbf{w}_{j-1})(\mathbf{w}_j - \mathbf{w}_{j-1})^T\right](\mathbf{h} - \mathbf{w}_{j-1}) \right\|}{\left\|\mathbf{w}_j - \mathbf{w}_{j-1}\right\|^3}$$

The fuel cost incurred by the i[th] UAV to travel across each edge of the Voronoi diagram from $\mathbf{w}_{j-1}$ to $\mathbf{w}_j$ is a function of the UAV's velocity and the length of the edge. The fuel required by the i[th] UAV is given by:

$$\hat{\mathbf{J}}_{fuel}(v_i, \mathbf{w}_j, \mathbf{w}_{j-1}) = \int_{t_{j-1}}^{t_j} \dot{f} dt = v_i^2(t_j - t_{j-1}) = v_i^2 \left\|\mathbf{w}_j - \mathbf{w}_{j-1}\right\| \qquad (3.10)$$

where $\left\|\mathbf{w}_j - \mathbf{w}_{j-1}\right\|$ is the length of an edge.

The total cost for traveling along an edge of the Voronoi diagram is a weighted sum of the threat cost and the fuel cost associated with a given edge, and is given by the equation:

$$\hat{\mathbf{J}}_{tc}(\mathbf{w}_j, \mathbf{w}_{j-1}) = (1-\kappa)\hat{\mathbf{J}}_{threat}(v_i, \mathbf{h}, \mathbf{w}_j, \mathbf{w}_{j-1}) + \kappa\hat{\mathbf{J}}_{fuel}(v_i, \mathbf{w}_j, \mathbf{w}_{j-1}) \qquad (3.11)$$

where:

$\kappa \in [0,1]$: weighting factor that can be used to prioritize either minimization of a vehicle's exposure to threats or the amount of fuel consumed.

Once the total cost associated with each edge is determined, the third stage involves searching the Voronoi diagram to find the best path, i.e., the lowest cost path between the initial location of each UAV and the location of the target(s). To this end, a shortest path algorithm is used, which produces a shortest path between a given source and destination such that a performance objective is minimized. We have used the Floyd-Warshall algorithm [43] to find the shortest path between the UAV and its destination such that the total cost incurred by the UAV is minimized. This algorithm solves the all-pairs shortest paths problem, which involves finding the shortest path (least-weight) between every pair of vertices $u, v \in V$ in a graph. The weight of a path is the sum of the weight of its constituent edges [43].

For the rendezvous mission, the best path for a UAV is one for which the vehicle will incur the lowest total cost for a given value of velocity. Over the given velocity range of a UAV, there can be multiple shortest paths. The total cost incurred by a vehicle for traveling along a path is equal to the weighted sum of the threat cost and the fuel cost associated with that path, and is given by:

$$\mathbf{J}_i(\mathbf{x}_i, \mathbf{u}_i) = (1-\kappa)\mathbf{J}_{threat}(\mathbf{x}_i, \mathbf{u}_i) \quad + \quad \kappa \mathbf{J}_{fuel}(\mathbf{x}_i, \mathbf{u}_i) \tag{3.12}$$

where:

$\mathbf{x}_i$: is the situation state of the ith UAV, which is given by: $\mathbf{x}_i = \begin{pmatrix} z_{io} \\ z_{if} \\ H \end{pmatrix}$, where

z_{io} : is the current position of the ith UAV.

z_{if} : is the destination of the ith UAV.

H : is the set of radar (threat) locations, which are known to all UAVs in the team.

$\mathbf{u}_i$: is the decision vector of the ith UAV, which is given by: $\mathbf{u}_i = \begin{pmatrix} v_i \\ W_i \end{pmatrix}$, where

v_i : is the velocity of the ith UAV chosen from within the range, $[v_{\min}, v_{\max}]$.

W_i : is the waypoint path from the ith UAV's current position to its destination. The waypoint path of the ith UAV is given by: $W_i = \{\mathbf{w}_{i1}, \mathbf{w}_{i2}, ..., \mathbf{w}_{iP}\}$, where $\mathbf{w}_{i1} = \mathbf{z}_{io}$ and $\mathbf{w}_{iP} = z_{if}$.

$\mathbf{J}_{threat}(\mathbf{x}_i, \mathbf{u}_i)$: the threat cost incurred by a UAV for traveling along a given path.

$\mathbf{J}_{fuel}(\mathbf{x}_i, \mathbf{u}_i)$: the fuel cost incurred by a UAV for traveling along a given path.

The threat cost incurred by a UAV for traveling along a specific waypoint path to its destination is equal to the sum of the threat costs associated with the constituent edges of the waypoint path, and is given by:

$$\mathbf{J}_{threat}(\mathbf{x}_i, \mathbf{u}_i) = \sum_{h \in H} \sum_{j=2}^{P} \hat{\mathbf{J}}_{threat}(v_i, \mathbf{h}, \mathbf{w}_j, \mathbf{w}_{j-1}) \tag{3.13}$$

The fuel required by the ith UAV to travel along a waypoint path from its current position to its destination is given by:

$$\mathbf{J}_{fuel}(\mathbf{x}_i, \mathbf{u}_i) = \sum_{j=2}^{P} \hat{\mathbf{J}}_{fuel}(v_i, \mathbf{w}_j, \mathbf{w}_{j-1}) = v_i^2 L(W_i) \tag{3.14}$$

where, $L(W_i) = \sum_{j=2}^{P} \left\| \mathbf{w}_{ij} - \mathbf{w}_{i(j-1)} \right\|$ is the length of the waypoint path, W_i.

The fuel cost and the threat cost associated with a given waypoint path are calculated based on the assumption that a UAV maintains a constant, uniform velocity while traveling along the path.

Once the *Path Planner* of a UAV has generated the shortest path(s) the vehicle can follow to reach its destination, and the associated total costs, it passes this information to the *Coordination Manager*. The goal of the Coordination Manager is to find the feasible time of arrival ranges of an UAV, and to determine the total cost that a vehicle would incur for following a given velocity and hence, for achieving a given time of arrival at the target (coordination function). The estimated time of arrival of the i^{th} UAV at its destination is given by:

$$T_i = \theta_i = f_i(\mathbf{x}_i, \mathbf{u}_i) = \frac{L(W_i)}{v_i} \tag{3.15}$$

Each vehicle's time of arrival depends on the length of the path the vehicle chooses to follow to its destination and its choice of velocity, selected from the vehicle's feasible velocity range, $[v_{\min}, v_{\max}]$. Hence, for a given waypoint path, W_i, the estimated time of arrival of the i^{th} vehicle can vary between the range $[L(W_i)/v_{\max}, L(W_i)/v_{\min}]$. Moreover, it is not necessary that only one best waypoint

path will be generated for each vehicle by the Floyd Warshall algorithm for the entire velocity range, $[v_{\min}, v_{\max}]$, of the vehicle. There might be different best waypoint paths generated for the ith vehicle for different velocity ranges, $[v_a, v_b]$, and $[v_c, v_d]$ (with v_a, v_b, v_c, v_d selected from within the feasible velocity range of the ith UAV given by $[v_{\min}, v_{\max}]$), and hence different sets of arrival times, given by $[L(W_i)/v_b, L(W_i)/v_a]$ and $[L(W_i)/v_d, L(W_i)/v_c]$, respectively.

The coordination function for the ith UAV describes the combined threat exposure and fuel cost (total cost, given by Equation (3.12)) incurred by the vehicle for traveling along a path of length, $L(W_i)$, at a velocity, v_i selected from the range $[v_{\min}, v_{\max}]$. As described earlier, over the feasible velocity range of the ith UAV, $v_{\min} \le v_i \le v_{\max}$, there might be several waypoint paths and hence, several arrival time ranges. Similarly, the total cost of a UAV also varies with the choice of waypoint path and associated velocity range. Hence, the coordination function of each vehicle describes the range of arrival times and the range of total cost associated with the different waypoint paths.

The coordination function for the ith UAV is given by:

$$\phi_i(\mathbf{x}_i, \theta_i) = \mathbf{J}_i(\mathbf{x}_i, \mathbf{u}_i) \tag{3.16}$$

where

$\mathbf{J}_i(\mathbf{x}_i, \mathbf{u}_i)$: is the total cost incurred by the ith UAV for traveling along a waypoint path

of length, $L(W_i)$ at velocity, v_i.

θ_i : the estimated time of arrival of the i^{th} UAV at its destination.

Cooperation among the UAV team is achieved through a centralized Coordination Manager algorithm, implemented by each vehicle. As shown in Figure 3.8, the Coordination Manager of each UAV in the team sends the range of feasible arrival times and the coordination function information via the Communication Manager to the other vehicles in the team. The role of the Coordination Manager of each vehicle is to then use the coordination function information and the range of arrival times received from each vehicle to find the coordination variable. The coordination variable is defined as the minimal amount of information needed by the team of vehicles to achieve the cooperation objective. For the mission scenario described in Section 3.2, the coordination variable for the rendezvous mission is the estimated time of arrival of the team (team ETA) at the pre-determined target location.

To choose the best value for the estimated time of arrival of the team, the Coordination Manager of each vehicle first uses the time of arrival ranges of all the vehicles in the team to determine a common range of arrival times for the team, which is given by:

$$\Theta_T = \bigcap_{i=1}^{N} \Theta_i(\mathbf{x}_i) \tag{3.17}$$

where:

N : the number of vehicles comprising the team,

$\Theta_i(\mathbf{x}_i) = \bigcup_{u_i \in U_i(x_i)} f_i(\mathbf{x}_i, \mathbf{u}_i)$ is the set of estimated time of arrival ranges of the ith vehicle in situation state, $\mathbf{x}_i$.

Next, the Coordination Manager of each vehicle uses the coordination functions of the individual vehicles to find the team cost values associated with the range of arrival times common to the team, Θ_T. The team cost is the sum of the individual vehicle costs (individual vehicle coordination functions), and is given by:

$$\mathbf{J}_{team}(\mathbf{J}_1, \mathbf{J}_2, ..., \mathbf{J}_N) = \sum_{i=1}^{N} \mathbf{J}_i(\mathbf{x}_i, \mathbf{u}_i) = \sum_{i=1}^{N} \phi_i(\mathbf{x}_i, \theta) \tag{3.18}$$

subject to

$$T_1 = T_2 = T_3 = ... = T_N = T_S = \theta$$

where, T_S is the estimated time of arrival of the team (Team ETA) at the target.

Once the range of arrival times for the team, and the team cost associated with these arrival times is determined by the Coordination Manager, it selects the estimated time of arrival of the team to be the one with the minimum associated team cost value. The chosen team cost function is given by:

$$\mathbf{J}_{team}(\mathbf{J}_1, \mathbf{J}_2, ..., \mathbf{J}_N) = \min \sum_{i=1}^{N} \mathbf{J}_i(\mathbf{x}_i, \mathbf{u}_i) \tag{3.19}$$

subject to

$$T_1 = T_2 = T_3 = ... = T_N = T_S$$

Hence, the Coordination Manager ensures that the cooperation objective of the team is satisfied by minimizing the collective threat exposure and conserving the fuel of the team and by ensuring simultaneous intercept. Once the team ETA is chosen, the Coordination Manager of each vehicle selects the waypoint path W_i that the vehicle should travel along at velocity v_i in order to reach the target at the time specified by the team ETA.

3.4 Simulation Results

As shown by Figure 3.9, three UAVs, represented by triangles, must simultaneously arrive at the target, represented by the star, while minimizing the team's threat exposure to 33 radar sites, represented by circles, and conserving fuel. Each UAV takes off form a different airbase. The entire area of operation is 3000 sq-km.

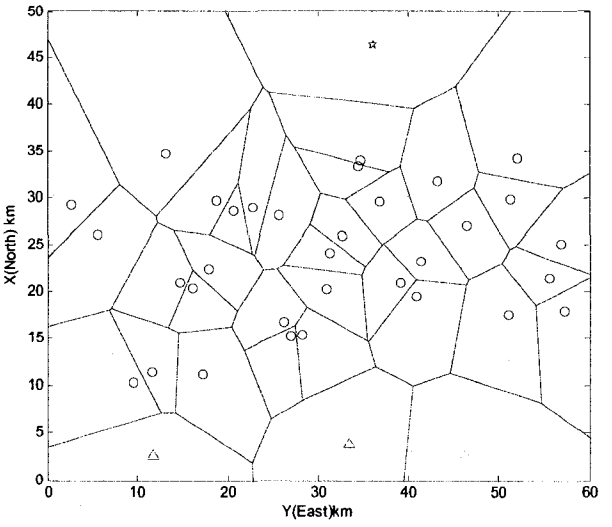

Figure 3.9: Mission scenario for the rendezvous problem showing the locations of the team of 3 UAVs, 33 radar sites and the target.

As stated in Section 3.2, it has been assumed that the positions of all the radar sites are known before the beginning of the mission. Hence, the UAVs follow pre-planned routes to their destination. For the following simulations, nominal velocity for all the vehicles has been chosen to be between 89m/s and 220m/s. The value of $\kappa = 0.5$ has been chosen to give equal weight to the conservation of fuel as well as avoidance of threats in determination of the vehicles' paths to the target. Moreover, for all the UAVs, the value of $\rho = 0.5$ has been chosen to indicate that there is a 50% chance that a UAV will be detected by the radars in the environment. The goal of the UAVs is to pre-plan threat avoiding routes to their destination while conserving fuel such that the total cost incurred by the team, which is a combination of the team's collective threat exposure and fuel consumption, is minimized, and simultaneous intercept is achieved.

In Section 3.4.1, we have shown team intercept at the target under nominal conditions, i.e., when neither a single nor multiple vehicles are suffering from an actuator fault. Here, a team of three UAVs, starting from geographically separate locations (airbases) is tasked to arrive simultaneously at a pre-determined high-valued target location in order to carry out a successful attack. While traveling to the target, the team must minimize its exposure to multiple radar sites and conserve fuel. The solution strategy outlined in Section 3.3 is employed in order to achieve simultaneous intercept.

In Section 3.4.2, velocity is used as the fault variable to simulate an actuator fault in both single and multiple UAVs, and its effect on the performance of the team is demonstrated. The extent of the actuator fault has been simulated through gradual reduction of the maximum velocity of the UAV.

As stated in Section 3.2, the type of actuator fault simulated in this thesis is the Loss of Effectiveness (LOE). Under nominal conditions, the output of the actuator is equal to the output of the controller. Moreover, the value of the effectiveness coefficient $k_i = 1$. In case of the LOE failure, $k_i < 1$, which leads to a lower value of the output of the actuator. Hence, the severity of the actuator fault depends on the value of k_i. As the value of k_i decreases, the severity of the actuator fault increases. Moreover, the fault in the actuator of a UAV results in the reduction in the vehicle's maximum velocity. Hence, we can assume that the percentage reduction in the value of k_i is directly proportional to the percentage reduction in maximum velocity of a UAV. For example, $k_i = 0.4$ will imply that the maximum velocity of a UAV has reduced to 40% of its nominal value.

It is assumed that the Loss of Effectiveness fault in the actuator of the affected vehicle occurs while the team is en route to the target. In response to the actuator fault, a new time of arrival at the target is generated for the team (using the solution strategy outlined in Section 3.3), and the affected vehicle as well as the healthy vehicles re-plan their routes to the target. However, if the degradation in a UAV's actuator is to such an extent that it can no longer rendezvous with the other vehicles at their pre-determined destination, a resource allocation problem must be solved in order to determine which vehicles should engage the target.

3.4.1 Performance Under Healthy Conditions

In this section, we have shown how intercept at the target is achieved without any faults in the UAV systems. The coordination functions of UAV1, UAV2, and UAV3 are shown by Tables 3.1, 3.2, and 3.3, respectively. Figures 3.10, 3.11, and 3.12 show the shortest paths to the target for UAV1, UAV2, and UAV3, respectively, for a given velocity range. Figure 3.13 shows the coordination function plots of UAV1, UAV2, and UAV3.

Table 3.1: The coordination function information of UAV1 for $\kappa = 0.5$ under healthy conditions.

kappa (κ)	Velocity Range of UAV1 $v_{\min} \le v_1 \le v_{\max}$ (m/s)	Range of Arrival times for UAV1, $T_{\min} \le T_1 \le T_{\max}$ (seconds)	Path Length of UAV1, $L(W_1)$ (km)	Total Cost of UAV1, $\mathbf{J}_1(\mathbf{x}_1, \mathbf{u}_1)$
0.5	89-100	922.6577-1.0367x10^3	92.2658	0.9827- 1.0107
	101-125	632.8627-783.2459	79.1078	1.0145- 1.1117
	126-220	290.4346-507.1081	63.8956	1.1173-1.8957

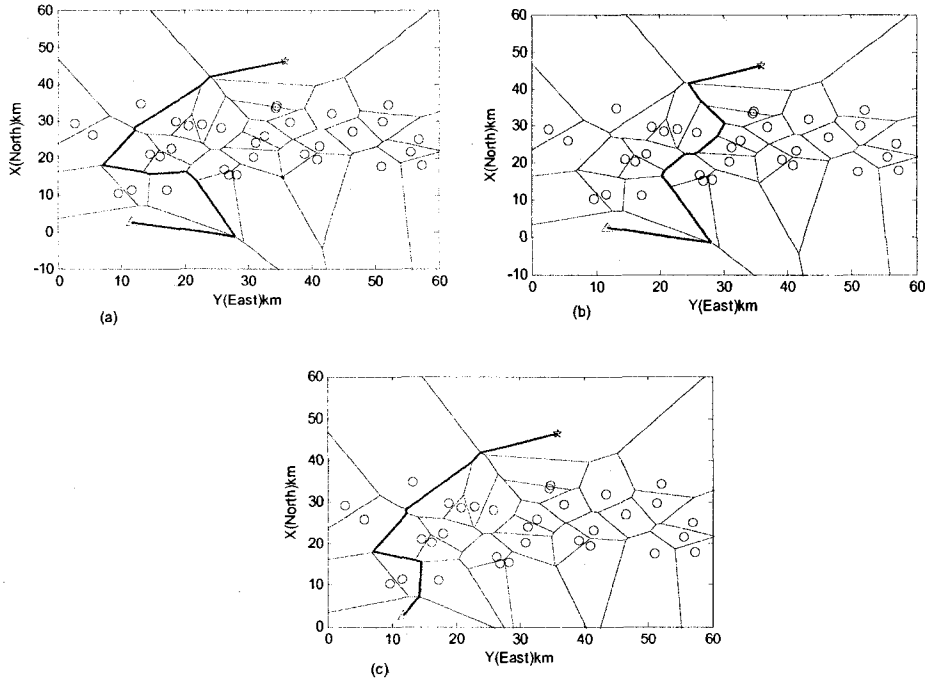

Figure 3.10: Optimal paths for UAV1 through the 33 radar sites to the target for (a) $89m/s \le v_1 \le 100m/s$, (b) $101m/s \le v_1 \le 125m/s$, (c) $126m/s \le v_1 \le 220m/s$.

Table 3.2: The coordination function information of UAV2 for $\kappa = 0.5$ under healthy conditions.

kappa (κ)	Velocity Range of UAV2 $v_{\min} \le v_2 \le v_{\max}$ (m/s)	Range of Arrival times for UAV2, $T_{\min} \le T_2 \le T_{\max}$ (seconds)	Path Length of UAV2, $L(W_2)$ (km)	Total Cost of UAV2 $\mathbf{J}_2(\mathbf{x}_2, \mathbf{u}_2)$
0.5	89-95	798.0935-851.8975	75.8189	0.9097- 0.9131
	96-112	483.4003-563.9670	54.1408	0.9076- 0.9122
	113-220	217.5252-423.5005	47.8556	0.9080-1.4675

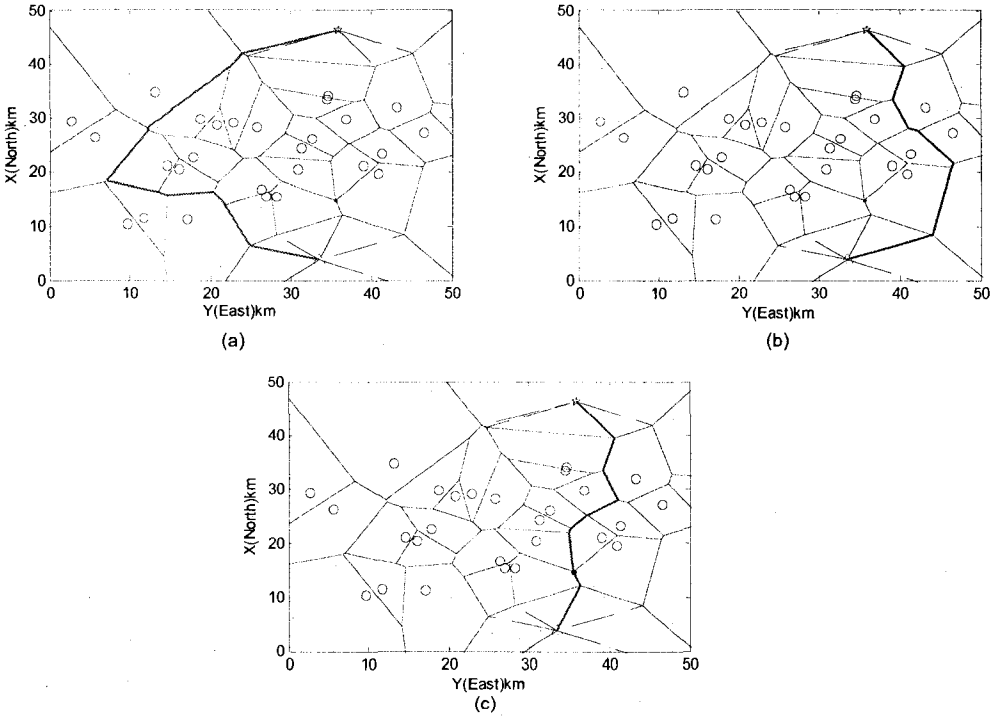

Figure 3.11: Optimal paths for UAV2 through the 33 radar sites to the target for (a) $89m/s \le v_2 \le 95m/s$, (b) $96m/s \le v_2 \le 112m/s$, (c) $113m/s \le v_2 \le 220m/s$.

Table 3.3: The coordination function information of UAV3 for $\kappa = 0.5$ under healthy conditions.

kappa (κ)	Velocity Range of UAV3 $v_{\min} \le v_3 \le v_{\max}$ (m/s)	Range of Arrival times for UAV3, $T_{\min} \le T_3 \le T_{\max}$ (seconds)	Path Length of UAV3 $L(W_3)$ (km)	Total Cost of UAV3 $\mathbf{J}_3(\mathbf{x}_3, \mathbf{u}_3)$
0.5	89-220	219.9692-543.7440	48.3932	0.8675- 1.4585

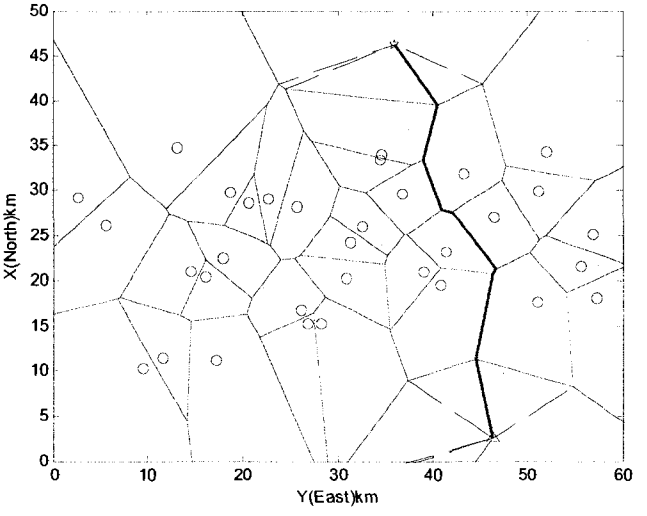

Figure 3.12: Optimal path for UAV3 through the 33 radar sites to the target.

Tables 3.1 and 3.2 show that three shortest paths are generated from the initial positions of UAV1 and UAV2 to the position of the target over the velocity range 89 m/s - 220 m/s. However, Table 3.3 shows that only a single shortest path is generated from the initial position of UAV3 to the target over the velocity range 89 m/s - 220 m/s. The Floyd Warshall algorithm generates only a single shortest path between a vehicle and a target for a given velocity range. While it may seem confusing that three shortest

paths are generated for UAV1 and UAV2, and only a single shortest path is generated for UAV3, it should be noted that factors such as the position of the UAV, the number and distribution of threats, and the position of the target also play a significant role in determining the number of paths generated over a given velocity range. To test this explanation, for the given mission scenario depicted in Figure 3.9, one can try varying the number and distribution of threats, and the position of the UAVs, and the target. In some sets of simulations, only a single shortest path will be generated for all vehicles over the velocity range 89 m/s – 220 m/s, whereas in others, multiple paths (not necessarily the same number of paths) will be generated for all three vehicles.

Figure 3.13 shows the total cost incurred by the three UAVs for achieving a given range of the arrival times. The total cost of UAV1 and UAV2 for the three different ranges of arrival times, decreases with an increase in arrival time. Whereas, for UAV3, at first, its total cost decreases until 441 sec, after which it starts to increase. Equations (3.9), (3.14), and (3.15) show that the fuel cost decreases with an increase in the arrival time (associated with a lower velocity), whereas the threat cost increases with an increase in the arrival time. Hence, a vehicle must travel at slow speeds and follow shorter paths to the target in order to conserve fuel. Whereas, avoiding threats involves higher speeds and longer paths to the target.

By setting $\kappa = 0.5$ in Equation (3.12), we give equal weight to the fuel cost and the threat cost in determination of the total cost for a given path for a given vehicle. However, the coordination functions of UAV1 and UAV2, and for the most part for

UAV3, show that the fuel cost is more influential in determining the overall cost as compared with the threat cost. The reason for this is that the units and hence, the values of the fuel cost and threat cost are different, making it difficult to equate the values of these two costs. The solution to this problem is to normalize the values of the threat and fuel cost so that they may be compared on a fair and equal basis.

Each edge in the Voronoi diagram has an associated fuel cost and threat cost, which are summed using Equation (3.11) to produce the total cost associated with a given edge. However, even after normalization, for a given velocity and arrival time, the constituent edges of a waypoint path may have higher fuel or threat costs. For example, at a higher velocity and thus, an early arrival time, the threat cost will be lower, whereas the fuel cost will be higher. Moreover, the proximity of the constituent edges of the waypoint path to the threats also affects the threat cost. The fuel cost is also affected by another factor, which is the length of the constituent edges of the waypoint path.

If a mission designer wishes to induce the same trend in the total cost versus the arrival time as in the threat cost or the fuel cost versus the arrival time, manipulation of the value of the weighting factor κ is essential. For $\kappa < 0.5$, the threat cost is given more weight than the fuel cost, and the coordination function graph generally tends to increase as the arrival time increases (i.e., as the velocity becomes lower). For $\kappa > 0.5$, the fuel cost is given more weight than the threat cost, and the coordination function graph generally tends to decrease as the arrival time increases. At $\kappa = 0.5$, the ratio of the values of the fuel cost and threat cost for each edge remains the same. Hence, if the

values of the fuel cost for each constituent edge of a given path are higher than the threat costs, the trends shown in Figure 3.13 for UAV1 and UAV2 can be generated. As for UAV3, the total cost decreases up until 441 seconds, after which it starts to increase. This shows that after 441 seconds (i.e., at lower velocities), the values of the threat cost of the constituent edges are higher than those of the fuel cost, and thus have a more significant impact on the total cost trend.

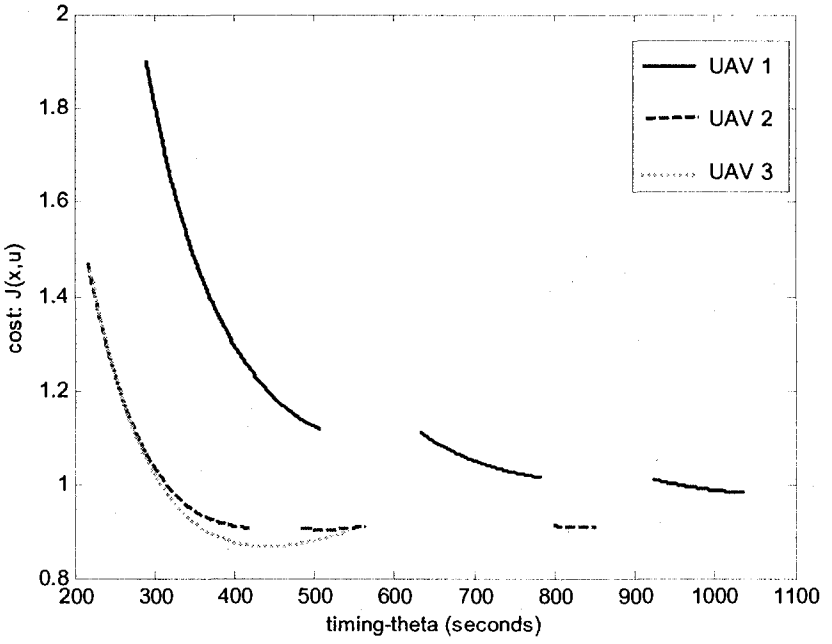

Figure 3.13: The range of arrival times and their associated costs for the three UAVs under nominal conditions.

The goal of the UAVs is to arrive at their destination simultaneously while minimizing the overall cost incurred by the team for accomplishing the rendezvous mission. The Coordination Manager of each vehicle uses the coordination functions to

determine the common range of arrival times for the team. The range of total cost incurred by each UAV for achieving the two separate common ranges of arrival times for the team is shown in Figures 3.14 and 3.15. For both the ranges, the Coordination Manager selects the arrival time with the lowest associated team cost. Table 3.4 shows that for the team arrival time range, $290\,\text{sec} \le \Theta_T \le 423\,\text{sec}$, the best choice for the team ETA is 423 seconds, and for $483\,\text{sec} \le \Theta_T \le 507\,\text{sec}$, the suitable choice of the team ETA is 507 seconds. Since the objective of the team is to arrive at the target while minimizing the combined threat cost and fuel cost, team ETA is chosen to be 507 seconds.

Table 3.4: Team ETA, team cost, and the associated individual vehicle costs and velocities for the time ranges: $290\,\text{sec} \le \Theta_T \le 423\,\text{sec}$, and $483\,\text{sec} \le \Theta_T \le 507\,\text{sec}$.

Team ETA T_S (sec)	v_1 (m/s)	v_2 (m/s)	v_3 (m/s)	Total Cost of UAV1 $\mathbf{J}_1(\mathbf{x}_1,\mathbf{u}_1)$	Total Cost of UAV2 $\mathbf{J}_2(\mathbf{x}_2,\mathbf{u}_2)$	Total Cost of UAV3 $\mathbf{J}_3(\mathbf{x}_3,\mathbf{u}_3)$	Team Cost $\mathbf{J}_{team}(\mathbf{J}_1,\mathbf{J}_2,\mathbf{J}_3)$
423	151.05	113.13	114.405	1.2379	0.9080	0.8693	3.0152
507	126	106.79	95.45	1.1174	0.9045	0.8828	2.9047

Table 3.4 also shows the velocities each vehicle will have to maintain to achieve the team ETA, and the associated costs that will be incurred by the individual vehicles. Comparing the individual vehicle costs at 423 seconds and 507 seconds, we can see that UAV1 and UAV2 incur lower costs, whereas UAV3 incurs a higher cost for achieving team ETA of 507 seconds. This result has been pointed out to show that the optimal

value of the team ETA is best from the team's perspective as opposed to the individual vehicle's perspective.

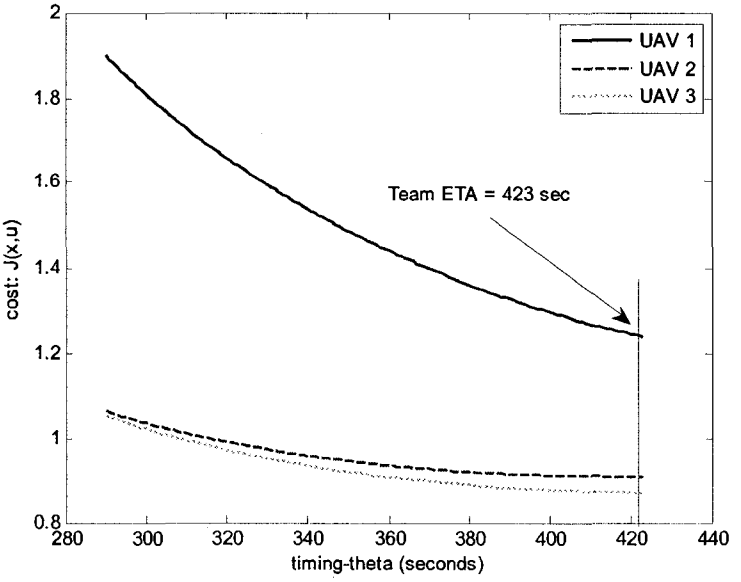

Figure 3.14: The estimated time of arrival of the team (Team ETA) for the common range of arrival times given by $290\,\text{sec} \leq \Theta_T \leq 423\,\text{sec}$.

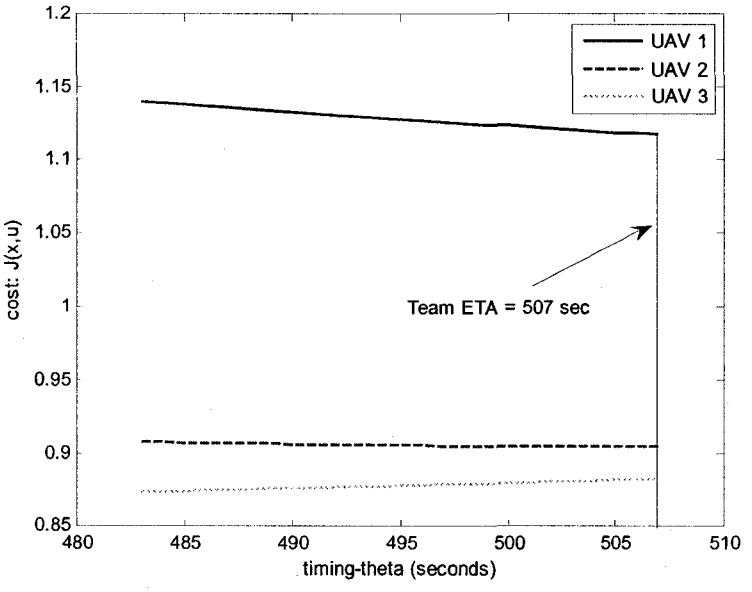

Figure 3.15: The estimated time of arrival of the team (Team ETA) for the common range of arrival times given by $483\text{sec} \leq \Theta_T \leq 507\text{sec}$.

3.4.2 Performance Under Actuator Fault

The type of actuator fault simulated here is the Loss of Effectiveness (LOE). It is assumed that the Loss of Effectiveness fault in the actuator of the affected vehicle occurs while the team is en route to the target. Velocity has been used as the fault variable to simulate the severity of the actuator fault in single and multiple UAVs. The extent of the actuator fault has been simulated through gradual reduction of the maximum velocity of the UAV. It is possible that the maximum velocity of a UAV may reduce multiple times during the rendezvous mission.

In response to the actuator fault and its subsequent diagnosis (detection and isolation), the affected UAV first communicates its new time of arrival range, and coordination function information to all its team members. Next, the other team members recalculate and send their time of arrival ranges and coordination functions across the team. As in the healthy case, based on the coordination functions and time of arrival ranges of all the team members, a new team ETA will be selected by the Coordination Manager of each vehicle. For simplicity, we have assumed that the overall time required in generating a new team ETA, i.e, the time required by each UAV to send its coordination function to its team members, and for the Coordination Manager of each vehicle to re-calculate the team ETA, is negligible.

The first set of simulations investigates the effect of the actuator fault in a single UAV (UAV1) on the arrival time ranges and total costs of UAV1, UAV2, and UAV3. Table 3.4 shows that the optimal team ETA occurs at 507 seconds, which requires UAV1, UAV2, and UAV3 to maintain velocities of 126 m/s, 106.79 m/s, and 95.45 m/s. Until UAV1's maximum velocity drops below 126 m/s, the vehicle can still arrive at the target without changing its path. Hence, to simulate the actuator fault during the mission, it is assumed that UAV1's velocity drops to 120 m/s at t = 100 seconds. The new maximum velocity of UAV1 (120 m/s) is 54.5% of the nominal maximum velocity, 220 m/s. This shows that the output of the actuator of UAV1 has decreased by (100-54.5) 45.5%. Since the output of the actuator is affected by the effectiveness coefficient k_i, we can state that the value of $k_i = 0.545$.

At t = 100 seconds, the instance of the first actuator fault, UAV1 re-calculates its coordination function and sends its arrival time range to UAV2 and UAV3. Both UAV2 and UAV3 also re-calculate their coordination functions and their arrival time (at the target) values. Table 3.5 shows the revised coordination function information for UAV1, UAV2, and UAV3.

Table 3.5: The coordination functions of UAV1, UAV2, and UAV3 after the actuator fault has occurred in UAV1 at t = 100 seconds.

	UAV1	UAV2	UAV3
Velocity Range $v_{\min} \le v_i \le v_{\max}$ (m/s)	89-120	89-220	89-220
Range of Arrival Times (sec)	422.0587-569.0679	195.8741-484.1831	176.5832-436.4977
Path Length (km)	50.6470	43.0923	38.8483
Total Cost	0.6165-0.6733	0.8331- 1.3283	0.8008-1.2299

From Table 3.5, it can be seen that the common range of arrival times for UAV1, UAV2, and UAV3 is between 422 sec and 436 sec. The range of total cost incurred by UAV1 for the common range of arrival times is shown in Figure 3.16, whereas those of UAV2 and UAV3 are shown in Figure 3.17. As in the nominal case, each vehicle's Coordination Manager selects the arrival time for the team such that the team cost is minimized. From Figure 3.16, it can be seen that the cost function for UAV1

monotonically decreases with time, whereas for UAV2 and UAV3, the total cost monotonically increases with time. Since the goal of the rendezvous mission is for the team to intercept at the target while minimizing the overall team cost, the team ETA is chosen to be the value with the lowest associated team cost. The minimum team cost occurs at 422 seconds (which is the intercept time at which the maximum cost for UAV1 and minimum cost for UAV2 and UAV3 occurs), and in order to achieve this intercept time, UAV1, UAV2, and UAV3 must maintain velocities of 120 m/s, 102 m/s, and 92 m/s, respectively. Hence, from takeoff, it will take the team 522 seconds to arrive at the target as opposed to 507 seconds under healthy conditions.

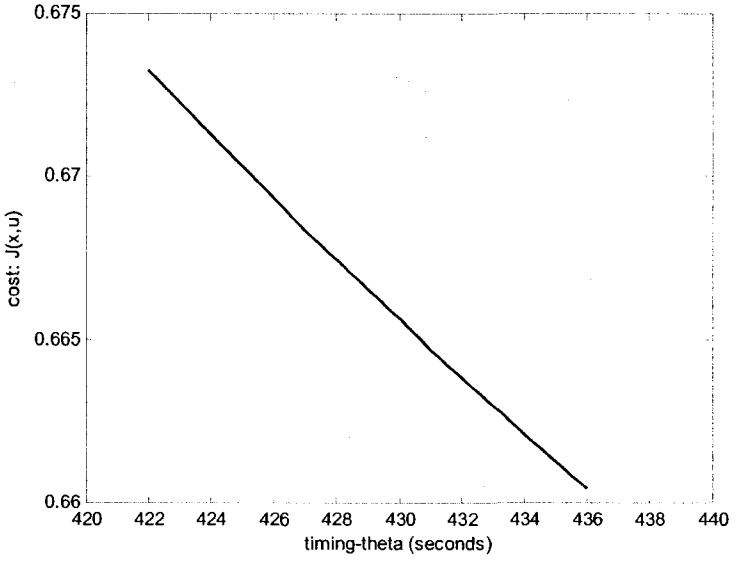

Figure 3.16: The range of total cost incurred by UAV1 for the common range of arrival times given by $422\,\text{sec} \leq \Theta_T \leq 436\,\text{sec}$.

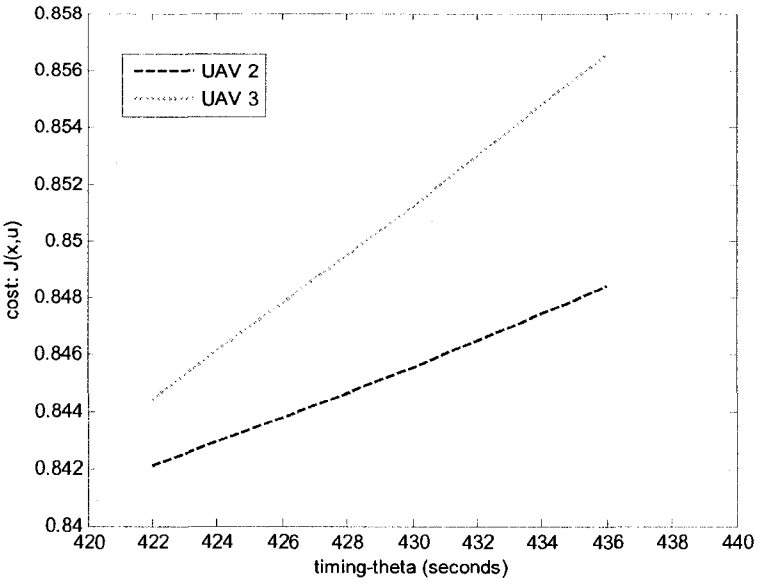

Figure 3.17: The range of total cost incurred by UAV2 and UAV3 for the common range of arrival times given by $422\,\text{sec} \leq \Theta_T \leq 436\,\text{sec}$.

It was stated earlier that the maximum velocity of the affected UAV may reduce multiple times during the rendezvous mission. Suppose that 200 seconds after the first instance of the actuator fault in UAV1 (which occurs at t = 100 seconds into the mission), a second fault occurs and UAV1's maximum velocity drops from 120 m/s to 110m/s. The new maximum velocity of UAV1 (110 m/s) is 50% of the nominal maximum velocity, 220 m/s. This shows that the output of the actuator of UAV1 has decreased by 50%. Since the output of the actuator is affected by the effectiveness coefficient k_i, we can state that the new value of $k_i = 0.50$.

From its original position at t = 100 seconds into the mission, in the subsequent 200 seconds, at a constant velocity of 120 m/s, UAV1 has traveled a distance of 24 km,

and its remaining distance to target along the chosen path is (50.6470 km - 24 km) 26.647 km. At its new maximum velocity of 110m/s, it will take UAV1 approximately another 242 seconds to arrive at the target. Hence, the earliest possible arrival time for UAV1 from the beginning of the mission will be (100 seconds + 200 seconds + 242 seconds) 542 seconds. However, the team has to intercept at the target in another 222 seconds (i.e., at 522 seconds from the beginning of the mission). Hence, UAV1 along with UAV2, and UAV3 must re-plan their route to the target. Table 3.6 shows the Coordination Function information for UAV1, UAV2, and UAV3 at t = 200 seconds from the instance of the first actuator fault, i.e., 300 seconds since the beginning of the mission.

Table 3.6: The coordination functions of UAV1, UAV2, and UAV3 after the second actuator fault has occurred in UAV1 at t = 300 seconds into the mission.

	UAV1	UAV2	UAV3
Velocity Range $v_{min} \leq v_i \leq v_{max}$ (m/s)	89-110	89-220	89-220
Range of Arrival Times (sec)	242.2461-299.4053	101.4897-250.8735	83.1763-205.6044
Path Length (km)	26.6471	22.3277	18.2988
Total Cost	0.2631-0.2887	0.4508-0.6869	0.3062-0.5374

From Table 3.6, it can be seen that there is no overlap in the arrival time ranges of UAV1 and UAV3, thereby making the team intercept at the target impossible. Hence, at this point, the Coordination Manager of each vehicle calls a Resource Allocation Manager (present on each vehicle), which in turn determines the composition of the team that should engage the target. Given the coordination functions and range of arrival times for all vehicles, the Resource Allocation Manager of each vehicle computes the minimum team cost for all possible team compositions. Table 3.7 shows the two possible team configurations.

Table 3.7: Team ETA, team cost, and the associated individual vehicle costs and velocities for the two possible team configurations.

Team Configuration	Team ETA T_S (sec)	v_1 (m/s)	v_2 (m/s)	v_3 (m/s)	Total Cost of UAV1 $J_1(x_1,u_1)$	Total Cost of UAV2 $J_2(x_2,u_2)$	Total Cost of UAV3 $J_3(x_3,u_3)$	Team Cost
Team 1	246	108.32	90.76		0.2858	0.4473		0.7331
Team 2	188		118.76	97.33		0.429	0.3004	0.7294

Team 1 comprises UAV1 and UAV2, whereas team 2 comprises UAV2 and UAV3. Table 3.7 shows that Team 1 can intercept at the target in 246 seconds (with a total rendezvous mission time of 100+200+246 = 546 seconds) whereas Team 2 can arrive at the target in 188 seconds (with a total rendezvous mission time of 100+200+188 = 488 seconds). Moreover, the overall team cost of Team 2 is lower than that of Team 1. Since the goal of the rendezvous mission is for a given team to arrive at

the target while minimizing the combined threat cost and the fuel cost, the Resource Allocation Manager assigns Team 2 to the target, and orders UAV1 to drop out of the coordinated strike mission. UAV1 then proceeds to the surveillance area to begin the surveillance mission. With Team 2 assigned to the target, it will take UAV2 and UAV3 (100 seconds + 200 seconds + 188 seconds) 488 seconds to arrive at the target.

The results in Tables 3.5, 3.6, and 3.7 show that even with degradation in the performance of the actuator in one of the vehicles, the team can still simultaneously arrive at the target. However, if at t = 300 seconds into the mission, UAV1's velocity drops to 105m/s instead of 110m/s, the earliest possible arrival time for UAV1 at the target would be 253.78 seconds. Thus, there would be no overlap in the time of arrival ranges of UAV1 and UAV2 as there is in Table 3.6. In this case, the Resource Allocation Manager would give preference to the team over the single vehicle for the chances of successfully engaging the target are increased with multiple vehicles. It should be noted that UAV2 and UAV3 will still have to re-calculate their paths to the target instead of continuing along the path chosen after the first instance of the actuator fault in UAV1. This is because the intercept time of 422 seconds generated at t =100 seconds was common to UAV1, UAV2, and UAV3. With UAV1 dropped from the team, the new intercept time for UAV2 and UAV3 should be one that ensures minimization of the overall cost of both UAVs.

The cases detailed above only address the actuator fault in a single UAV. Moreover, in Table 3.7, it was straightforward to choose Team 2 over Team 1 because

Team 2 has an earlier intercept time as well as a lower cost than Team 1. However, that is not always the case. To this end, in the next scenario, we assume the actuator fault occurs in two vehicles. Suppose at t = 300 seconds into the coordinated strike mission, both UAV1 and UAV2 suffer from an actuator fault resulting in a further drop of UAV1's maximum velocity from 120 m/s to 110 m/s (as shown in Table 3.6), and a drop in UAV2's maximum velocity from 220 m/s to 110 m/s. Table 3.8 shows the coordination function information of all the three vehicles.

Table 3.8: The coordination functions of UAV1, UAV2, and UAV3 after the velocities of UAV1 and UAV2 drop to 110m/s at t = 300 seconds.

	UAV1	UAV2	UAV3
Velocity Range $v_{\min} \le v_i \le v_{\max}$ (m/s)	89-110	89-110	89-220
Range of Arrival Times (sec)	242.2461-299.4053	202.9795-250.8735	83.1763-205.6044
Path Length (km)	26.6471	22.3277	18.2988
Total Cost	0.2631-0.2887	0.4283- 0.4508	0.3062-0.5374

Table 3.8 shows that there are two distinct arrival time ranges common to different members of the team. UAV1 and UAV2 have a common arrival time range of 242.2461-250.8735 seconds, whereas UAV2 and UAV3 have a common arrival time range of 202.9795-205.6044 seconds. Given the coordination function information in

Table 3.8, the Resource Allocation Manager computes the minimum team cost and the associated team ETA for both team configurations.

Table 3.9: Team ETA, team cost, and the associated individual vehicle costs and velocities for the two possible team configurations.

Team Configuration	Team ETA T_S (sec)	v_1 (m/s)	v_2 (m/s)	v_3 (m/s)	Total Cost of UAV1 $\mathbf{J}_1(\mathbf{x}_1,\mathbf{u}_1)$	Total Cost of UAV2 $\mathbf{J}_2(\mathbf{x}_2,\mathbf{u}_2)$	Total Cost of UAV3 $\mathbf{J}_3(\mathbf{x}_3,\mathbf{u}_3)$	Team Cost
Team 1	246	108.32	90.76		0.2858	0.4473		0.7331
Team 2	203		110	90.14		0.4283	0.3051	0.7334

As shown in Table 3.9, Team1 has a higher team ETA but a lower cost than Team 2. In Table 3.7, Team 2 was assigned to the target since it had both a lower cost as well as a lower team ETA than Team 1. If the goal of the mission designer is to achieve a minimum team ETA at the expense of the overall cost to the team, Team 2 would be a better choice. Similarly, Team 1 would be a better choice if minimizing the overall cost at the expense of team ETA was the mission goal. However, realistically, both team ETA and the fuel cost as well as threat cost should play a role in determining the team composition. To this end, we have defined the coordinated strike mission (or coordinated rendezvous mission) cost, given by Equation (3.20), to be a weighted sum of the combined threat and the fuel cost of the team and the team ETA, namely.

$$J_{mission}(J_1, J_2, ..., J_N) = (1-\lambda) * J_{team}(J_1, J_2, ..., J_N) + \lambda * \tau * T_S \qquad (3.20)$$

where

$T_S = T_i, \quad i = 1,...,N$

$\lambda \in [0,1]$: scaling factor chosen by the mission designer to emphasize on either minimization of team cost or the team ETA.

$\tau = \frac{average\_J_{team}}{average\_T_S}$: scaling factor that is used to equate the values of team cost and team ETA.

For Team 1 and Team 2 in Table 3.8, we have selected $\lambda = 0.5$ to give equal weight to the team cost and the team ETA.

In Figures 3.18 and 3.19, the mission cost values for Team 1 (UAV1, UAV2), and Team 2 (UAV2, UAV3) are plotted against the common range of arrival times for the respective teams. The Resource Allocation Manager compares the minimum mission cost values for both teams, and finally selects the team with the lower minimum mission cost value. For the chosen team, the team ETA value is selected to correlate with the minimum value of the mission cost. For the teams in Table 3.8, comparison of the minimum mission cost values of Team 1 and Team 2 results in the selection of Team1 for the coordinated strike mission. Hence, UAV1 and UAV2 will head to the target while UAV3 will be dropped from the team and assigned to travel to the surveillance region. From Figure 3.18, it can be seen that the team ETA for UAV1 and UAV2 is 242 seconds.

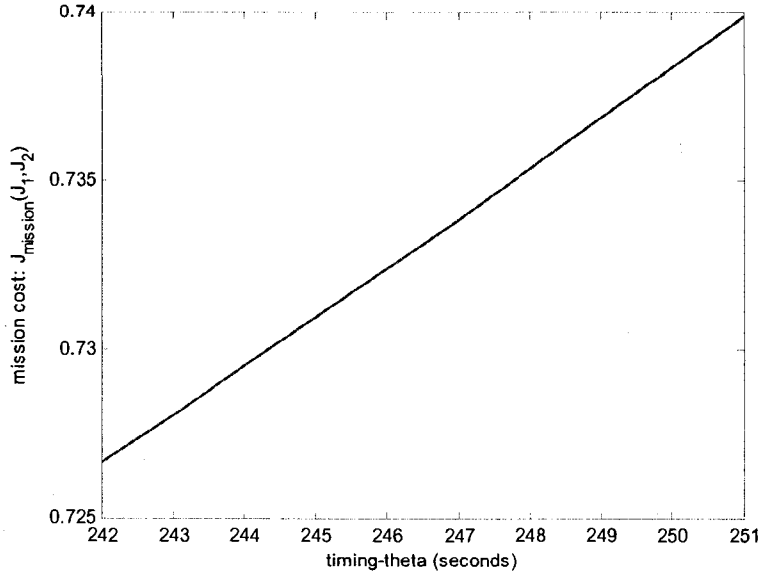

Figure 3.18: The mission cost of Team 1 for the common range of arrival times,

$$242\,\text{sec} \le \Theta_T \le 251\,\text{sec}.$$

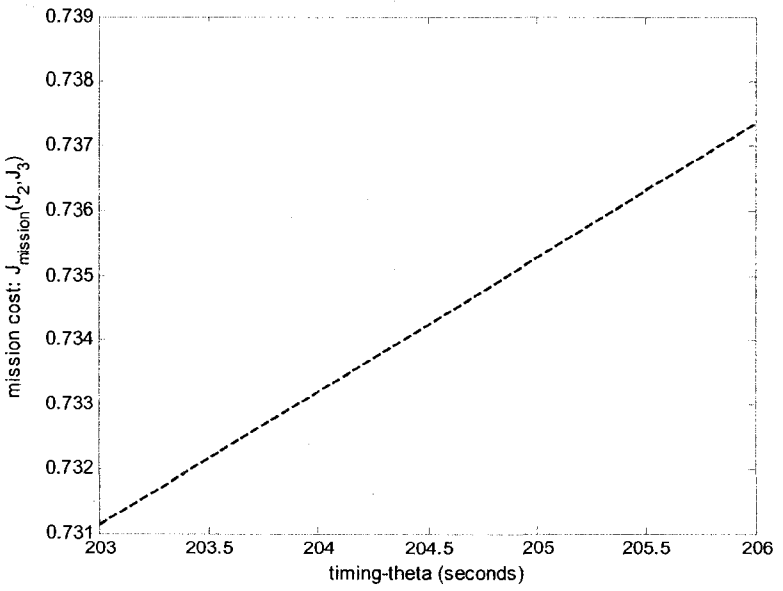

Figure 3.19: The mission cost of Team 2 for the common range of arrival times,

$$203\,\text{sec} \le \Theta_T \le 206\,\text{sec}.$$

3.5 Conclusions

In this chapter, the coordinated rendezvous problem has been illustrated through an example scenario involving a team of 3 UAVs, which must travel through an area containing 33 radar sites to simultaneously arrive at a single high priority target to carry out a coordinated strike. While traveling to the target, the team must minimize its combined exposure to radars and conserve fuel.

Two cases have been simulated. One is the healthy case in which all UAVs are functioning normally, and where the team ETA, selected through collaboration among team members, is associated with the minimum combined threat and fuel cost of the team (team cost). In the second case, velocity has been used as the control variable to simulate an actuator fault in single and multiple UAVs. The extent of the actuator fault, which occurs during the rendezvous mission, has been simulated through gradual reduction of the maximum velocity of the affected vehicle(s).

Four set of simulations have been carried out to simulate the actuator fault. In the first set of simulations, the maximum velocity of a single UAV is slightly reduced, thereby requiring a re-plan. In the second set of simulations, the maximum velocity of the already affected vehicle is further reduced. However, this time, there is an overlap in the arrival time ranges of the affected vehicle and only one other vehicle, thereby making the team intercept at the target impossible. Results show that two possible team configurations are generated by a Resource Allocation Manager, which then assigns the

team with both the lower team cost and team ETA to the target. It has also been pointed out that if the affected vehicle's velocity were further reduced, there would be no overlap in the time of arrival ranges of the other vehicles and the affected vehicle. Hence, in this case, the Resource Allocation Manager chooses the team over the single vehicle to perform the coordinates strike mission.

The fourth set of simulations has been carried out to simulate the actuator fault in multiple vehicles as well as to show that the results of the second set of simulations are not always possible, and there can be times when one team has a lower overall cost than the other team, whereas the other team has a lower team ETA. Moreover, realistically, both team ETA and the fuel cost as well as the threat cost should play a role in determining the team composition. Hence, a new coordinated strike mission cost has been introduced, which is a weighted sum of the combined threat and fuel cost of the team and the team ETA. The weighting factor in the mission cost equation allows the mission designer to either give equal, or more or less weight to the team ETA or the overall team cost. For our results, we gave equal weight to the team ETA and the overall team cost. As seen from the results, the Resource Allocation Manager selects the team with the lower minimum mission cost value to perform the mission.

Chapter 4

Multiple UAV Surveillance Mission

4.1 Problem Formulation

In this chapter, the *Multiple UAV Surveillance* problem is addressed. In the previous chapter, multiple UAVs were tasked to simultaneously arrive at a high priority target to carry out a coordinated strike mission. In this chapter, it is assumed that upon completion of the coordinated strike mission, the UAV team must travel to a region of known dimensions along a border between two countries. Upon arriving at the border, the team must monitor the given region. In the previous chapter, the vehicles communicated with one another in order to re-plan their paths to the target or to decide which vehicles should engage the target. However, for the purpose of the surveillance mission, each UAV periodically communicates with a central command and control station through a satellite in orbit, and not with its team members. The goal of the UAVs is to carry out surveillance of the entire environment of operation while minimizing the team cost, which is a function of the individual vehicle costs. Each vehicle's cost is a function of the amount of fuel consumed by the vehicle during the surveillance mission and the time required to complete the mission.

As shown in Figure 4.1, a team of three homogeneous UAVs has to perform a surveillance mission in a rectangular region spanning 600 sq-km. A central command

and control station divides the search region equitably among the UAVs, and assigns each vehicle to monitor a section of the region. Hence, the surveillance paths of the vehicles do not overlap. It is assumed that each vehicle will perform only one sortie.

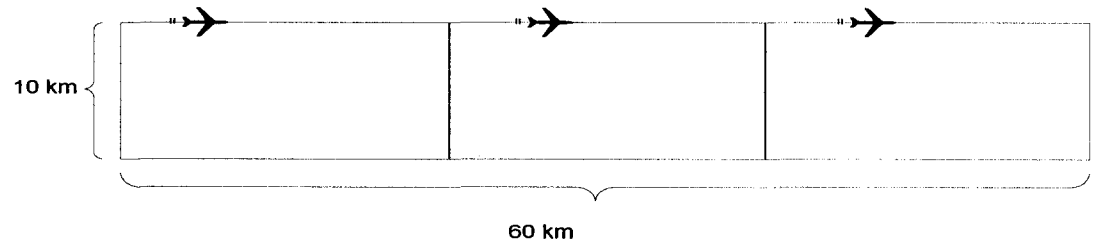

Figure 4.1: A team of 3 UAVs is performing surveillance in a 600sq-km region.

As an added dimension to the surveillance problem, the mission is carried out by a team of three vehicles where a single vehicle is assumed to be suffering from a fault. It is assumed that the fault occurs in either the actuator (Loss of Effectiveness, as mentioned in Chapter 3) or the sensor or both the actuator and the sensor of the affected vehicle. In [46], five types of sensor failures have been mentioned, which are: (1) Total sensor failure; (2) Stuck with constant bias sensor failure; (3) Drift or additive-type sensor failure; (4) Multiplicative-type sensor failure; and (5) Outlier data sensor failure.

Total sensor failure is a catastrophic failure, in which at a given point in time, the sensor stops functioning. The output of the sensor is then a constant zero. This failure can be caused by electrical or communication problems. In (stuck with constant bias sensor failure), the sensor gets stuck with a constant bias, and the output (thereafter)

remains constant [46]. Drift or additive-type sensor failure is a very common failure in analog sensors [46]. It is caused by internal temperature changes or calibration problems. The sensor output has an added constant term (the drift) [46]. A scaling error in the sensor output is responsible for the multiplicative-type sensor failure. (In this failure type), a multiplicative factor is applied to the sensor nominal value [46]. Outlier data sensor failure occurs in GPS sensors. It is a temporal failure. The GPS sensor outputs a single point with a large error. However, the measurements following this error are correct. Possible causes of the error are failures in the GPS internal signal processing algorithms, and temporary satellite signal blocking.

The Multiplicative-type sensor failure has been simulated in this thesis. The sensor range (sensor output) has been used as the fault variable to simulate the sensor fault in a single UAV. Despite the presence of either the Loss of Effectiveness actuator fault and/or the Multiplicative-type sensor failure, the goal of the surveillance mission remains the same, which is minimization of the team cost. However, a fault in either the sensor, or actuator or both requires the mission designer to address a resource allocation problem, i.e, whether to carry out the mission using all the three vehicles or two healthy, perfectly functioning vehicles. The team chosen to perform the surveillance mission is the one that incurs the minimum cost for performing the mission.

4.2 Cost Assignment

The objective of the team of UAVs is to carry out surveillance of the given region while minimizing the cost incurred by the team. The team cost is a function of the individual vehicle costs, and is given as follows:

$$J_{team} = \sum_{i=1}^{N} J_{sm_i} \tag{4.1}$$

where:

N: the number of UAVs.

J_{sm_i} : the total cost incurred by the i[th] UAV for carrying out surveillance of the area assigned to it.

The individual vehicle cost is a function of the fuel cost incurred by the vehicle and the total mission time, and is given by:

$$J_{sm_i} = (1-\alpha) J_{fuel_i} + \alpha t_{s_i} \tag{4.2}$$

where:

$\alpha \in [0,1]$: is a scaling factor that gives the mission designer flexibility to emphasize on either minimization of fuel cost or minimization of the i[th] UAV's mission time.

The function J_{fuel_i} is the fuel cost incurred by the i[th] UAV. The fuel cost is a function of the vehicle's velocity and the length of the path covered by the vehicle during the mission. While each vehicle's velocity is constrained to be between a given range, $v_{\min} \le v \le v_{\max}$, it is assumed that while covering the surveillance region, a vehicle maintains a constant, uniform velocity. The fuel cost chosen here is based on the fuel cost in [7], where it has been assumed that the fuel consumption rate is proportional to the aerodynamic drag force, which is proportional to the velocity squared. Hence, the fuel required by the i[th] UAV to search the region it is assigned to, is given by:

$$J_{fuel_i} = v_i^2 D_i \tag{4.3}$$

where:

v_i : the velocity of the i[th] UAV constrained to be between $v_{\min} \le v \le v_{\max}$.

D_i : the distance or the length of the path covered by the i[th] UAV.

The distance covered by the i[th] UAV depends on the path taken, and the sensor range of the vehicle, and is given by:

$$D_i = \left(LRA_i \left(\frac{WRA}{SR\_UAV_i} \right) \right) + WRA \tag{4.4}$$

where:

LRA_i : is the length of the rectangular area to be covered by the i[th] UAV.

WRA : is the width of the entire rectangular area.

SR_UAV_i : is the sensor range of the i[th] UAV.

$\frac{WRA}{SR\_UAV_i}$: is the number of times a UAV has to travel along the breadth (or the length, LRA_i) of the rectangular area assigned to it in order to complete its surveillance mission.

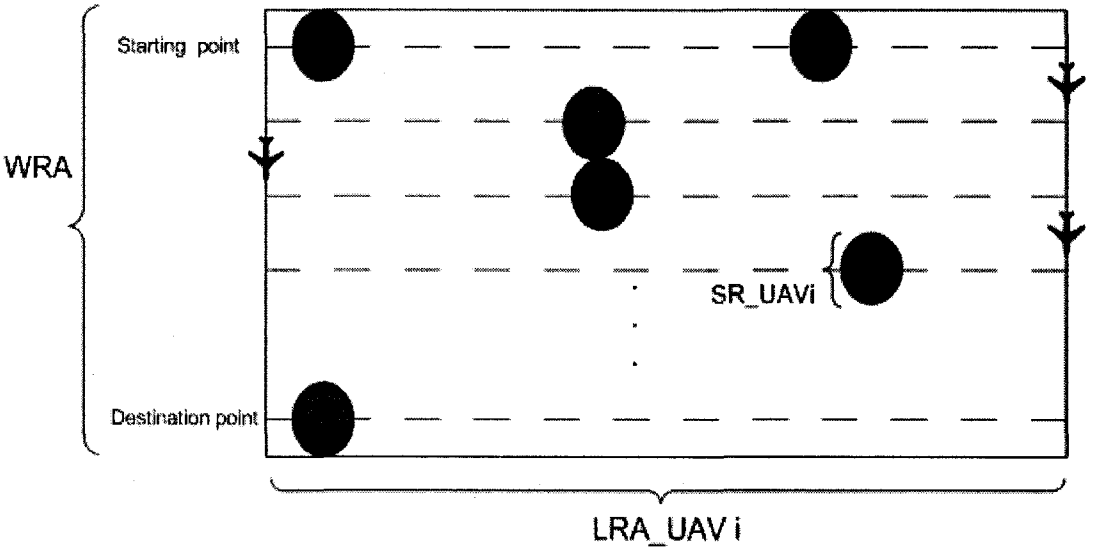

Figure 4.2: The surveillance path followed by the i^{th} UAV.

In Figure 4.2, the surveillance path of a UAV is shown by the dashed lines. The sensor range of the vehicle, represented by the circle, determines the number of times a vehicle has to travel along the length of the rectangular area in order to complete its surveillance mission. Under nominal conditions, the sensor range of each vehicle is assumed to be the same.

The second term in Equation (4.2) is the time taken by a UAV to complete its surveillance mission, and is a function of the distance covered by the UAV in Equation

(4.4) and the vehicle's velocity. Hence, the surveillance mission time of the i^{th} UAV is given by:

$$t_{s_i} = \frac{D_i}{v_i} \tag{4.5}$$

Each vehicle uses Equation (4.2) to determine the cost it will incur for completing its surveillance mission. This cost is a function of the fuel cost in Equation (4.3) and the surveillance mission time in Equation (4.5). These two metrics are in turn controlled by the velocity and the sensor range of the vehicle. Hence, manipulation of velocity and sensor range determines the cost that a vehicle would incur. As seen from Equations (4.3) and (4.5), an increase in velocity would result in an increase in the fuel cost but a decrease in the surveillance mission time. Similarly, as seen from Equation (4.4), an increase in the sensor range would result in a decrease in the distance covered by a UAV, which in turn decreases the fuel cost as well as the surveillance mission time.

It has been assumed that the three vehicle team is operating under either an actuator fault, or sensor fault, or a fault in both the sensor and the actuator of an individual vehicle. The goal is to determine which team configuration is better suited for performing the surveillance mission i.e., either a three vehicle team or a two vehicle team. Hence, in the following simulations, using 1) velocity, 2) sensor range, and 3) a combination of velocity and sensor range of the vehicles as fault variables, the performance of a team of three vehicles is compared with a team of two normally functioning vehicles to determine which team is better suited for the surveillance mission and under what conditions.

4.3 Simulation Results

For the following simulations, nominal velocity for all the vehicles is chosen to be between 89m/s and 220m/s. The nominal sensor range of each vehicle is assumed to be 100 meters. As shown by Figure 4.1, the entire rectangular area is 600 sq-km. For all simulations, UAV1 has been chosen as the vehicle suffering from the actuator fault, the sensor fault or both the actuator and the sensor faults.

For each type of fault, two cases are simulated to determine whether the team of three vehicles (two healthy and one faulty) or the team of two healthy vehicles is better suited for performing the mission.

In the first case, the team is composed of three vehicles, where one vehicle (UAV1) is suffering from an actuator fault and two (UAV2, and UAV3) are healthy vehicles. As shown by Figure 4.3, it is assumed that a central command and control station assigns each UAV to cover an equal portion of the rectangular surveillance region.

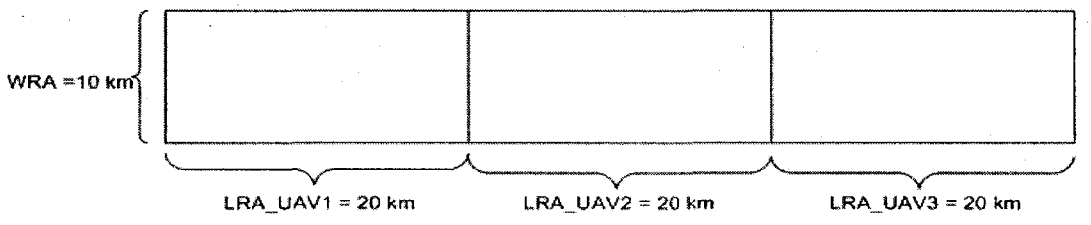

Figure 4.3: The surveillance region divided among a team of 3 UAVs.

In the second case, the team is composed of only two healthy vehicles (UAV2, and UAV3), which, as shown by Figure 4.4, are assigned to cover an area of 300 sq-km each.

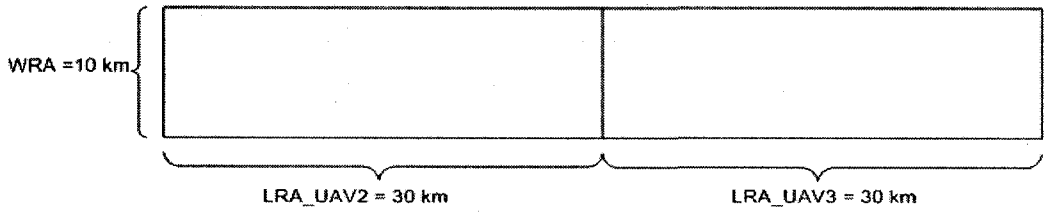

Figure 4.4: The surveillance region divided among a team of 2 UAVs.

The goal of each team is to cover the entire surveillance region while minimizing the team cost. The team that is chosen to perform the mission is the one which incurs the minimum cost, given by Equation (4.1). For the simulations below, the following equations are solved for determining the minimum value of the team cost for a team of 3 UAVs and a team of 2 UAVs. It should be noted that the fuel cost and surveillance mission time shown in the following equations are calculated by using Equations (4.3) and (4.5). However, for calculating the individual vehicle costs, slight modifications to Equation (4.2) have to be made to take into account the following: 1) Differing velocity ranges of the vehicles (actuator fault in UAV1), and/or 2) Differing search distances of the vehicles (sensor fault in UAV1). For the actuator and/or sensor fault, the surveillance mission cost for each UAV is calculated using the following equations. The surveillance mission cost of UAV1 is given by:

$$J_{sm_1} = (1-\alpha)J_{fuel_1} + \alpha\beta(t_{s_1}) \tag{4.6}$$

where:

$\beta = \dfrac{average\_J_{fuel_1}}{average\_t_{s_1}}$: is a scaling factor that is used to normalize the fuel cost and surveillance mission time values for UAV1.

Since UAV2 and UAV3 do not suffer from an actuator and/or sensor fault, they both have the same fuel cost and surveillance mission time, and hence the same surveillance mission cost, as given by:

$$J_{sm_2} = (1-\alpha)J_{fuel_2} + \alpha\gamma(t_{s_2}) \tag{4.7}$$

$$J_{sm_3} = (1-\alpha)J_{fuel_3} + \alpha\gamma(t_{s_3}) \tag{4.8}$$

where:

$\gamma = \dfrac{average\_J_{fuel_2}}{average\_t_{s_2}}$ or $\gamma = \dfrac{average\_J_{fuel_3}}{average\_t_{s_3}}$: is a scaling factor that is used to normalize the fuel cost and surveillance mission time values for UAV2 and UAV3.

The scaling factors β and γ are used because the units of surveillance mission time (seconds) and fuel cost (km^3/sec^2), and the respective values of these terms are different, and thus must be normalized so that they can be compared on a fair and equal basis using the scaling factor α. The scaling factor γ in Equations (4.7) and (4.8) is different from the scaling factor β in Equation (4.6) because: 1) for the actuator fault, the velocity range of UAV1 is different from that of UAV2 and UAV3, 2) for the sensor fault, the sensor range and hence the distance covered by UAV1 is different from that of UAV2 and UAV3, and 3) for a combination of the sensor and actuator faults, both the velocity range and the distance covered by UAV1 is different.

For each team configuration, the surveillance mission cost of each vehicle in Equations (4.6), (4.7), and (4.8) is calculated for $\alpha = 0.1$ to $\alpha = 0.9$ (in increments of 0.1). Subsequently, for each α, the minimum team cost for both teams is then determined using Equation (4.1). Next, depending on the value of α preferred by the mission designer (i.e., whether the minimization of the individual vehicle's fuel cost or its mission time is more important or both are given equal weighting), the team costs for both teams are compared. For the given α, the team with the minimum cost is chosen to perform the surveillance mission. For the following simulations, we do not choose one value of α over the other. We just compare the minimum team cost for both team configurations for all values of α between 0.1 and 0.9 to show the effects of the choice of α on the Minimum Team cost.

4.4 Performance Under an Actuator Fault

Velocity has been used as a fault variable to simulate the Loss of Effectiveness actuator fault in a single UAV, chosen to be UAV1. It is assumed that the fault in the actuator of UAV1 occurs before the beginning of the surveillance mission. The extent of the actuator fault has been simulated through gradual reduction of the maximum velocity of UAV1. To simulate the gradual degradation of the actuator of UAV1, its maximum velocity is reduced to 90% (Velocity Set 1) to 80% (Velocity Set 2) to 70% (Velocity Set 3) to 60% (Velocity Set 4) and finally to 50% (Velocity Set 5) of the nominal maximum velocity, which is 220 m/s. Since UAV2 and UAV3 are in a healthy

state, their velocity range remains between 89m/s and 220m/s for the duration of the mission. In Table 4.1, a description of the terms that will be used in the results is given.

Table 4.1: Description of terms

Term	Description
α (alpha)	Scaling factor that gives the mission designer flexibility to emphasize on either minimization of fuel cost or minimization of total mission time
v_i (m/s)	Velocity of the i^{th} UAV
$\min\_J_{sm_i}$	Minimum Surveillance Mission cost of the i^{th} UAV
J_{fuel_i} (km^3/sec^2)	Fuel cost of the i^{th} UAV
t_{s_i} (seconds)	Surveillance Mission time of the i^{th} UAV

In the following tables, the results for only two velocity sets are given. These are Velocity Set 1 and Set 5 in which the maximum velocity of UAV1 is 90% and 50% of the maximum velocity of UAVs 2 and 3. The results for the Velocity Set 2, Set 3, and Set 4 (80%, 70%, and 60%) are given in the Appendix A.

In the tables, for the three member and the two member team, the value of α in Equations (4.6), (4.7), and (4.8) is varied between 0.1 and 0.9, and the corresponding *Minimum Surveillance Mission cost of the i^{th} UAV*, $\min\_J_{sm_i}$, is recorded. The fuel cost incurred by a vehicle and its surveillance mission time, associated with $\min\_J_{sm_i}$, for a given α, are also recorded. Figures have also been included to show the effect of

velocity and the scaling factor α on the Minimum Surveillance Mission cost of each vehicle.

For all the velocity sets, for case I (team of 3 vehicles) as well as case II (team of 2 vehicles), the Minimum Surveillance Mission costs for both UAV2 and UAV3 only need to be found once. This is because the velocity range of these vehicles remains the same throughout the simulations, i.e., they do not suffer from an actuator fault. UAV1 is the only vehicle in which the actuator fault is simulated, and hence its *Minimum Surveillance Mission* cost values will change as its maximum velocity is reduced. Thus, the minimum team cost values of the team of three vehicles will change but that of the team of two vehicles will remain the same.

In the following section, i.e., Section 4.4.1, we will consider Velocity Set 1 in which the maximum velocity of UAV1 is limited to 90% of its nominal maximum velocity, 220 m/s. Two cases are considered, namely case I and case II. In case I, a team of three vehicles (two healthy and one faulty) carries out the surveillance mission. The results for case I are tabulated in Tables 4.2 and 4.3, which show, for α (scaling factor in Equation (4.2)) ranging from 0.1 to 0.9, the Minimum Surveillance mission cost along with the associated fuel cost and surveillance mission time of the individual vehicles in the three vehicle team (UAV1, UAV2, and UAV3). In case II, a team of two healthy vehicles (UAV2 and UAV3) is tasked to perform surveillance. The Minimum Surveillance mission cost, the fuel cost, and the surveillance mission time of UAV2 and UAV3 are tabulated in Table 4.4.

4.4.1 Velocity Set 1: UAV1: 89-198m/s, UAV2: 89-220m/s, UAV3: 89-220m/s

Case I: Two healthy vehicles, 1 faulty vehicle performing surveillance

Table 4.2: Minimum Surveillance mission costs of UAV1 when its maximum velocity is at 90% of the nominal value, 220m/s.

alpha (α)	v_1 (m/s)	min_J_{sm_1}	J_{fuel_1} (km^3/sec^2)	t_{s_1} (hours)
0.1	89	20.97	15.92	6.273
0.2	89	26.02	15.92	6.273
0.3	89	31.07	15.92	6.273
0.4	98	35.71	19.3	5.697
0.5	113	38.99	25.67	4.941
0.6	129	40.88	33.45	4.328
0.7	149	41.16	44.62	3.747
0.8	179	39.30	64.40	3.119
0.9	198	34.75	78.80	2.82

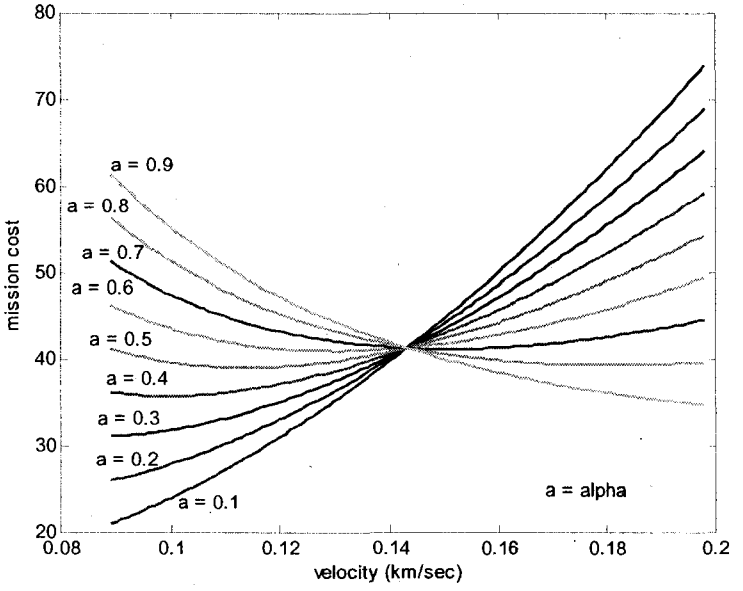

Figure 4.5: Surveillance Mission Costs of UAV1 for the velocity range: $89m/s \leq v_1 \leq 198m/s$.

Table 4.2 shows, for each value of α, the Minimum Surveillance mission cost incurred by UAV1. The velocity at which the minimum cost is incurred and the associated fuel cost and the surveillance mission time are also given. Figure 4.5 shows the effects of varying the value of α on the Surveillance Mission Cost of UAV1, given by Equation (4.6).

At lower values of α, the weight given to the minimization of fuel cost is more than that given to the minimization of the surveillance mission time. As shown by Figure 4.6, fuel cost increases monotonically with an increase in velocity. Whereas, Figure 4.7 shows that the surveillance mission time decreases monotonically with an increase in velocity. Hence, as expected, Figure 4.5 shows that for α = 0.1 to 0.3, the Surveillance Mission cost of UAV1 increases monotonically with an inease in velocity. Table 4.2 also shows that for α = 0.1 to 0.3, the minimum Surveillance Mission cost is incurred by UAV1 at its minimum velocity, 89m/s. The minimum value of the fuel cost, 15.92 km^3/sec^2, also occurs when UAV1 is flying at its minimum velocity of 89m/s. However the surveillance mission time, 6.273 hours, is maximum at 89m/s. As the value of α increases to 0.4 and then up to 0.9 (i.e., as the mission designer places more emphasis on the minimization of the surveillance mission time), the velocity of UAV1 increases, which leads to an increase in the fuel cost and a decrease in the surveillance mission time. Finally, the minimum value of the surveillance mission time, 2.82 hours, occurs when the velocity of UAV1 is at its maximum, 198m/s. At this velocity, the fuel cost of UAV1 reaches its maximum value of 78.80km^3/sec^2.

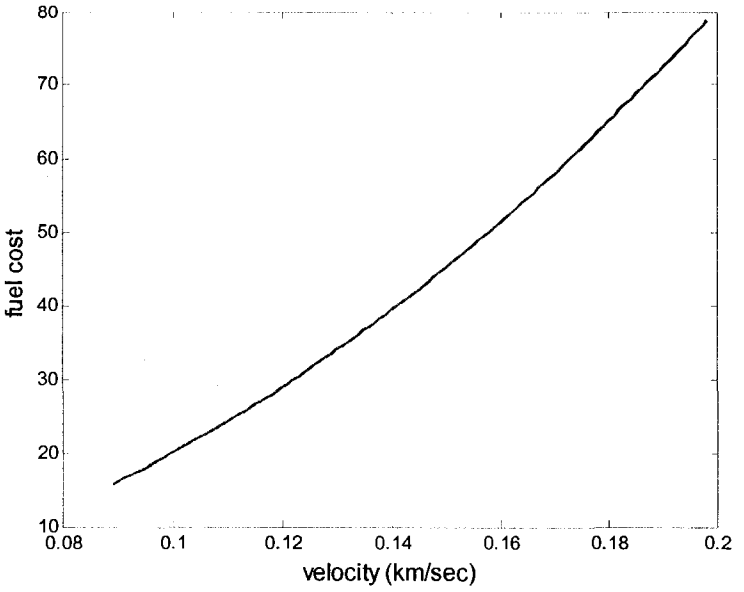

Figure 4.6: Fuel cost of UAV1 for the velocity range: $89m/s \leq v_1 \leq 198m/s$.

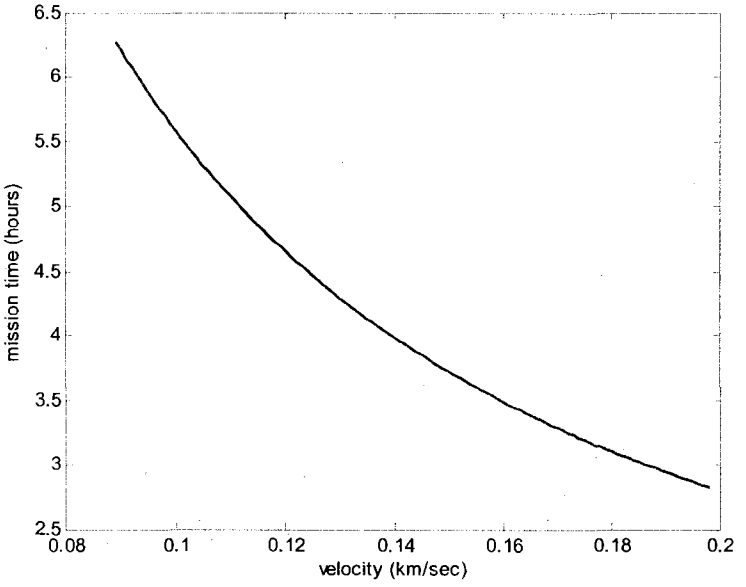

Figure 4.7: Surveillance Mission time of UAV1 for the velocity range: $89m/s \leq v_1 \leq 198m/s$.

Table 4.3 shows, for each value of α, the Minimum Surveillance mission cost incurred by UAV2 and UAV3. Unlike UAV1, these vehicles function normally throughout the mission. Hence, their Minimum Surveillance mission cost, for each value of α, always remains the same, and hence will only be found once. Here, as in the case of UAV1, for lower values of α, UAV2 and UAV3 incur the minimum Surveillance mission cost at lower velocities. As shown by Figure 4.8, with an increase in α, the minimum Surveillance mission cost for UAV2 and UAV3 occurs at higher velocities.

Table 4.3: Minimum Surveillance mission cost of UAV2 and UAV3 for case I.

alpha (α)	v_2, v_3 (m/s)	$\min\_J_{sm_2}$ $\min\_J_{sm_3}$	J_{fuel_2}, J_{fuel_3} (km^3/sec^2)	t_{s_2}, t_{s_3} (hours)
0.1	89	22.6	15.92	6.273
0.2	89	29.28	15.92	6.273
0.3	91	35.91	16.64	6.136
0.4	106	41.32	22.58	5.267
0.5	122	45.12	29.92	4.577
0.6	139	47.30	38.84	4.017
0.7	160	47.63	51.46	3.49
0.8	192	45.48	74.10	2.908
0.9	220	39.84	97.28	2.538

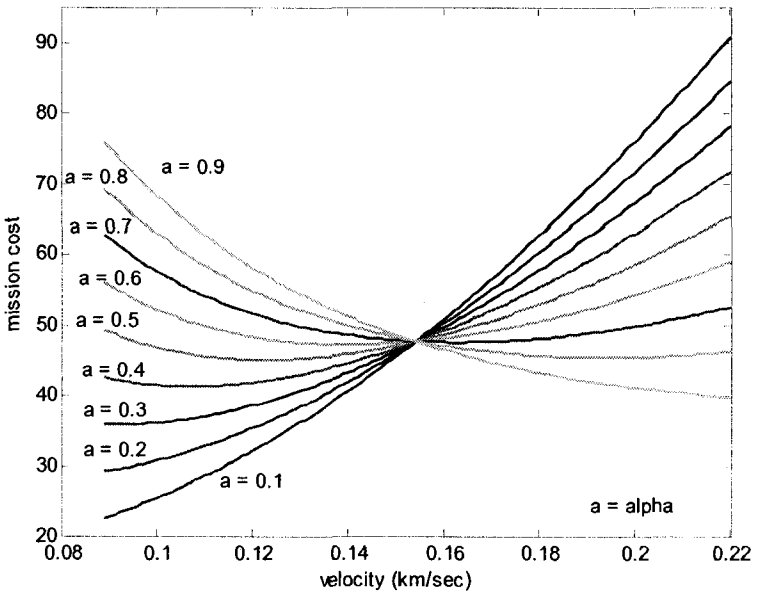

Figure 4.8: Surveillance Mission Costs of UAV2 and UAV3 for case I, and for the nominal velocity range: $89m/s \leq v_{2,3} \leq 220m/s$.

In Table 4.4, the results of case II (where only two healthy vehicles are performing the surveillance mission) are tabulated, which show the Minimum Surveillance Mission cost incurred by UAV2 and UAV3. Figure 4.9 shows the effects of varying the value of α on the Surveillance Mission cost of UAV2 and UAV3, given by Equations (4.7), and (4.8).

Comparing Tables 4.2, 4.3, and 4.4, one can see that in case II, the fuel cost and the surveillance mission time, and hence the surveillance mission cost of UAV2 and UAV3 is higher than that of each vehicle (UAV1, UAV2, and UAV3) in case I. This is because the search distance of UAV2 and UAV3 (300 sq-km each) in case II is greater than that of UAV1, UAV2, and UAV3 (200 sq-km each) in case I.

Case II: Two healthy vehicles performing surveillance

Table 4.4: Minimum Surveillance mission cost of UAV2 and UAV3 for case II.

alpha (α)	v_2, v_3 (m/s)	$\min\_J_{sm_2}$ $\min\_J_{sm_3}$	J_{fuel_2}, J_{fuel_3} (km^3/sec^2)	t_{s_2}, t_{s_3} (hours)
0.1	89	33.84	23.84	9.395
0.2	89	43.84	23.84	9.395
0.3	92	53.77	25.48	9.088
0.4	106	61.88	33.82	7.888
0.5	122	67.57	44.80	6.853
0.6	140	70.83	59	5.972
0.7	161	71.32	78.02	5.193
0.8	194	68.10	113.3	4.31
0.9	220	59.65	145.7	3.801

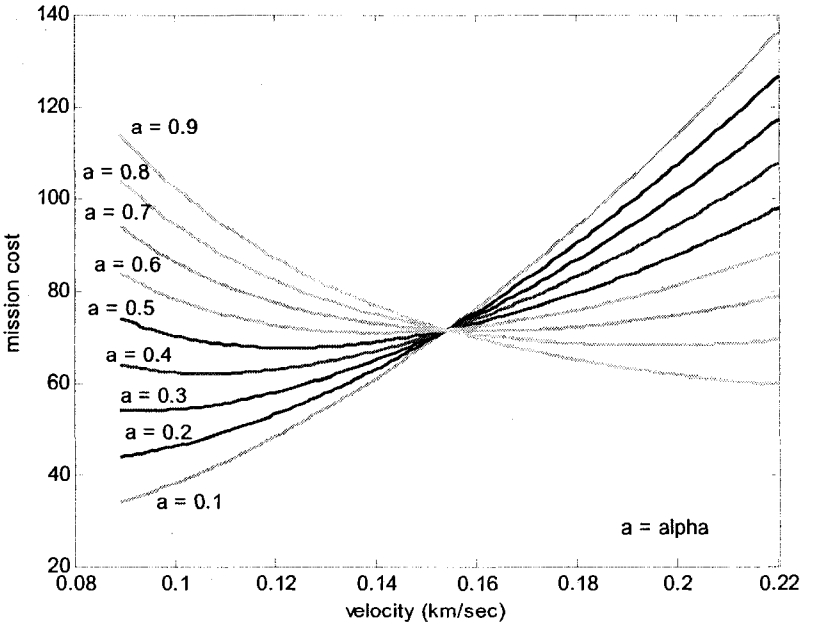

Figure 4.9: Surveillance Mission Costs of UAV2 and UAV3 for case II, and for the nominal velocity range: $89m/s \leq v_{2,3} \leq 220m/s$.

Finally, Table 4.5, given below, shows that for all values of α, as expected, the Minimum Team Cost of the three vehicle team is always lower than that of the two vehicle team. As seen from Tables 4.2, 4.3, and 4.4, the Minimum Surveillance Mission cost values of the individual vehicles (UAV1, UAV2, and UAV3) in the three vehicle team are always lower than that of the two vehicle team. This is because both UAV2 and UAV3 have to cover a greater distance as compared with each of the vehicles in the three vehicle team.

Table 4.5: Comparison of Minimum Team Cost values for case I and case II when the velocity range of UAV1 is: $89m/s \leq v_1 \leq 198m/s$

alpha (α)	$\min \sum_{i=1}^{N} J_{sm_i}$ (Minimum Team Cost)	
	Case I (N = 3)	**Case II (N = 2)**
0.1	66.17	67.68
0.2	84.57	87.68
0.3	102.89	107.54
0.4	118.35	123.76
0.5	129.23	135.14
0.6	135.48	141.66
0.7	136.42	142.64
0.8	130.26	136.20
0.9	114.43	119.30

To see if further lowering the velocity of UAV1 will have any impact on the overall team cost of the three vehicle team (i.e., whether it will remain lower or become higher than that of the two vehicle team), we gradually decrease UAV1's maximum velocity. In Section 4.4.2, the maximum velocity of UAV1 is further lowered to 50% of the nominal maximum velocity, 220m/s (same for all three vehicles). The simulation

results for the cases where the maximum velocity of UAV1 is decreased to 80%, 70% and 60% of its nominal maximum value are shown in the Appendix A. As in Section 4.4.1, wherein the maximum velocity of UAV1 is limited to 90% of the nominal maximum velocity, two cases, namely case I and case II are considered in Section 4.4.2 as well. However, it should be noted that for case I, only the results for UAV1 are tabulated in Table 4.6. The results for UAV2 and UAV3 are tabulated in Table 4.3 for case I and in Table 4.4 for case II. This is because the velocity range of these vehicles remains the same throughout the simulations, (89m/s – 220m/s) i.e., they do not suffer from an actuator fault. UAV1 is the only vehicle in which the actuator fault is simulated, and hence its results have to be tabulated for each velocity set.

4.4.2 Velocity Set 5: UAV1: 89-110m/s, UAV2: 89-220m/s, UAV3: 89-220m/s

Case I: Two healthy vehicles, 1 faulty vehicle performing surveillance

Table 4.6: Minimum Surveillance mission cost of UAV1 when its maximum velocity is at 50% of the nominal value, 220m/s.

alpha (α)	v_1 (m/s)	min_J_{sm_1}	J_{fuel_1} (km^3/sec^2)	t_{s_1} (hours)
0.1	89	16.55	15.92	6.273
0.2	89	17.19	15.92	6.273
0.3	89	17.82	15.92	6.273
0.4	89	18.45	15.92	6.273
0.5	89	19.08	15.92	6.273
0.6	90	19.71	16.28	6.204
0.7	103	19.85	21.32	5.421
0.8	110	19.26	24.32	5.076
0.9	110	18.63	24.32	5.076

Table 4.6 shows that UAV1 incurs its minimum Surveillance Mission cost at α = 0.1, and at its minimum velocity of 89m/s. For α = 0.2 to 0.5, UAV1 maintains the same velocity (89m/s) as well as fuel cost (15.92 km^3/sec^2) and surveillance mission time (6.273 hours) as in α = 0.1. However, its minimum Surveillance Mission cost increases as α increases from 0.1 to 0.5. This is because the weighting given to the surveillance mission time (which remains constant at its maximum value of 6.273 hours from α = 0.1 to 0.5) increases with an increasing α , which in turn leads to an increase in the value of the minimum Surveillance Mission cost.

In Table 4.7, the Minimum Team Cost values of the three vehicle team (Case I: UAV1, UAV2, and UAV3) and the two vehicle team (Case II: UAV2 and UAV3) are tabulated.

Table 4.7: Comparison of Minimum Team Cost values for case I and case II when the velocity range of UAV1 is: $89m/s \le v_1 \le 110m/s$.

alpha (α)	$\min \sum_{i=1}^{N} J_{sm_i}$ (Minimum Team Cost)	
	Case I (N = 3)	**Case II (N = 2)**
0.1	61.75	67.68
0.2	75.75	87.68
0.3	89.64	107.54
0.4	101.09	123.76
0.5	109.32	135.14
0.6	114.31	141.66
0.7	115.11	142.64
0.8	110.22	136.20
0.9	98.31	119.30

Comparing the Minimum Team Cost values for case II in Tables 4.5 and 4.7, one can see that these values are the same. This is because UAV2 and UAV3 do not suffer from an actuator fault, and hence their Minimum Surveillance Mission cost values do not change from one Velocity Set to the next. However, since the velocity range of UAV1 is reduced from 89m/s-198m/s in Section 4.4.1 to 89m/s-110m/s in Section 4.4.2, the Minimum Team Cost values of the three vehicle team in case I are affected, and hence, these values change from Table 4.5 to Table 4.7.

From Tables 4.5 and 4.7, and the simulation results for the three cases included in the Appendix A, it can be seen that even when the maximum velocity of UAV1 is reduced from 90% down to 50% of its nominal value, the team of three vehicles is still a better choice for performing the surveillance mission. This is because the Minimum Team Cost of the three vehicle team is always (i.e., for $\alpha = 0.1$ to 0.9) lower than that of the team of two healthy vehicles (UAV2 and UAV3). Hence, one may conclude from these results that when we consider the actuator fault to be in a single vehicle in a team of only three vehicles, it is not the extent of the fault in the actuator but rather the search distance to be covered by each vehicle that determines whether a team of two or three vehicles is better suited for performing the given mission.

4.5 Performance Under a Sensor Fault

In the second set of simulations, sensor range has been used as a fault variable to simulate a sensor fault in a single UAV. The extent of the sensor fault has been

simulated through gradual reduction of the sensor range of the affected vehicle. As in the case of the actuator fault, the goal here is to determine whether a team of three vehicles is better suited for the surveillance mission or a team of two vehicles.

The nominal circular sensor range of each vehicle is 100 meters. It is assumed that the fault in the sensor of UAV1 occurs before the beginning of the surveillance mission. To simulate the sensor fault, the sensor range of UAV1 is gradually reduced from 80 meters to 50 meters and finally to 25 meters. Since UAV2 and UAV3 are in a healthy state, their sensor range remains at 100 meters for the duration of the mission. Hence, the results of UAV2 and UAV3 are not shown in the simulations that follow. These results are available in Tables 4.3, and 4.4., and Figures 4.8, and 4.9 respectively. It should be noted that the velocity range of each vehicle is assumed to be between the nominal range, $89m/s \leq v_{1,2,3} \leq 220m/s$. In the following tables, the results for the sensor ranges of 80 meters and 50 meters are given, while the results for the sensor range of 25 meters are given in the Appendix A.

In Sections 4.5.1 and 4.5.2, the sensor range of UAV1 is reduced to 80% and 50% of its nominal range of 100 meters, respectively. As in the case of the Actuator Fault in Section 4.4, two cases are considered, namely case I and case II, in order to determine whether a team of three vehicles (two healthy and one faulty) or a team of two healthy vehicles is better suited for performing the surveillance mission.

4.5.1 Sensor Range: UAV1: 80 meters, UAV2: 100 meters, UAV3: 100 meters

Case I: Two healthy vehicles, 1 faulty vehicle performing surveillance

Table 4.8: Minimum Surveillance mission cost of UAV1 when its sensor range is at 80% of the nominal value, 100 meters.

alpha (α)	v_1 (m/s)	min_J_{sm_1}	J_{fuel_1} (km^3/sec^2)	t_{s_1} (hours)
0.1	89	28.22	19.88	7.834
0.2	89	36.56	19.88	7.834
0.3	92	44.84	21.24	7.579
0.4	106	51.60	28.20	6.578
0.5	122	56.34	37.36	5.715
0.6	139	59.06	48.50	5.016
0.7	162	59.47	65.87	4.304
0.8	193	56.79	93.49	3.613
0.9	220	49.74	121.5	3.169

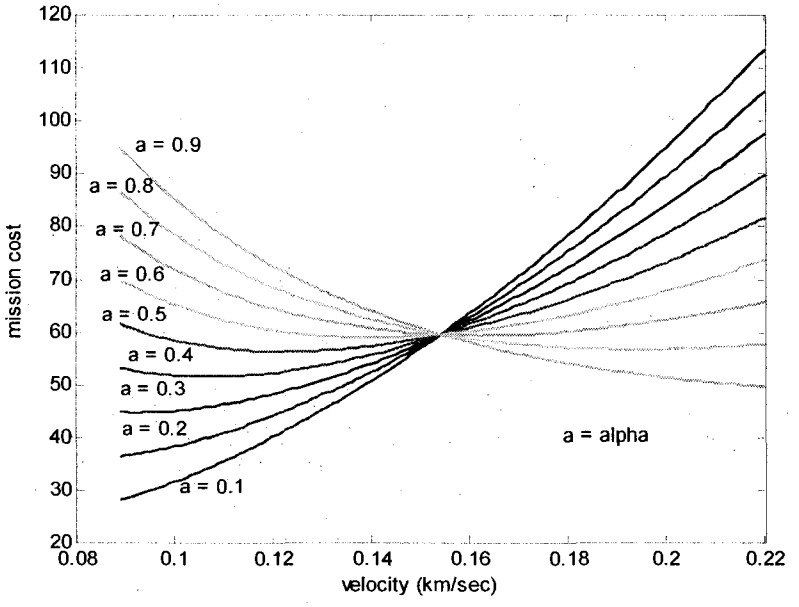

Figure 4.10: Surveillance Mission Costs of UAV1 for a sensor range of 80 meters.

For case I, the results of only UAV1 are tabulated in Table 4.8 and graphed in Figure 4.10. The results for UAV2 and UAV3, for both case I and case II, are not tabulated since we assume that these vehicles function within normal parameters, i.e., they maintain a velocity within the nominal velocity range of 89 m/s – 220 m/s and have a nominal sensor range spanning 100 meters. Hence, as was pointed out in Section 4.4, the results for UAV2 and UAV3, for both case I and case II, only need to be found once, and are tabulated in Tables 4.3 and 4.4.

For the results in Table 4.8 and Table 4.9, it is assumed that the sensor range of UAV1 is 80 meters as compared with the nominal sensor range of 100 meters for UAV2 and UAV3. As seen from Equation (4.4), reducing the sensor range of UAV1 leads to an increase in the value of the term, $\frac{WRA}{SR\_UAV_i}$, which, for UAV1, represents the number of times UAV1 has to travel along the length of the rectangular region. An increase in the value of the term $\frac{WRA}{SR\_UAV_i}$, leads to an increase in the distance covered by UAV1, which in turn leads to an increase in both the fuel cost (given by Equation (4.3)) and the surveillance mission time (given by Equation (4.5)) of UAV1. According to Equation (4.6), an increase in the fuel cost and surveillance mission time of UAV1 leads to an increase in the surveillance mission cost of UAV1. Hence, a reduced sensor range leads to an increase in the surveillance mission cost.

Observing the results of Table 4.8 and Figure 4.10 in entirety will not help us in understanding the effect of a reduced sensor range on the fuel cost and surveillance

mission time of UAV1. However, comparing the results of the fuel cost and the surveillance mission time for $\alpha = 0.1$ in Table 4.8 with those in Tables 4.2 and 4.6, we can see that for a given velocity of 89 m/s, the fuel cost and the surveillance mission time of UAV1 increase as its sensor range is reduced.

Table 4.9 shows that even with a limited reduction in the sensor range in a single vehicle in a three vehicle team, the team of two healthy vehicles always (i.e., for $\alpha = 0.1$ to 0.9) incurs a lower Minimum Team Cost than a team of two healthy vehicles and one faulty vehicle.

Table 4.9: Comparison of Minimum Team Cost values for case I and case II when the sensor range of UAV1 is 80 meters.

alpha (α)	$\min \sum_{i=1}^{N} J_{sm_i}$ (Minimum Team Cost)	
	Case I (N = 3)	**Case II (N = 2)**
0.1	73.42	67.68
0.2	95.12	87.68
0.3	116.66	107.54
0.4	134.24	123.76
0.5	146.58	135.14
0.6	153.66	141.66
0.7	154.72	142.64
0.8	147.75	136.20
0.9	129.42	119.30

From the results in Tables 4.5 and 4.7, we have seen that even with either a limited or a significant reduction in the maximum velocity of a single vehicle in a three vehicle team, a three vehicle team always incurs a lower Minimum Team Cost than a

team of two healthy vehicles. However, for those results, the sensor range of all three vehicles was assumed to be nominal, i.e., 100 meters, which is not the case for the results in Table 4.9, where the sensor range of UAV1 is limited to 80 meters. Comparison of these results shows that for our chosen surveillance scenario, a reduced sensor range and hence an increase in the distance covered by a vehicle has a more significant impact on a team's performance than a fault in a vehicle's actuator.

In Section 4.5.2, the sensor range of UAV1 is further reduced to 50% of its nominal range of 100 meters, respectively.

4.5.2 Sensor Range: UAV1: 50 meters, UAV2: 100 meters, UAV3: 100 meters

Case I: Two healthy vehicles, 1 faulty vehicle performing surveillance

Table 4.10: Minimum Surveillance mission cost of UAV1 when its sensor range is at 50% of the nominal value, 100 meters.

alpha (α)	v_1 (m/s)	min_J_{sm_1}	J_{fuel_1} (km^3/sec^2)	t_{s_1} (hours)
0.1	89	45.08	31.76	12.52
0.2	89	58.40	31.76	12.52
0.3	92	71.64	33.94	12.11
0.4	107	82.43	45.91	10.41
0.5	122	90.02	59.68	9.13
0.6	140	94.36	78.60	7.956
0.7	162	95.01	105.2	6.876
0.8	193	90.73	149.4	5.771
0.9	220	79.47	194.1	5.063

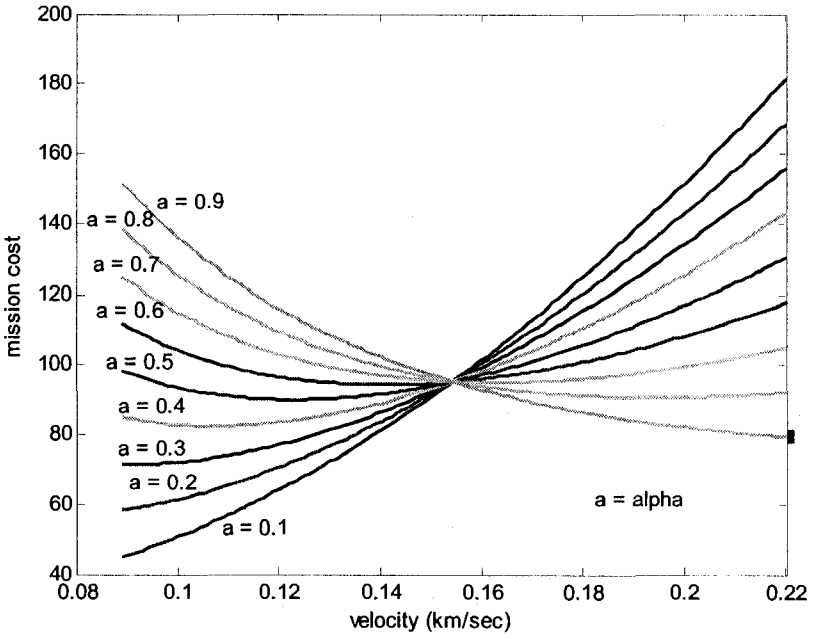

Figure 4.11: Surveillance Mission Costs of UAV1 for a sensor range of 50 meters.

For reasons given in Section 4.5.1, the results in Section 4.5.2 also only include case I for UAV1 (Table 4.10 and Figure 4.11) and the comparison of the Minimum Team Cost values for case I and case II (Table 4.11).

Comparing the results in Tables 4.8 and 4.10, we can see that for equivalent velocities, the fuel cost and the surveillance mission time values are higher in Table 4.10 than in Table 4.8. These results are expected since the sensor range of UAV1 for the results in Table 4.10 is limited to 50 meters as compared with 80 meters for Table 4.8. Following the results from Tables 4.8 and 4.10, a comparison of the Minimum Team Cost values for case I in Table 4.11 with those in Table 4.9 also shows that a further

decrease in the sensor range of UAV1 from 80 meters to 50 meters leads to a higher Minimum Team Cost value for $\alpha = 0.1$ to 0.9.

Table 4.11: Comparison of Minimum Team Cost values for case I and case II when the sensor range of UAV1 is 50 meters.

alpha (α)	$\min \sum_{i=1}^{N} J_{sm_i}$ (Minimum Team Cost)	
	Case I (N = 3)	**Case II (N = 2)**
0.1	90.28	67.68
0.2	116.96	87.68
0.3	143.46	107.54
0.4	165.07	123.76
0.5	180.26	135.14
0.6	188.96	141.66
0.7	190.27	142.64
0.8	181.69	136.20
0.9	159.15	119.30

From Tables 4.9, 4.11, and A.8 (Appendix A. These are the results for a sensor range of 25 meters for UAV1.), it can be seen that for all the values of α, the Minimum Team Cost value of the team of two vehicles is always lower than that of the team of three vehicles, making the team of 2 healthy vehicles (UAV2 and UAV3) a better choice for performing the surveillance mission. The explanation for these results is that as the sensor range of UAV1 decreases, its search distance increases, leading to an increase in its fuel cost and surveillance mission time, which in turn lead to an increase in its Minimum Surveillance mission costs (for $\alpha = 0.1$ to 0.9). With a sensor range of 80 meters, the distance covered by UAV1 is 2510 km (see Equation (4.4)), which increases to 4010 km as its sensor range reduces to 50 meters. Moreover, when the sensor range of

UAV1 is 80 meters, the overall distance to be covered by the three vehicle team is 6530 km (UAV1: 2510 km, UAV2: 2010 km, UAV3: 2010 km), which increases to 8030 km (UAV1: 4010 km, UAV2: 2010 km, UAV3: 2010 km) as the sensor range of UAV1 decreases to 50 meters. In comparison, the overall distance to be covered by the two vehicle team remains at 6020 km (UAV2: 3010 km, UAV3: 3010 km). Hence, from these results, it can be concluded that the team whose search distance is lower is the one that should be chosen to perform the surveillance mission.

4.6 Performance Under Sensor and Actuator Faults

In the third set of simulations, both sensor range and velocity have been used as fault variables to simulate a sensor and an actuator fault in a single UAV. It is assumed that before the start of the surveillance mission, the actuator of UAV1 is suffering from Loss of Effectiveness, whereas the sensor is subject to a multiplicative type sensor failure. To simulate these two faults simultaneously, two sets of simulations have been carried out.

In the first set, the sensor range of UAV1 is assumed to be limited to 80 meters, whereas that of UAV2 and UAV3 is 100 meters. The maximum velocity of UAV1 is reduced to: 90% (198 m/s), 80% (176 m/s), 70% (154 m/s), 60% (132 m/s), and 50% (110 m/s) of its nominal maximum velocity, 220 m/s. As before, the velocity range of UAV2 and UAV3 remains between 89 m/s and 220 m/s for the duration of the mission.

In the second set of simulations, the sensor range of UAV1 is assumed to be limited to 50 meters. For this sensor range, the maximum velocity of UAV1 is reduced to 60% (132 m/s), and 50% (110 m/s) of the maximum velocity, 220 m/s. For the third set of simulations, the sensor range of UAV1 is further reduced to 25 meters, and its maximum velocity is dropped to 110 m/s. As in the cases of the actuator fault and the sensor fault, the mission designer must use minimization of the team cost as a performance measure to select either a team of all three vehicles or a team of two healthy vehicles to perform the surveillance mission.

4.6.1 Results of Simulation Set 1: Sensor Range: UAV1: 80 meters, UAV2: 100 meters, UAV3: 100 meters

4.6.1.1 Velocity Range: UAV1: 89-198 m/s, UAV2: 89-220 m/s, UAV3: 89-220 m/s

The results tabulated in Table 4.12 show, for α = 0.1 to 0.9, the Minimum Surveillance Mission cost, the fuel cost, and the surveillance mission time of UAV1 when it is suffering from a simultaneous sensor and actuator fault. As explained in the previous section, the results for UAV2 and UAV3 for both cases, i.e., case I and case II only need to be recorded once (the results for case I are recorded in Table 4.3 whereas those of case II are recorded in Table 4.4) since these vehicles are considered to be healthy. Table 4.13 compares the Minimum Team Cost values of the three vehicle team with those of the two vehicle team.

Table 4.12: Minimum Surveillance Mission costs of UAV1 when its maximum velocity is at 90% and its sensor range is at 80% of the nominal values.

alpha (α)	v_1 (m/s)	min_J_{sm_1}	J_{fuel_1} (km^3/sec^2)	t_{s_1} (hours)
0.1	89	26.1891	19.88	7.834
0.2	89	32.4965	19.88	7.834
0.3	89	38.8039	19.88	7.834
0.4	99	44.5908	24.6	7.043
0.5	113	48.6918	32.05	6.17
0.6	130	51.0432	42.42	5.363
0.7	149	51.3952	55.72	4.679
0.8	179	49.0783	80.42	3.895
0.9	198	43.3995	98.40	3.521

Table 4.13: Comparison of Minimum Team Cost values for case I and case II when the maximum velocity of UAV1 is 198 m/s and its sensor range is 80 meters.

alpha (α)	$\min \sum_{i=1}^{N} J_{sm_i}$ (Minimum Team Cost)	
	Case1 (N = 3)	**Case2 (N = 2)**
0.1	71.3856	67.68
0.2	91.0471	87.68
0.3	110.6187	107.54
0.4	127.2306	123.76
0.5	138.9329	135.14
0.6	145.6420	141.66
0.7	146.6467	142.64
0.8	140.0351	136.20
0.9	123.0709	119.30

From Table 4.13, it can be seen that when the maximum velocity of UAV1 is 198m/s (90% of the maximum velocity under nominal conditions), and its sensor range

is 80 meters, the Minimum Team Cost of the team of two vehicles is always lower than that of the team of three vehicles.

To understand these results, one has to observe the effect of the actuator fault in Tables 4.2 and 4.5, and the sensor fault in Tables 4.8 and 4.9 on the performance of the team of three vehicles. In Table 4.5, it has been shown that when UAV1 is operating under an actuator fault with its maximum velocity reduced to 90% (198m/s) of the nominal value, 220m/s, the team of three vehicles is better suited to perform the mission. We have seen that this happens because the distance to be covered by each vehicle in the two vehicle team (UAV2: 3010 km, UAV3: 3010 km) is 1000 km more than that of each vehicle in the three vehicle team (UAV1: 2010 km, UAV2: 2010 km UAV3: 2010 km). Hence, for the team of two vehicles, a greater distance translates into an increase in fuel cost and surveillance mission time, which lead to an increase in the individual vehicle costs. Table 4.9 shows that when UAV1 is operating with a perfectly functioning actuator but a reduced sensor range of 80 meters, the team of two healthy vehicles is the better option. Here, a reduced sensor range of UAV1 leads to an increase in its surveillance distance, which leads to an increase in the mission cost of UAV1, and ultimately the team cost. However, an increased team cost for the team of three vehicles does not necessarily mean that this cost will always be higher than that of the team of two UAVs. For the given case (i.e., the results in Tables 4.12 and 4.13), the overall search distance of the team of three vehicles (UAV1: 2510 km + UAV2: 2010 km + UAV3: 2010 km = 6530 km) is greater than that of the team of two vehicles (6020 km) and as the results in the previous section (sensor fault) have shown, the team with the

overall lower surveillance distance is the one that incurs the lower Minimum Team cost for $\alpha = 0.1$ to 0.9.

Given the aforementioned results, one would expect and the results show that for all values of α, the minimum team cost values for the three vehicle team in Table 4.13 would be lower than those in Table 4.9 (sensor fault) but higher than those of Table 4.5 (actuator fault). While the surveillance distance of UAV1 (for the results in Tables 4.12 and 4.13) is the same (equal to 2510 km) as in the reduced sensor range scenario in Tables 4.8 and 4.9, its maximum velocity is lower (equal to 198 m/s), which leads to a decreased average fuel cost but an increased average surveillance mission time (as compared with the results in Table 4.8). Hence, the value of β (the scaling factor in Equation (4.6)) is lower, which leads to a decreased Minimum Surveillance Mission cost of UAV1 for $\alpha = 0.1$ to 0.9. This can be seen when the results showing the Minimum Surveillance Mission costs of UAV1 in Table 4.8 (sensor fault) and Table 4.12 (sensor and actuator fault) are compared. As for the actuator fault, the Minimum Surveillance Mission costs of UAV1 are lower than the sensor and actuator fault case due to UAV1's lower search distance (2010 km).

However, even knowing that the Minimum Team costs for the three vehicle team, where one vehicle is suffering from a simultaneous actuator and sensor fault, are lower than the case involving the sensor fault, and higher than the case involving the actuator fault, one still cannot predict that the Minimum Team cost values of the three vehicle team in Table 4.13 will be higher than that of the two vehicle team.

To see if further lowering the velocity of UAV1 will have any impact on the overall team cost of the three vehicle team, we gradually decrease UAV1's maximum velocity. The next sets of simulation results show the effect of lowering the velocity of UAV1 to 80% (176 m/s), 70% (154 m/s), 60% (132 m/s), and 50% (110 m/s) of its nominal maximum velocity, 220 m/s.

4.6.1.2 Velocity Range: UAV1: 89-176 m/s, UAV2: 89-220 m/s, UAV3: 89-220 m/s

The results tabulated in Table 4.14 show, for α = 0.1 to 0.9, the Minimum Surveillance Mission cost, the fuel cost, and the surveillance mission time of UAV1 when it is suffering from a simultaneous sensor and actuator fault. Here, as in Table 4.12, the sensor range of UAV1 is limited to 80 meters, whereas the maximum velocity of UAV1 is further reduced to 80% of its nominal value (176 m/s). For UAV2 and UAV3, the results for case I are recorded in Table 4.3 whereas those of case II are recorded in Table 4.4. Table 4.15 compares the Minimum Team Cost values of the three vehicle team with those of the two vehicle team.

Table 4.14: Minimum Surveillance Mission costs of UAV1 when its maximum velocity is at 80% and its sensor range is at 80% of the nominal values.

alpha (α)	v_1 (m/s)	min_J_{sm_1}	J_{fuel_1} (km^3/sec^2)	t_{s_1} (hours)
0.1	89	24.4373	19.88	7.834
0.2	89	28.9929	19.88	7.834
0.3	89	33.5484	19.88	7.834
0.4	91	38.0682	20.79	7.662
0.5	104	41.5694	27.15	6.704
0.6	119	43.5773	35.54	5.859
0.7	138	43.8779	47.80	5.052
0.8	165	41.8994	68.33	4.226
0.9	176	37.5565	77.75	3.961

Table 4.15: Comparison of Minimum Team Cost values for case I and case II when the maximum velocity of UAV1 is 176 m/s and its sensor range is 80 meters.

alpha (α)	$\min \sum_{i=1}^{N} J_{sm_i}$ (Minimum Team Cost)	
	Case I (N = 3)	**Case II (N = 2)**
0.1	69.6338	67.68
0.2	87.5435	87.68
0.3	105.3633	107.54
0.4	120.7080	123.76
0.5	131.8105	135.14
0.6	138.1761	141.66
0.7	139.1293	142.64
0.8	132.8562	136.20
0.9	117.2279	119.30

4.6.1.3 Velocity Range: UAV1: 89-154 m/s, UAV2: 89-220 m/s, UAV3: 89-220 m/s

The results tabulated in Table 4.16 show, for α = 0.1 to 0.9, the Minimum Surveillance Mission cost, the fuel cost, and the surveillance mission time of UAV1 when it is suffering from a simultaneous sensor and actuator fault. Here, as in Tables 4.12 and 4.14, the sensor range of UAV1 is limited to 80 meters, whereas the maximum velocity of UAV1 is further reduced to 70% of its nominal value (154 m/s). For UAV2 and UAV3, the results for case I are recorded in Table 4.3 whereas those of case II are recorded in Table 4.4. Table 4.17 compares the Minimum Team Cost values of the three vehicle team with those of the two vehicle team.

Table 4.16: Minimum Surveillance Mission costs of UAV1 when its maximum velocity is at 70% and its sensor range is at 80% of the nominal values.

α	v_1 (m/s)	$\min\_J_{sm_1}$	J_{fuel_1} (km^3/sec^2)	t_{s_1} (hours)
0.1	89	22.9463	19.88	7.834
0.2	89	26.0108	19.88	7.834
0.3	89	29.0754	19.88	7.834
0.4	89	32.1399	19.88	7.834
0.5	95	34.9876	22.65	7.339
0.6	109	36.6771	29.82	6.397
0.7	127	36.9297	40.48	5.49
0.8	153	35.2647	58.76	4.557
0.9	154	32.2335	59.53	4.527

Table 4.17: Comparison of Minimum Team Cost values for case I and case II when the maximum velocity of UAV1 is 154 m/s and its sensor range is 80 meters.

alpha (α)	$\min \sum_{i=1}^{N} J_{sm_i}$ (Minimum Team Cost)	
	Case I (N = 3)	**Case II (N = 2)**
0.1	68.1428	67.68
0.2	84.5615	87.68
0.3	100.8902	107.54
0.4	114.7797	123.76
0.5	125.2287	135.14
0.6	131.2759	141.66
0.7	132.1812	142.64
0.8	126.2215	136.20
0.9	111.9049	119.30

4.6.1.4 Velocity Range: UAV1: 89-132 m/s, UAV2: 89-220 m/s, UAV3: 89-220 m/s

The results tabulated in Table 4.18 show, for α = 0.1 to 0.9, the Minimum Surveillance Mission cost, the fuel cost, and the surveillance mission time of UAV1 when it is suffering from a simultaneous sensor and actuator fault. Here, as in Tables 4.12, 4.14, and 4.16, the sensor range of UAV1 is limited to 80 meters, whereas the maximum velocity of UAV1 is further reduced to 60% of its nominal value (132 m/s). For UAV2 and UAV3, the results for case I are recorded in Table 4.3 whereas those of case II are recorded in Table 4.4. Table 4.19 compares the Minimum Team Cost values of the three vehicle team with those of the two vehicle team.

Table 4.18: Minimum Surveillance Mission costs of UAV1 when its maximum velocity is at 60% and its sensor range is at 80% of the nominal values.

alpha (α)	v_1 (m/s)	min_J_{sm_1}	J_{fuel_1} (km^3/sec^2)	t_{s_1} (hours)
0.1	89	21.6975	19.88	7.834
0.2	89	23.5132	19.88	7.834
0.3	89	25.3290	19.88	7.834
0.4	89	27.1447	19.88	7.834
0.5	89	28.9605	19.88	7.834
0.6	100	30.3530	25.10	6.972
0.7	116	30.5621	33.77	6.011
0.8	132	29.2650	43.73	5.282
0.9	132	27.4563	43.73	5.282

Table 4.19: Comparison of Minimum Team Cost values for case I and case II when the maximum velocity of UAV1 is 132 m/s and its sensor range is 80 meters.

alpha (α)	$\min \sum_{i=1}^{N} J_{sm_i}$ (Minimum Team Cost)	
	Case I (N = 3)	**Case II (N = 2)**
0.1	66.8940	67.68
0.2	82.0638	87.68
0.3	97.1438	107.54
0.4	109.7845	123.76
0.5	119.2016	135.14
0.6	124.9517	141.66
0.7	125.8135	142.64
0.8	120.2218	136.20
0.9	107.1278	119.30

4.6.1.5 Velocity Range: UAV1: 89-110 m/s, UAV2: 89-220 m/s, UAV3: 89-220 m/s

The results tabulated in Table 4.20 show, for α = 0.1 to 0.9, the Minimum Surveillance Mission cost, the fuel cost, and the surveillance mission time of UAV1 when it is suffering from a simultaneous sensor and actuator fault. Here, as in Tables 4.12, 4.14, 4.16, and 4.18, the sensor range of UAV1 is limited to 80 meters, whereas the maximum velocity of UAV1 is further reduced to 50% of its nominal value (110 m/s). For UAV2 and UAV3, the results for case I are recorded in Table 4.3 whereas those of case II are recorded in Table 4.4. Table 4.21 compares the Minimum Team Cost values of the three vehicle team with those of the two vehicle team.

Table 4.20: Minimum Surveillance Mission costs of UAV1 when its maximum velocity is at 50% and its sensor range is at 80% of the nominal values.

alpha (α)	v_1 (m/s)	min_J_{sm_1}	J_{fuel_1} (km^3/sec^2)	t_{s_1} (hours)
0.1	89	20.6716	19.88	7.834
0.2	89	21.4615	19.88	7.834
0.3	89	22.2513	19.88	7.834
0.4	89	23.0412	19.88	7.834
0.5	89	23.8311	19.88	7.834
0.6	89	24.6155	19.88	7.834
0.7	105	24.7849	27.67	6.64
0.8	110	24.0558	30.37	6.338
0.9	110	23.2664	30.37	6.338

Table 4.21: Comparison of Minimum Team Cost values for case I and case II when the maximum velocity of UAV1 is 110 m/s and its sensor range is 80 meters.

alpha (α)	$\min \sum_{i=1}^{N} J_{sm_i}$ (Minimum Team Cost)	
	Case I (N = 3)	**Case II (N = 2)**
0.1	65.8681	67.68
0.2	80.0121	87.68
0.3	94.0662	107.54
0.4	105.6810	123.76
0.5	114.0722	135.14
0.6	119.2143	141.66
0.7	120.0364	142.64
0.8	115.0125	136.20
0.9	102.9378	119.30

Contrary to the results of Table 4.13, Tables 4.15 and 4.17 show that when the maximum velocity of UAV1 drops to 176 m/s and 154 m/s, the Minimum Team cost of the three vehicle team is lower than that of the two vehicle team for all values of α except $\alpha = 0.1$. For the last two cases, where in one the maximum velocity of UAV1 is 132 m/s (Table 4.19), and the other, the maximum velocity of UAV1 is 110 m/s (Table 4.21), the Minimum Team cost of the three vehicle team is always lower than that of the two vehicle team. Hence, for these two cases, the team of 3 vehicles is always better suited to perform the surveillance mission than the team of 2 vehicles. These results show that the Minimum Surveillance Mission cost of the team of three vehicles is lower than that of the team of two healthy vehicles if the sensor fault in a single vehicle (in the three vehicle team) is limited and its maximum velocity is low (i.e., there is an increased degradation in the performance of its actuator).

The results of Simulation Set 1 have shown that when the maximum velocity of UAV1 drops down to 60% (132 m/s), and 50% (110 m/s) of its nominal value, the minimum team cost of the three vehicle team is always lower than that of the two vehicle team. However, for the first set of simulations, the sensor fault is limited (i.e., the sensor range of UAV1 is assumed to be 80 meters as compared with 100 meters, which is the sensor range of the two healthy vehicles, UAV2 and UAV3). Hence, the goal of simulation set 2 is to determine the impact of further decreasing the sensor range of UAV1 on the performance of the three vehicle team. To this end, the maximum velocity of UAV1 is decreased to 132 m/s and 110 m/s, and its sensor range is limited to 50 meters.

4.6.2 Results of Simulation Set 2: Sensor Range: UAV1: 50 meters, UAV2: 100 meters, UAV3: 100 meters

As stated in the previous section, the goal of simulation set 2 is to determine the impact of further decreasing the sensor range of UAV1 on the performance of the three vehicle team. Hence, in the second set of simulations, the sensor range of UAV1 is assumed to be limited to 50 meters. For this sensor range, the maximum velocity of UAV1 is reduced to 60% (132 m/s), and 50% (110 m/s) of the nominal maximum velocity, 220 m/s.

4.6.2.1 Velocity Range: UAV1: 89-132 m/s, UAV2: 89-220 m/s, UAV3: 89-220 m/s

The results tabulated in Table 4.22 show, for α = 0.1 to 0.9, the Minimum Surveillance Mission cost, the fuel cost, and the surveillance mission time of UAV1 when it is suffering from a simultaneous sensor and actuator fault. Here, the sensor range of UAV1 is limited to 50 meters, whereas the maximum velocity of UAV1 is limited to 60% of its nominal value (132 m/s). For UAV2 and UAV3, the results for case I are recorded in Table 4.3 whereas those of case II are recorded in Table 4.4. Table 4.23 compares the Minimum Team Cost values of the three vehicle team with those of the two vehicle team.

Table 4.22: Minimum Surveillance Mission costs of UAV1 when its maximum velocity is at 60% and its sensor range is at 50% of the nominal values.

alpha (α)	v_1 (m/s)	min_J_{sm_1}	J_{fuel_1} (km^3/sec^2)	t_{s_1} (hours)
0.1	89	34.6641	31.76	12.52
0.2	89	37.5649	31.76	12.52
0.3	89	40.4658	31.76	12.52
0.4	89	43.3667	31.76	12.52
0.5	89	46.2676	31.76	12.52
0.6	100	48.4922	40.10	11.14
0.7	115	48.8263	53.03	9.686
0.8	132	46.7540	69.87	8.439
0.9	132	43.8645	69.87	8.439

Table 4.23: Comparison of Minimum Team Cost values for case I and case II when the maximum velocity of UAV1 is 132 m/s and its sensor range is 50 meters.

alpha (α)	$\min \sum_{i=1}^{N} J_{sm_i}$ (Minimum Team Cost)	
	Case I (N = 3)	**Case II (N = 2)**
0.1	79.8606	67.68
0.2	96.1156	87.68
0.3	112.2807	107.54
0.4	126.0065	123.76
0.5	136.5087	135.14
0.6	143.0910	141.66
0.7	144.0777	142.64
0.8	137.7108	136.20
0.9	123.5359	119.30

From Table 4.23, it can be seen that when the maximum velocity of UAV1 is 132 m/s, and its sensor range is 50 meters, the minimum value of team cost of the three vehicle team is always higher (i.e., for all values of α) than that of the two vehicle team. However, it can be seen from Table 4.25 that when the maximum velocity of UAV1 is 110 m/s, and its sensor range is 50 meters, the minimum team cost of the three vehicle team is lower than that of the two vehicle team for all values of α except $\alpha = 0.1$ and $\alpha = 0.2$. These results show that if a greater emphasis is placed on minimization of the surveillance mission time as compared with the fuel cost of UAV1, i.e., a higher value of α is chosen for UAV1, the minimum team cost of the team of three vehicles is lower than that of the team of two vehicles.

4.6.2.2 Velocity Range: UAV1: 89-110 m/s, UAV2: 89-220 m/s, UAV3: 89-220 m/s

The results tabulated in Table 4.24 show, for α = 0.1 to 0.9, the Minimum Surveillance Mission cost, the fuel cost, and the surveillance mission time of UAV1 when it is suffering from a simultaneous sensor and actuator fault. Here, the sensor range of UAV1 is limited to 50 meters, whereas the maximum velocity of UAV1 is limited to 50% of its nominal value (110 m/s). For UAV2 and UAV3, the results for case I are recorded in Table 4.3 whereas those of case II are recorded in Table 4.4. Table 4.25 compares the Minimum Team Cost values of the three vehicle team with those of the two vehicle team.

Table 4.24: Minimum Surveillance Mission costs of UAV1 when its maximum velocity is at 50% and its sensor range is at 50% of the nominal values.

alpha (α)	v_1 (m/s)	min_J_{sm_1}	J_{fuel_1} (km^3/sec^2)	t_{s_1} (hours)
0.1	89	33.0251	31.76	12.52
0.2	89	34.2870	31.76	12.52
0.3	89	35.5490	31.76	12.52
0.4	89	36.8109	31.76	12.52
0.5	89	38.0728	31.76	12.52
0.6	89	39.3260	31.76	12.52
0.7	104	39.5966	43.37	10.71
0.8	110	38.4317	48.52	10.13
0.9	110	37.1705	48.52	10.13

Table 4.25: Comparison of Minimum Team Cost values for case I and case II when the maximum velocity of UAV1 is 110 m/s and its sensor range is 50 meters.

alpha (α)	$\min \sum_{i=1}^{N} J_{sm_i}$ (Minimum Team Cost)	
	Case I (N = 3)	**Case II (N = 2)**
0.1	78.2217	67.68
0.2	92.8377	87.68
0.3	107.3638	107.54
0.4	119.4506	123.76
0.5	128.3139	135.14
0.6	133.9247	141.66
0.7	134.8481	142.64
0.8	129.3885	136.20
0.9	116.8420	119.30

The results in Table 4.25 show that when the sensor range of a single vehicle in a three vehicle team is limited to 50% of its nominal value, the team cost of the team of three vehicles (two healthy and one operating under a sensor and an actuator fault) would only be lower than that of the team of two healthy vehicles if the following conditions are satisfied: 1) The maximum velocity of a single vehicle (UAV1) is reduced to 50% of its nominal value (110 m/s), and 2) A value of $\alpha = 0.3$ or higher is chosen for each vehicle in both team configurations. However, as shown in the Appendix A, if the sensor range is further reduced to 25% of its nominal value, then the team of two healthy vehicles is better suited to perform the surveillance mission, for it incurs a lower cost for all the values of α.

4.7 Conclusions

In this chapter, the multiple UAV Surveillance problem has been investigated using a scenario involving a UAV team tasked to monitor a region of known dimensions along a border between two countries. The goal of the UAVs is to cover the entire surveillance region, while minimizing the team cost, which is a function of each vehicle's fuel consumption and mission time.

It has been assumed that the three vehicle team is operating under either an actuator fault (Loss of Effectiveness), or (a Multiplicative type) sensor fault, or a fault in both the sensor and the actuator of an individual vehicle. The goal of the central controller (mission designer or ground operator) is to determine which team configuration is better suited for performing the surveillance mission i.e., either a three vehicle team or a two vehicle team. Hence, in the simulations, using velocity, sensor range, and a combination of velocity and sensor range of the vehicles as fault variables, the performance of a team of three vehicles is compared with a team of two normally functioning vehicles to determine which team is better suited for the mission and under what conditions.

In the first set of simulations, velocity has been used as a fault variable to simulate an actuator fault in a single UAV. The results show that even when the maximum velocity of a single vehicle in a three vehicle team is reduced from 90% to 50% of its nominal value, the team of three vehicles incurs a lower cost than the team of two healthy vehicles.

In the second set of simulations, sensor range has been used as a fault variable to simulate a sensor fault in a single UAV. The results show that for the three cases of a reduced sensor range of 80 meters, 50 meters and 25 meters, the minimum team cost of the team of two vehicles is always lower than that of the team of three vehicles, thus making the team of 2 healthy vehicles a better choice for performing the surveillance mission. The explanation for these results is that as the sensor range of the affected vehicle decreases, its surveillance distance increases, leading to an increase in its fuel cost and mission time, which in turn lead to an increase in its mission cost, and hence the overall mission cost of the three vehicle team. The conclusion drawn from these results is that the team whose surveillance distance is lower should be chosen to perform the mission.

In the third set of simulations, both sensor range and velocity have been used as fault variables to simulate a sensor and an actuator fault in a single UAV. To simulate these two faults simultaneously, three sets of simulations have been carried out. In the first set, the sensor range of UAV1 is assumed to be limited to 80 meters, whereas that of UAV2 and UAV3 is 100 meters. The maximum velocity of UAV1 is then reduced to 90% (198 m/s), 80% (176 m/s), 70% (154 m/s), 60% (132 m/s), and 50% (110 m/s) of its nominal maximum velocity, 220 m/s. The velocity range of UAV2 and UAV3 remains between 89 m/s and 220 m/s for the duration of the mission. In the second set of simulations, the sensor range of UAV1 is assumed to be limited to 50 meters, and the maximum velocity of UAV1 is reduced to 60% (132 m/s), and 50% (110 m/s) of the maximum velocity, 220 m/s. For the third set of simulations, the sensor range of UAV1

is assumed to be limited to 25 meters, and the maximum velocity of UAV1 is reduced to 110 m/s.

For the first set of simulations, when the maximum velocity of UAV1 is 198 m/s, and its sensor range is 80 meters, the minimum team cost of the team of two vehicles is always lower than that of the team of three vehicles. However, when the maximum velocity of UAV1 drops to 176 m/s and 154 m/s, the minimum team cost of the three vehicle team is lower than that of the two vehicle team for all values of α except $\alpha = 0.1$. For the last two cases, where the maximum velocity of UAV1 is reduced to 132 m/s and 110 m/s respectively, the minimum team cost of the three vehicle team is always lower than that of the two vehicle team. Hence, for these two cases, the team of three vehicles is always better suited to perform the surveillance mission than the team of two vehicles. These results show that the minimum surveillance mission cost of the team of three vehicles is lower than that of the team of two healthy vehicles if the sensor fault in a single vehicle (in the three vehicle team) is limited and there is an increased degradation in the performance of its actuator (which limits the affected vehicle's maximum velocity, and hence its fuel cost).

The objective of the second set of simulations is to determine the impact of further decreasing the sensor range of UAV1 on the performance of the three vehicle team. To this end, the maximum velocity of UAV1 is decreased to 132 m/s and 110 m/s, and its sensor range is limited to 50 meters. The results show that when the sensor range of a single vehicle in a three vehicle team is limited to 50% of its nominal value, the

team cost of the team of three vehicles (two healthy and one operating under a sensor and an actuator fault) would only be lower than that of the team of two healthy vehicles if the following conditions are satisfied: 1) The maximum velocity of a single vehicle (UAV1) is reduced to 50% (110 m/s) or lower of its nominal value, and 2) A value of $\alpha = 0.3$ or higher is chosen for each vehicle in both team configurations.

Finally, for the third set of simulations (see Appendix A), the results show that if the sensor range is decreased to 25 meters, then the team of two healthy vehicles is better suited to perform the surveillance mission, for it incurs a lower minimum team cost value for all values of α.

Chapter 5

Conclusions and Future Work

Due to the complexities of modern warfare, autonomous systems such as UAVs are being employed at an ever increasing pace by the military, which has utilized these vehicles for surveillance and strike missions in operations in Iraq and Afghanistan. Thus far, military organizations have only employed single vehicles operated by ground controllers for completing given missions. However, to enhance its capability of using these vehicles more efficiently, the military is shifting its focus from single vehicle missions to multiple vehicle missions. To this end, researchers in both the military and civilian domains have turned their attention to developing strategies that will allow a group of vehicles to work together to achieve common goals.

In this thesis, we have addressed the problem of employing multiple vehicles for carrying out two disjoint missions, i.e., *Coordinated Strike* and *Multiple UAV Surveillance*. In Chapter 2, we have given an overview of the Coordinated Rendezvous and the *Multiple UAV Search and Surveillance* problems. A brief literature review on the topic of fault detection and identification of sensor and actuator failures has also been included.

The area of cooperative control is relatively new and to date, no unified framework has been developed for categorizing cooperative control problems. Due to this reason, it is difficult to compare different cooperative control algorithms, which are developed for a unique set of problems. In Chapter 3, the cooperative control problem has been illustrated through a simulated Coordinated Rendezvous (*Coordinated Strike*) mission. The objective of the mission is for a team of multiple UAVs to simultaneously arrive at a single high priority target to carry out a coordinated strike. While traveling to the target, the team must minimize its combined exposure to multiple radar sites, and conserve fuel. We have used the coordination strategy based on coordination variables and coordination functions, originally developed by Chandler et al ([8], [9], [10], and [15]) and Beard et al ([4], [5], [6], [7], and [16]). While the aforementioned authors have only tested their strategy under nominal conditions for the rendezvous problem, we have extended it to include an actuator fault in single as well as multiple vehicles in order to determine the effect of faults on the performance of the coordination strategy.

In Chapter 4, we have developed a hypothetical *Multiple UAV Border Surveillance Mission*, wherein the goal of the UAVs is to cover the entire surveillance region, while minimizing the team cost, which is a function of each vehicle's fuel consumption and mission time. It has been assumed that the three vehicle team is operating under either an actuator fault (Loss of Effectiveness), or (a Multiplicative type) sensor fault, or a fault in both the sensor and the actuator of an individual vehicle. The goal of the central controller (mission designer or ground operator) is to determine which team configuration is better suited for performing the surveillance mission i.e.,

either a three vehicle team or a two vehicle team. Hence, in the simulations, using velocity, sensor range, and a combination of velocity and sensor range of the vehicles as fault variables, the performance of a team of three vehicles is compared with a team of two normally functioning vehicles to determine which team is better suited for the mission and under what conditions.

5.1 Future Work

Since the ultimate goal of research into multiple UAVs is to develop coordination algorithms for teams of UAVs performing a wide variety of missions, a possible direction for further research could be to develop a coordination strategy for the combined problems of coordinated strike and multiple UAV search and surveillance. To this end, the environment of operation can be altered to include multiple UAV teams with differing capabilities, multiple hostile (stationary and mobile) targets, and threats, and no-fly zones. To assess the robustness of the coordination strategy, the effect of communication constraints on the performance of multiple UAV teams should be explored. Communication constraints may include a limited range of communication, availability of incomplete or partial crucial information to vehicles, and a transmitter or receiver fault in a single and/or multiple vehicles. We have utilized a distributed architecture for the coordinated strike problem. However, for completeness, performance measures should be developed to compare the centralized and distributed architectures. Finally, robust and efficient algorithms for path planning, trajectory generation, and target assignment (resource allocation) must be developed.

5.2 Thesis Contributions

In this thesis, two disjoint missions, i.e., Coordinated Rendezvous and Multiple UAV Surveillance have been investigated. The Coordinated Rendezvous problem has been studied under nominal conditions by Chandler et al ([8], [9], [10], and [15]) and Beard et al ([4], [5], [6], [7], and [16]). We have extended the Coordinated Rendezvous problem to include an actuator fault in single as well as multiple vehicles in order to determine the effect of actuator faults on the performance of the coordination strategy. The type of actuator fault simulated in this thesis is the Loss of Effectiveness (LOE). Velocity has been used as the fault variable to simulate an actuator fault in single and multiple UAVs. The extent of the actuator fault has been simulated through gradual reduction of the maximum velocity of the UAV. In response to the actuator fault, all UAVs re-generate and share coordinating information with one another in order to re-plan their routes to the target. However, if the degradation in a UAV's actuator is to such an extent that it can no longer rendezvous with the other vehicles at the target, a resource allocation problem is solved in order to determine which vehicles should engage the target.

We have investigated the Multiple UAV Surveillance problem by developing a hypothetical *Border Surveillance Mission*, wherein a (three vehicle) UAV team is tasked to monitor a region of known dimensions along a border between two countries. The goal of the UAVs is to cover the entire surveillance region, while minimizing the team cost, which is a function of each vehicle's fuel consumption and mission time. To

emulate real world situations, where a fault in one or more of the vehicles in a team can occur at any time, we have simulated three cases of faults in different sub systems of a single vehicle in a team in order to determine the effect of the faults on the performance of the team. The affected vehicle is assumed to be suffering from a fault in either its actuator or sensor or both its actuator and sensor. As in the Coordinated Strike mission, the type of actuator fault simulated here is the Loss of Effectiveness (LOE). The type of sensor fault simulated here is called the Multiplicative-type sensor failure. The sensor range (sensor output) has been used as the fault variable to simulate the sensor fault in a single UAV. Despite the presence of either the Loss of Effectiveness actuator fault and/or the Multiplicative-type sensor failure, the goal of the surveillance mission remains the same, which is minimization of the team cost. However, a fault in either the sensor, or actuator or both requires the mission designer to address a resource allocation problem, i.e, whether to carry out the mission using all the three vehicles or two healthy, perfectly functioning vehicles. The team chosen to perform the surveillance mission is the one that incurs the minimum cost for performing the mission.

Bibliography

[1] U.S. Department of Defense (DOD) Dictionary of Military and Associated Terms 2007, http://www.dtic.mil/doctrine/jel/doddict/data/u/05736.html.

[2] UAV Technologies and combat operations, Technical Report, SAB-TR-96-01, USAF Scientific Advisory Board, November 1996.

[3] R. W. Beard, T. W. McLain, D. B. Nelson, D. Kingston, and D. Johansson, "Decentralized Cooperative Aerial Surveillance Using Fixed-Wing Miniature UAVs", Proceedings of the IEEE, Vol.94, No.7, July 2006.

[4] R. W. Beard, T. W. McLain, and M. A. Goodrich, "Coordinated Target Assignment and Intercept for Unmanned Air Vehicles", Proceedings of the IEEE International Conference on Robotics and Automation, Washington D.C., May 2002.

[5] R. W. Beard, T. W. McLain, M. A. Goodrich, and E. P. Anderson, "Coordinated Target Assignment and Intercept for Unmanned Air Vehicles", IEEE Transactions on Robotics and Automation, Vol. 18, No.6, December 2002.

[6] T. W. McLain and R. W. Beard, "Cooperative Path Planning for Timing Critical Missions", Proceedings of the American Control Conference, Denver, Colorado, USA, June 4-6, 2003.

[7] T.W. McLain and R.W. Beard, "Coordination Variables, Coordination Functions, and Cooperative-Timing Missions", AIAA Journal of Guidance, Control, and Dynamics, Vol.28, No.1, January-February, 2005.

[8] T. W. McLain, P. R. Chandler, and M. Pachter, "A Decomposition Strategy for Optimal Coordination of Unmanned Air Vehicles", Proceedings of the American Control Conference, Chicago, Illinois, USA, June 2000.

[9] T. W. McLain, P. R. Chandler, S. Rasmussen, and M. Pachter, "Cooperative Control of UAV Rendezvous", Proceedings of the American Control Conference, Arlington, VA, June 25-27, 2001.

[10] P. R. Chandler, M. Pachter, and S. Rasmussen, "UAV Cooperative Control", Proceedings of the American Control Conference, Arlington, VA, June 25-27, 2001.

[11] P. R. Chandler and M. Pachter, "Hierarchical Control for Autonomous Teams", Proceedings of the AIAA Guidance, Navigation and Control Conference, and Exhibit, Montreal, Canada, 6-9 August 2001.

[12] P. R. Chandler, M. Pachter, D. Swaroop, J. M. Fowler, J. K. Howlett, S. Rasmussen, C. Schumacher, and K. Nygrad, "Complexity in UAV Cooperative Control", Proceedings of the American Control Conference, Anchorage, AK, May 8-10, 2002.

[13] E. Paul Anderson, "Extremal Control and Unmanned Air Vehicle Trajectory Generation", Master of Science Thesis, Brigham Young University, April 2002.

[14] K. B. Judd, "Trajectory Planning Strategies for Unmanned Air Vehicles", Master of Science Thesis, Brigham Young University, August 2001.

[15] P. R. Chandler, S. Rasmussen, and M. Pachter, "UAV Cooperative Path Planning", Proceedings of the AIAA Guidance, Navigation and Control Conference, and Exhibit, Denver, Colorado, USA, 14-17 August 2000.

[16] T. W. McLain and R. W. Beard, "Trajectory Planning for Coordinated Rendezvous of Unmanned Air Vehicles", Proceedings of AIAA Guidance, Navigation, and Control Conference, August 2000.

[17] S. A. Bortoff, "Path Planning for UAVs", Proceedings of the American Control Conference, Chicago, Illinois, USA, June 2000.

[18] P. R. Chandler, "Cooperative Control for a Team of UAVs for Tactical Missions", Proceedings of AIAA 1st Intelligent Systems Technical Conference, Chicago, Illinois, USA, 20-22 September, 2004.

[19] P. B. Sujit and D. Ghose, "Optimal Uncertainty Reduction using the k-Shortest Path Algorithm", Proceedings of the American Control Conference, Denver, CO, USA, 4th-6th June, 2003.

[20] P. B. Sujit and D. Ghose, "Search Using Multiple UAVs with Flight Time Constraints", IEEE Transactions on Aerospace and Electronic Systems, Vol. 40, No.2, April 2004.

[21] P. B. Sujit and D. Ghose, "Multiple Agent Search of an Unknown Environment Using Game Theoretical Models", Proceedings of the 2004 American Control Conference, Boston, MA, USA, June 30th – July 2nd, 2004.

[22] P. B. Sujit and D. Ghose, "Multiple UAV Search Using Agent Based Negotiation Scheme", Proceedings of the 2005 American Control Conference, Portland, OR, USA, June 8th -10th, 2005.

[23] P. B. Sujit and D. Ghose, "Self-Assessment Schemes for Multi-Agent Cooperative Search", Proceedings of the 2006 American Control Conference, Minneapolis, Minnesota, USA, June 14-16, 2006.

[24] M. M. Polycarpou, Y. Yang, and K. M. Passino, "A Cooperative Search Framework for Distributed Agents", Proceedings of the 2001 IEEE International Symposium on Intelligent Control, Mexico City, Mexico, September 5-7, 2001.

[25] M. Flint, M. Polycarpou, and E. F-Gaucherand, "Cooperative Control for Multiple Autonomous UAV's Searching for Targets", Proceedings of the 41st IEEE Conference on Decision and Control, Las Vegas, Nevada, USA, December 2002.

[26] M. Flint, M. Polycarpou, and E. F-Gaucherand, "Cooperative Control for UAV's Searching Risky Environments for Targets", Proceedings of the 42nd IEEE Conference on Decision and Control, Las Vegas, Nevada, USA, December 2003.

[27] Y. Jin, A. A. Miani, and M. M. Polycarpou, "Cooperative Real-Time Search and Task Allocation in UAV Teams", Proceedings of the 42nd IEEE Conference on Decision and Control, Maui, Hawaii, USA, December 2003.

[28] Y. Yang, A. A. Minai, and M. M. Polycarpou, "Decentralized Cooperative Search by Networked UAVs in an Uncertain Environment", Proceedings of the 2004 American Control Conference, Boston, MA, USA, June 30th-July 2nd, 2004.

[29] Y. Jin, Y. Liao, M. M. Polycarpou, and A. A. Minai, "Balancing Search and Target Response in Cooperative UAV Teams", Proceedings of the 43rd IEEE Conference on Decision and Control, Atlantis, Paradise Island, Bahamas, December 14-17, 2004.

[30] Y. Jin, Y. Liao, A. A. Minai, and M. M. Polycarpou, "Balancing Search and Target Response in Cooperative Unmanned Aerial Vehicle (UAV) Teams", IEEE

Transactions on Systems, Man, and Cybernetics - Part B: Cybernetics, Vol. 36, No.3, June 2006.

[31] Y. Liao, Y. Jin, A. A. Minai, and M. M. Polycarpou, "Information Sharing in Cooperative Unmanned Aerial Vehicle Teams", Proceedings of the 44th IEEE Conference on Decision and Control, and the European Control Conference 2005, Seville, Spain, December 12-15, 2005.

[32] R. W. Beard and T. W. McLain, "Multiple UAV Cooperative Search under Collision Avoidance and Limited Range Communication Constraints", Proceedings of the 42nd IEEE Conference on Decision and Control, Maui, Hawaii, USA, December 2003.

[33] M. L. Baum and K. M. Passino, "A Search-Theoretic Approach to Cooperative Control for Uninhabited Air Vehicles", Proceedings of the AIAA Guidance Navigation, and Control Conference, and Exhibit, Monterey, CA, USA, 5-8 August 2002.

[34] D. Enns, D. Bugajski, and S. Pratt, "Guidance and Control for Cooperative Search", Proceedings of the American Control Conference, Anchorage, AK, USA, 8th-10th May, 2002.

[35] L. F. Bertuccelli and J. P. How, "Robust UAV Search for Environments with Imprecise Probability Maps", Proceedings of the 44th IEEE Conference on Decision and Control, and the European Control Conference 2005, Seville, Spain, December 12-15, 2005.

[36] L. F. Bertuccelli and J. P. How, "Search for Dynamic Targets with Uncertain Probability Maps", Proceedings of the 2006 American Control Conference, Minneapolis, Minnesota, USA, June 14-16, 2006.

[37] G. L. Slater, "Cooperation between UAVs in a Search and Destroy Mission", Proceedings of the AIAA Guidance, Navigation, and Control Conference, and Exhibit, Austin, Texas, USA, 11th-14th August, 2003.

[38] D. W. Casbeer, R. W. Beard, T. W. McLain, Sai-Ming Li, and R. K. Mehra, "Forest Fire Monitoring With Multiple Small UAVs", Proceedings of the 2005 American Control Conference, Portland, OR, USA, June 8th-10th, 2005.

[39] D. W. Casbeer, D. B. Kingston, R. W. Beard, T. W. McLain, Sai-Ming Li, and R. K. Mehra, "Cooperative Forest Fire Surveillance Using a Team of Small Unmanned Air Vehicles", International Journal of Systems Science, Volume 37, Issue 6, May 2006, pages 351-360.

[40] D. Kingston, R. Holt, R. W. Beard, T. W. McLain, and D. W. Casbeer, "Decentralized Perimeter Surveillance Using a Team of UAVs", Proceedings of the AIAA Guidance, Navigation, and Control Conference, and Exhibit, San Francisco, CA, USA, 15th-18th August, 2005.

[41] T. Samad, J. S. Bay, and D. Godbole, "Network-Centric Systems for Military Operations in Urban Terrain: The Role of UAVs", Proceedings of the IEEE, Vol.95, No.1, January 2007.

[42] M. de Berg, M. van Kreveld, M. Overmars, and O. Schwarzkopf, "Computational Geometry: Algorithms and Applications", 2nd, rev. ed., Berlin; New York, Springer 2000.

[43] T. H. Cormen, C. E. Leiserson, and R. L. Rivest, "Introduction to Algorithms", The MIT Press, 1990.

[44] W. C. Stirling and M. A. Goodrich, "Conditional Preferences for Social Systems", Proceedings of the IEEE International Conference on Systems, Man, and Cybernetics, Vol.2, 7th-10th October, 2001.

[45] J. D. Boskovic, S. E. Bergstorm, and R. K. Mehra, "Retrofit Reconfigurable Flight Control in the Presence of Control Effector Damage", Proceedings of the 2005 American Control Conference, Portland, OR, USA, June 8-10, 2005.

[46] G. Heredia, A. Ollero, R. Mahtani, and M. Bejar, "Detection of Sensor Faults in Autonomous Helicopters", Proceedings of the 2005 IEEE International Conference on Robotics and Automation, Barcelona, Spain, April 2005.

[47] C. Rago, R. Prasanth, R. K. Mehra, and R. Fortenbaugh, "Failure Detection and Identification and Fault Tolerant Control using the IMM-KF with applications to the Eagle-Eye UAV", Proceedings of the 37th IEEE Conference on Decision and Control, Tampa, FL, USA, December 1998.

[48] S. M. Magrabi and P. W. Gibbens, "Decentralised Fault Detection and Diagnosis in Navigation Systems for Unmanned Aerial Vehicles", Proceedings of the 2000 IEEE Position, Location and Navigation Symposium, 13th-16th March, 2000.

Appendix A

Simulation Results for the Surveillance Mission

Results for the Actuator Fault

Velocity Set 2: UAV1: 89-176 m/s, UAV2: 89-220 m/s, UAV3: 89-220 m/s

Case I: Two healthy vehicles, 1 faulty vehicle performing surveillance

Table A.1: Minimum Surveillance mission costs of UAV1 when its maximum velocity is at 80% of the nominal value, 220m/s.

α	v_1 (m/s)	$\min\_J_{sm_1}$	J_{fuel_1} (km^3/sec^2)	t_{s_1} (hours)
0.1	89	19.57	15.92	6.273
0.2	89	23.22	15.92	6.273
0.3	89	26.87	15.92	6.273
0.4	92	30.48	17.01	6.069
0.5	104	33.29	21.74	5.369
0.6	119	34.90	28.46	4.692
0.7	138	35.14	38.28	4.046
0.8	166	33.55	55.39	3.363
0.9	176	30.08	62.26	3.172

Table A.2: Comparison of Minimum Team Cost values for case I and case II when the velocity range of UAV1 is: $89m/s \le v_1 \le 176m/s$.

alpha (α)	$\min \sum_{i=1}^{N} J_{sm_i}$ (Minimum Team Cost)	
	Case I (N = 3)	**Case II (N = 2)**
0.1	64.77	67.68
0.2	81.78	87.68
0.3	98.69	107.54
0.4	113.12	123.76
0.5	123.53	135.14
0.6	129.50	141.66
0.7	130.40	142.64
0.8	124.51	136.20
0.9	109.76	119.30

Note: The results for UAV2 and UAV3 for case I and case II are given in Tables 4.3 and 4.4, respectively.

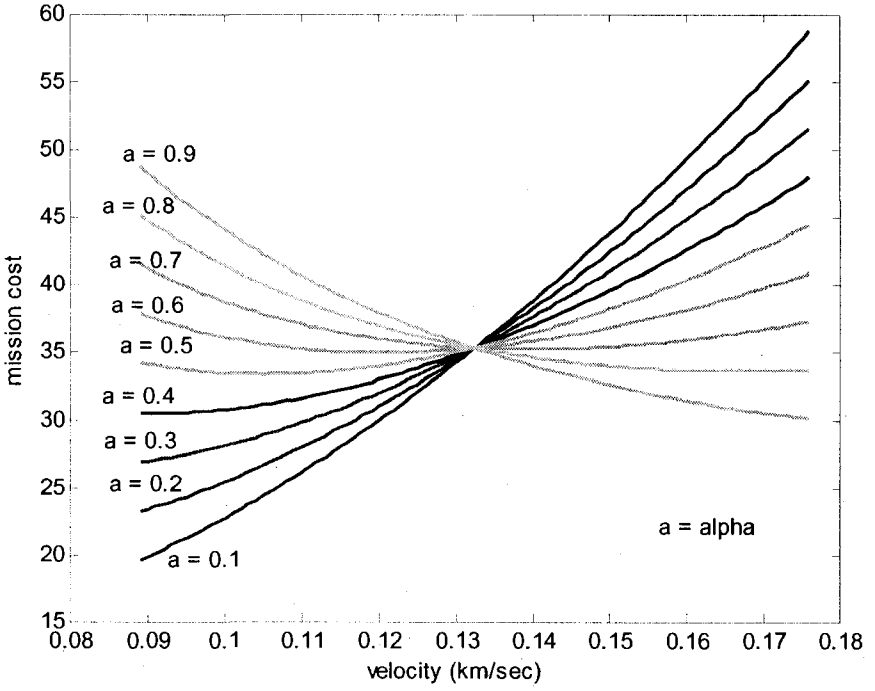

Figure A.1: Surveillance Mission Costs of UAV1 for the velocity range:

$$89m/s \le v_1 \le 176m/s\,.$$

Velocity Set 3: UAV1: 89-154 m/s, UAV2: 89-220 m/s, UAV3: 89-220 m/s

Case I: Two healthy vehicles, 1 faulty vehicle performing surveillance

Table A.3: Minimum Surveillance mission costs of UAV1 when its maximum velocity is at 70% of the nominal value, 220m/s.

α	v_1 (m/s)	$\min\_J_{sm_1}$	J_{fuel_1} (km^3/sec^2)	t_{s_1} (hours)
0.1	89	18.37	15.92	6.273
0.2	89	20.83	15.92	6.273
0.3	89	23.28	15.92	6.273
0.4	89	25.74	15.92	6.273
0.5	95	28.02	18.14	5.877
0.6	110	29.37	24.32	5.076
0.7	127	29.57	32.42	4.396
0.8	151	28.24	45.83	3.698
0.9	154	25.81	47.67	3.626

Table A.4: Comparison of Minimum Team Cost values for case I and case II when the velocity range of UAV1 is: $89m/s \le v_1 \le 154m/s$.

alpha (α)	$\min \sum_{i=1}^{N} J_{sm_i}$ (Minimum Team Cost)	
	Case I (N = 3)	**Case II (N = 2)**
0.1	63.57	67.68
0.2	79.39	87.68
0.3	95.10	107.54
0.4	108.38	123.76
0.5	118.26	135.14
0.6	123.97	141.66
0.7	124.83	142.64
0.8	119.20	136.20
0.9	105.49	119.30

Note: The results for UAV2 and UAV3 for case I and case II are given in Tables 4.3 and 4.4, respectively.

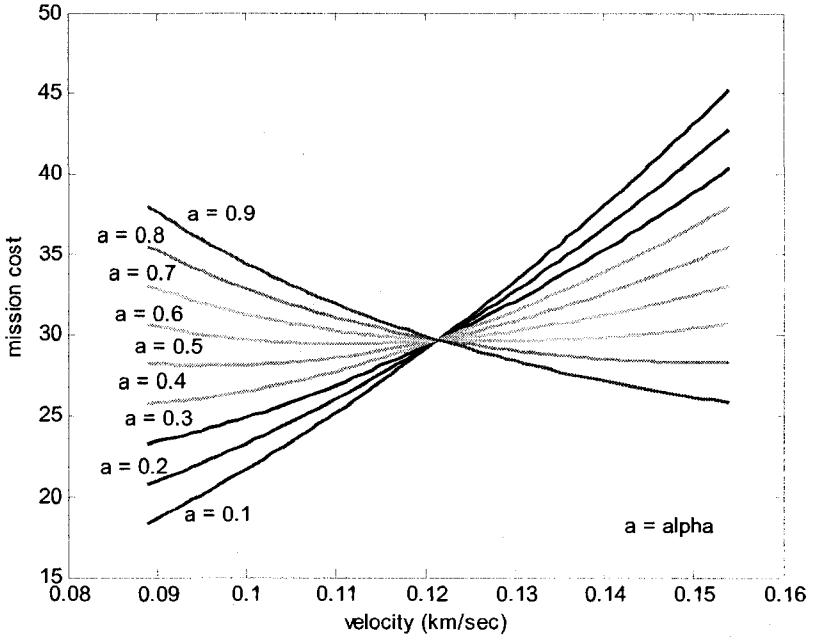

Figure A.2: Surveillance Mission Costs of UAV1 for the velocity range:

$$89m/s \le v_1 \le 154m/s.$$

Velocity Set 4: UAV1: 89-132 m/s, UAV2: 89-220 m/s, UAV3: 89-220 m/s

Case I: Two healthy vehicles, 1 faulty vehicle performing surveillance

Table A.5: Minimum Surveillance mission costs of UAV1 when its maximum velocity is at 60% of the nominal value, 220m/s.

α	v_1 (m/s)	$\min\_J_{sm_1}$	J_{fuel_1} (km^3/sec^2)	t_{s_1} (hours)
0.1	89	17.37	15.92	6.273
0.2	89	18.83	15.92	6.273
0.3	89	20.28	15.92	6.273
0.4	89	21.74	15.92	6.273
0.5	89	23.19	15.92	6.273
0.6	99	24.31	19.70	5.64
0.7	116	24.47	27.05	4.813
0.8	132	23.43	35.02	4.23
0.9	132	21.99	35.02	4.23

Table A.6: Comparison of Minimum Team Cost values for case I and case II when the velocity range of UAV1 is: $89m/s \le v_1 \le 132m/s$.

alpha (α)	$\min \sum_{i=1}^{N} J_{sm_i}$ (Minimum Team Cost)	
	Case I (N = 3)	**Case II (N = 2)**
0.1	62.57	67.68
0.2	77.38	87.68
0.3	92.10	107.54
0.4	104.38	123.76
0.5	113.43	135.14
0.6	118.91	141.66
0.7	119.73	142.64
0.8	114.39	136.20
0.9	101.67	119.30

Note: The results for UAV2 and UAV3 for case I and case II are given in Tables 4.3 and 4.4, respectively.

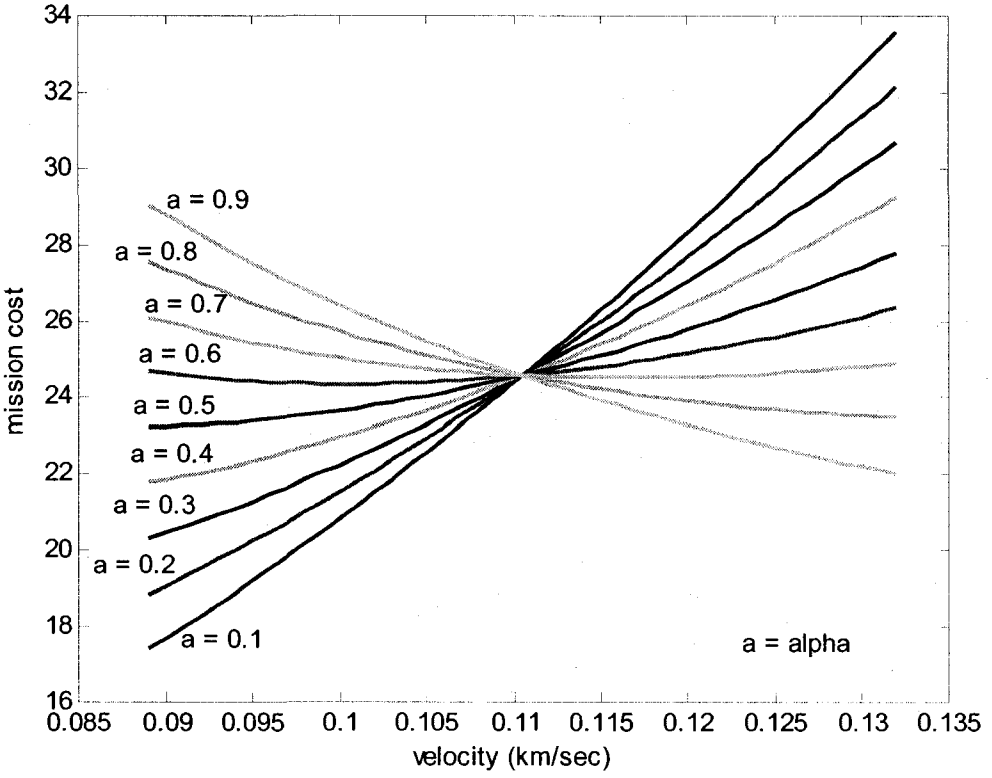

Figure A.3: Surveillance Mission Costs of UAV1 for the velocity range:

$$89m/s \le v_1 \le 132m/s.$$

Results for the Sensor Fault

Sensor Range: UAV1: 25 meters, UAV2: 100 meters, UAV3: 100 meters

Case I: Two healthy vehicles, 1 faulty vehicle performing surveillance

Table A.7: Minimum Surveillance mission cost of UAV1 when its sensor range is at 25% of the nominal value, 100 meters.

α	v_1 (m/s)	$\min\_J_{sm_1}$	J_{fuel_1} (km^3/sec^2)	t_{s_1} (hours)
0.1	89	90.06	63.45	25
0.2	89	116.66	63.45	25
0.3	91	143.09	66.33	24.45
0.4	105	164.66	88.31	21.19
0.5	121	179.81	117.3	18.39
0.6	138	188.49	152.5	16.12
0.7	160	189.79	205.10	13.91
0.8	193	181.23	298.40	11.53
0.9	220	158.75	387.7	10.11

Table A.8: Comparison of Minimum Team Cost values for case I and case II when the sensor range of UAV1 is 25 meters.

alpha (α)	$\min \sum_{i=1}^{N} J_{sm_i}$ (Minimum Team Cost)	
	Case I (N = 3)	**Case II (N = 2)**
0.1	135.25	67.68
0.2	175.22	87.68
0.3	214.91	107.54
0.4	247.30	123.76
0.5	270.05	135.14
0.6	283.09	141.66
0.7	285.05	142.64
0.8	272.19	136.20
0.9	238.43	119.30

Note: The results for UAV2 and UAV3 for case I and case II are given in Tables 4.3 and 4.4, respectively.

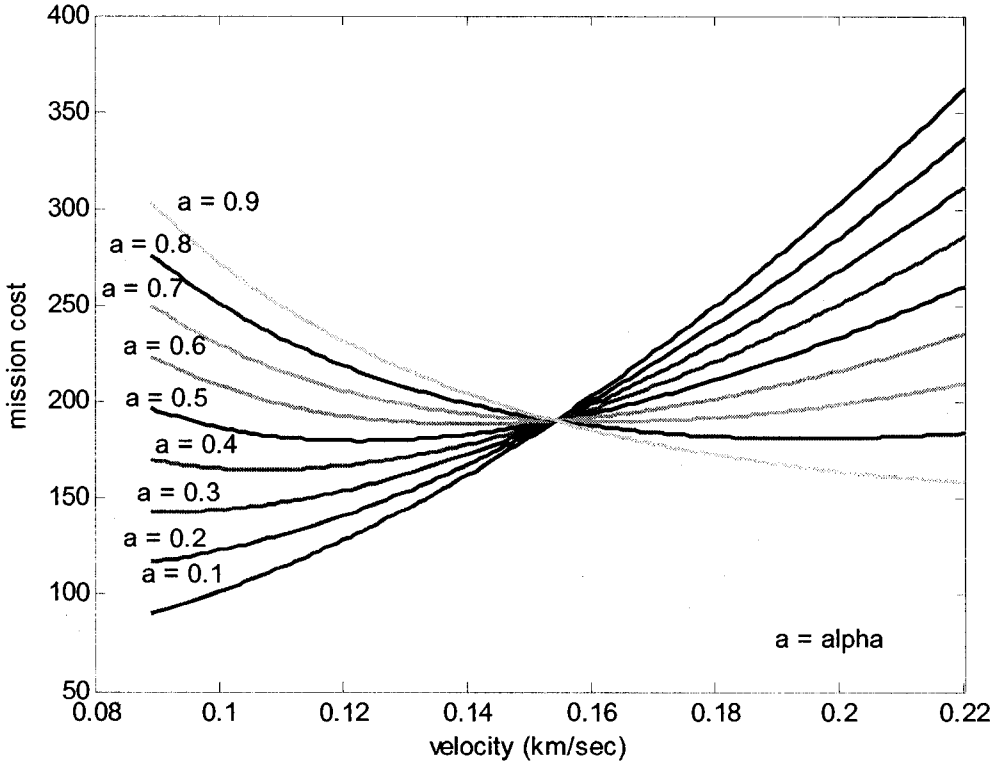

Figure A.4: Surveillance Mission Costs of UAV1 for a sensor range of 25 meters.

Results for the Sensor and the Actuator Faults

Velocity Range: UAV1: 89-110 m/s, UAV2: 89-220 m/s, UAV3: 89-220 m/s

Sensor Range: UAV1: 25 meters, UAV2: 100 meters, UAV3: 100 meters

Table A.9: Minimum Surveillance Mission costs of UAV1 when its maximum velocity is at 50% and its sensor range is at 25% of the nominal values.

α	v_1 (m/s)	$\min\_J_{sm_1}$	J_{fuel_1} (km^3/sec^2)	t_{s_1} (hours)
0.1	89	65.9679	63.45	25
0.2	89	68.4886	63.45	25
0.3	89	71.0093	63.45	25
0.4	89	73.5300	63.45	25
0.5	89	76.0507	63.45	25
0.6	90	78.5538	64.88	24.72
0.7	105	79.0945	88.31	21.19
0.8	110	76.7676	96.92	20.23
0.9	110	74.2484	96.92	20.23

Table A.10: Comparison of Minimum Team Cost values for case I and case II when the maximum velocity of UAV1 is 110 m/s and its sensor range is 25 meters.

alpha (α)	$\min \sum_{i=1}^{N} J_{sm_i}$ (Minimum Team Cost)	
	Case I (N = 3)	**Case II (N = 2)**
0.1	111.1644	67.68
0.2	127.0392	87.68
0.3	142.8241	107.54
0.4	156.1697	123.76
0.5	166.2918	135.14
0.6	173.1526	141.66
0.7	174.3459	142.64
0.8	167.7244	136.20
0.9	153.9198	119.30